

# **Characterization of Phosphofructokinase B-Type Kinases from *Arabidopsis thaliana* Leading to the Identification of a Plastid Inosine Kinase**

Von der Naturwissenschaftlichen Fakultät der  
Gottfried Wilhelm Leibniz Universität Hannover

zur Erlangung des Grades  
Doktor der Naturwissenschaften (Dr. rer. nat.)

genehmigte Dissertation  
von  
Xiaoguang Chen, Master of Science (China)

2022

Referent: Prof. Dr. Claus-Peter Witte

Korreferent: Prof. Dr. rer. nat. Hans-Peter Braun

Tag der Promotion: 27.09.2022

## Abstract

Nucleotide metabolism is vital for plant development and dependent on the support of various enzymes including the phosphofructokinase B-type (PfkB) sugar kinases. Although some PfkB kinases such as adenosine kinase (ADK), ribokinase (RBSK), and pseudouridine kinase (PUKI) have been successfully identified and characterized in recent years, much is still unknown about these kinases. In this study, PfkB kinases from *Arabidopsis thaliana* were functionally screened leading to the identification of a plastid inosine kinase (PINK) that is involved in the feedback regulation of *de novo* purine synthesis and of kinase 6-2 (K6-2), which may be involved in negative regulation of purine synthesis.

According to bioinformatic analyses, PINK is highly conserved in the plant kingdom, Subcellular localization and *in vitro* kinase activity analyses revealed that PINK is a plastid kinase that phosphorylates inosine, uridine, and 5-aminoimidazole-4-carboxamide ribonucleoside (AICAr). Furthermore, metabolite analysis was performed of *Arabidopsis* seedlings in which *PINK* expression was varied, which showed that PINK is not only involved in the inosine salvage but also likely contributes to feedback inhibition of *de novo* purine biosynthesis by regulating the plastid IMP pool. Moreover, PINK is possibly involved in pyrimidine nucleotide synthesis, at least in the context of defective uridine degradation.

Additionally, another member of the PfkB family, kinase 6-2 (K6-2) was partially characterized in this work. K6-2 is localized in the chloroplast and *in vitro* biochemical analysis showed that K6-2 can phosphorylate AICAr, inosine, and guanosine. Furthermore, an *in vivo* functional study suggested that K6-2 is a negative regulator of purine *de novo* biosynthesis, as the biosynthesis of purine nucleotides was enhanced in the knock-down mutant of *K6-2*. Moreover, the reduced expression of *K6-2* in *Arabidopsis* led to a phenotype that involved yellowing and suppressed leaf growth.

Keywords: PfkB kinases, inosine kinase, purine *de novo* biosynthesis, nucleotide metabolism, *Arabidopsis*

## Zusammenfassung

Der Nukleotid-Stoffwechsel ist für die Pflanzenentwicklung von entscheidender Bedeutung und hängt von der Aktivität verschiedener Enzyme ab, darunter die Zuckerkinasen vom Typ Phosphofruktokinase B (PfkB). Obwohl einige PfkB-Kinasen wie die Adenosin-Kinase (ADK), die Ribokinase (RBSK) und die Pseudouridin-Kinase (PUKI) in den letzten Jahren identifiziert und charakterisiert wurden, ist noch vieles über diese Kinasen unbekannt. In dieser Studie wurden PfkB-Kinasen aus *Arabidopsis thaliana* funktionell untersucht, was zur Identifizierung einer plastiden Inosin-Kinase (PINK) führte, die an der Rückkopplungsregulierung der *De-novo*-Purinsynthese beteiligt ist, sowie der Kinase 6-2 (K6-2), die möglicherweise zur negativen Regulierung der Purinsynthese einen Beitrag leistet.

Bioinformatischer Analysen zufolge ist PINK im Pflanzenreich hoch konserviert. Analysen der subzellulären Lokalisierung und der *In-vitro*-Kinaseaktivität ergaben, dass PINK eine plastide Kinase ist, die Inosin, Uridin und 5-Aminoimidazol-4-Carboxamid-Ribonukleosid (AICAr) phosphoryliert. Darüber hinaus zeigte die Metabolitenanalyse von Arabidopsis-Keimlingen, in denen die PINK-Expression variiert wurde, dass PINK nicht nur am Inosin-*Salvage* beteiligt ist, sondern wahrscheinlich auch zur Rückkopplungshemmung der *De-novo*-Purin-Biosynthese beiträgt, indem sie den plastiden IMP-Pool reguliert. Darüber hinaus ist PINK möglicherweise an der Synthese von Pyrimidinnukleotiden beteiligt, zumindest im Zusammenhang mit einem gestörten Uridinabbau.

Des Weiteren wurde in dieser Arbeit ein weiteres Mitglied der PfkB-Familie, die Kinase 6-2 (K6-2), teilweise charakterisiert. K6-2 ist im Chloroplasten lokalisiert, und eine biochemische *In-vitro*-Analyse zeigte, dass K6-2 AICAr, Inosin und Guanodin phosphorylieren kann. Eine *In-vivo*-Funktionsstudie deutet außerdem darauf hin, dass K6-2 ein negativer Regulator der Purin-*de-novo*-Biosynthese ist, da die Biosynthese von Purinnukleotiden in der *Knock-down*-Mutante von K6-2 offenbar erhöht war. Eine reduzierte Expression von K6-2 in Arabidopsis führte phänotypisch zu vermehrter Blattvergilbung und unterdrücktem Wachstum.

Schlüsselwörter: PfkB-Kinasen, Inosin-Kinase, Purin-*de-novo*-Biosynthese, Nukleotid-Stoffwechsel, *Arabidopsis thaliana*

## Contents

Abstract .....	I
Zusammenfassung .....	II
Contents .....	III
Abbreviations .....	VI
List of Figures .....	VIII
List of Tables .....	X
<b>1 Introduction .....</b>	<b>1</b>
1.1 Nucleotides .....	1
1.1.1 Nucleotides are essential for plant development .....	1
1.1.2 Structure .....	1
1.1.3 Nucleotide metabolism .....	2
1.2 Purine metabolism in plants .....	3
1.2.1 <i>De novo</i> purine biosynthesis .....	3
1.2.2 Purine salvage .....	6
1.2.3 Purine catabolism .....	7
1.3 Pyrimidine metabolism in plants .....	8
1.3.1 Pyrimidine <i>de novo</i> synthesis .....	8
1.3.2 Pyrimidine salvage .....	8
1.3.3 Pyrimidine degradation .....	9
1.4 PfkB sugar kinases in plants .....	11
1.5 Aim of this study .....	14
<b>2 Material and Methods .....</b>	<b>15</b>
2.1 Material .....	15
2.1.1 Antibiotics .....	15
2.1.2 Bacterial strains .....	15
2.1.3 Buffers and solutions .....	16

## CONTENTS

---

2.1.4	Media.....	19
2.1.5	Plants .....	20
2.1.6	Primers .....	21
2.1.7	Vectors and constructs .....	24
2.1.8	Substrate candidates for kinase assay.....	26
2.1.9	Software and databases .....	27
2.2	Methods .....	28
2.2.1	Plants .....	28
2.2.2	Microbiology.....	29
2.2.3	Molecular biology .....	30
2.2.4	Biochemistry .....	32
2.2.5	Metabolite analysis.....	36
2.2.6	Bioinformatic analysis.....	38
2.2.7	Statistical analysis .....	38
3	Results .....	40
3.1	<i>In vitro</i> biochemical analyses of PfkB kinases .....	40
3.1.1	Cloning, expression, and protein purification of PfkB kinases.....	40
3.1.2	Kinase activity screen of PfkB kinases .....	43
3.1.3	Summary of <i>in vitro</i> characterization of PfkB kinases .....	47
3.2	Functional analyses of PINK.....	48
3.2.1	Bioinformatic analysis of PINK.....	48
3.2.2	Subcellular localization of PINK .....	49
3.2.3	Enzyme kinetics of PINK.....	50
3.2.4	Characterization of <i>PINK</i> variants .....	52
3.2.5	Antibody preparation of PINK.....	53
3.2.6	Phenotype of the <i>PINK NSH1</i> double mutant .....	55
3.2.7	Metabolite analysis of <i>PINK</i> variants.....	56

## CONTENTS

---

3.2.8	Summary of PINK functional analyses .....	64
3.3	Functional analyses of K6-2 .....	65
3.3.1	Bioinformatic analysis of K6-2 .....	65
3.3.2	Subcellular localization of K6-2 .....	67
3.3.3	Enzyme kinetics of K6-2 .....	67
3.3.4	Characterization of the <i>K6-2</i> knock-down mutant .....	69
3.3.5	Phenotype of the <i>K6-2</i> knock-down mutant .....	70
3.3.6	Metabolite analysis of <i>K6-2</i> variants .....	71
4	Discussion .....	74
4.1	Characterization of PfkB kinases from Arabidopsis .....	74
4.2	Purine <i>de novo</i> purine biosynthesis .....	74
4.3	Functional analysis of PINK .....	75
4.3.1	PINK is an inosine kinase and should be involved in the feedback regulation of purine biosynthesis .....	75
4.3.2	PINK under cold stress .....	78
4.3.3	PINK in pyrimidine homeostasis .....	78
4.4	Functional analysis of K6-2 .....	80
4.4.1	K6-2 is a negative regulator of purine nucleotide synthesis .....	80
4.4.2	K6-2 may be an AICAr kinase in Arabidopsis .....	81
4.4.3	K6-2 is more likely a guanosine kinase .....	81
4.5	Conclusion .....	82
	References .....	83
	Acknowledgement .....	90
	Appendix of Figures .....	91
	Appendix of Tables .....	102
	Curriculum Vitae .....	104
	Publications .....	105

## Abbreviations

---

AICAr	5-aminoimidazole-4-carboxamide ribonucleoside
AICAR	5-aminoimidazole-4-carboxamide ribonucleotide
Amp	ampicillin
AP	alkaline phosphatase
APS	ammonium persulfate
BCIP	5-bromo-4-chloro-3'-indolyphosphate
BSA	bovine serum albumin
Carb	carbenicillin
cDNA	complementary deoxyribonucleic acid
DCM	dichloromethane
DMF	dimethylformamide
DNA	deoxyribonucleic acid
DTT	dithiothreitol
EDTA	ethylenediaminetetraacetic acid
FW	fresh weight
Gent	gentamycin
HEPES	4-(2-hydroxyethyl)-1-piperazineethanesulfonic acid
HPLC	high-performance liquid chromatography
IMP	inosine monophosphate
ISTDs	internal standards
Kan	kanamycin
KO	knock out
LB	lysogeny broth
LC-MS	liquid chromatography coupled to mass spectrometry
MES	2-(N-morpholino) ethanesulfonic acid



## ABBREVIATIONS

---

MS	Murashige and skoog medium
m <sup>6</sup> A	N <sup>6</sup> -methyladenosine
m <sup>6</sup> AMP	N <sup>6</sup> -methyl-AMP
NAD	nicotinamide adenine dinucleotide
NADH	nicotinamide adenine dinucleotide reduced disodium salt
NBT	nitro-blue tetrazolium chloride
PEP	phosphoenolpyruvate
PfkB	phosphofructokinase B
PRPP	5-phosphoribosyl-1-pyrophosphate
rDNase	recombinant deoxyribonuclease
Rif	rifampicin
RNA	ribonucleic acid
RNase	ribonuclease
RT-PCR	reverse transcription polymerase chain reaction
SDS	sodium dodecyl sulfate
SDS-PAGE	sodium dodecyl sulfate polyacrylamide gel electrophoresis
TBA	tetrebtylammonium bisulfate
TCA	trichloroacetic acid
TEMED	tetramethylethylenediamine
TOA	trioctylamine
Tris	tris(hydroxymethyl)aminomethane
YEB	yeast extract beef broth

---

## List of Figures

Figure 1. Structure of nucleosides, nucleotides, and nucleobases.....	2
Figure 2. Scheme of purine metabolism in Arabidopsis. ....	4
Figure 3. Scheme of pyrimidine metabolism in Arabidopsis. ....	10
Figure 4. Scheme of nucleoside kinase activity.....	12
Figure 5. Phylogenetic analysis of PfkB kinases in plants. ....	13
Figure 6. Affinity purification of Arabidopsis PfkB kinases.....	42
Figure 7. HPLC analyses of the kinase activity screen for ADK1. ....	44
Figure 8. HPLC analyses of the kinase activity screen for ADK2. ....	45
Figure 9. HPLC analyses of the kinase activity screen for K6-2.....	46
Figure 10. HPLC analyses of the kinase activity screen for PINK. ....	47
Figure 11. Phylogenetic analysis of PINK and functionally related PfkB kinases. ....	49
Figure 12. Subcellular localization of PINK. ....	50
Figure 13. Kinetic analysis of PINK. ....	51
Figure 14. Characterization of PINK variants. ....	53
Figure 15. Inclusion body characterization and detection of PINK with antibodies.....	54
Figure 16. Phenotype of 21-day-old seedlings of PINK variants. ....	55
Figure 17. Metabolite analysis of the PINK mutant under different light conditions. ....	56
Figure 18. Metabolite analysis of PINK variants with different duration of light.....	57
Figure 19. Metabolite analysis of seedlings varying in PINK expression in the NSH1 background. ....	59
Figure 20. Metabolite analysis of seedlings varying in PINK expression in the HGPRT mutant background and upon XDH inhibition during the day.....	61
Figure 21. Metabolite analysis of wild type seedlings with cold treatment.....	62
Figure 22. Metabolite analysis in seedlings of PINK variants after short-term cold exposure.....	63
Figure 23. Phylogenetic analysis of KINASE 6-2 and PfkB nucleoside or ribo-kinases..	66
Figure 24. Subcellular localization of K6-2.....	67
Figure 25. Kinetic analysis of K6-2.....	68
Figure 26. Characterization of a K6-2 knock-down mutant. ....	70
Figure 27. Phenotype of 16-day-old seedlings with varying K6-2 expression.....	71
Figure 28. Metabolite analysis of 10-day-old seedlings varying in K6-2 expression.....	72
Figure 29. Model of inosine salvage by PINK in the context of purine metabolism. ....	80

## LIST OF FIGURES

---

<b>Figure A-1. Multiple protein sequence alignment of PfkB kinases. ....</b>	<b>91</b>
<b>Figure A-2. Expression overviews of pink and k6-2 in Arabidopsis. ....</b>	<b>96</b>
<b>Figure A-3. Metabolite analysis in seedlings of the PINK mutant under different light conditions. ....</b>	<b>97</b>
<b>Figure A-4. Metabolite analysis in seedlings of PINK variants with different durations of light. ....</b>	<b>98</b>
<b>Figure A-5. Metabolite analysis of Arabidopsis wild type seedlings with cold treatment. ....</b>	<b>99</b>
<b>Figure A-6. Metabolite analysis in seedlings of PINK variants with short-term cold exposure. ....</b>	<b>99</b>
<b>Figure A-7. Specific activity of K6-2. ....</b>	<b>101</b>

## List of Tables

<b>Table 2.1-1: Antibiotics.</b> .....	15
<b>Table 2.1-2: Bacterial strains.</b> .....	15
<b>Table 2.1-3. Buffer for <i>Nicotiana benthamiana</i> infiltration.</b> .....	16
<b>Table 2.1-4. Buffers for Strep tagged protein extraction and purification.</b> .....	16
<b>Table 2.1-5. Buffers associated with SDS polyacrylamide gel.</b> .....	16
<b>Table 2.1-6. Solutions for the colloidal Coomassie stain in SDS-PAGE.</b> .....	17
<b>Table 2.1-7. Buffers and solutions for immunoblot.</b> .....	17
<b>Table 2.1-8. Buffers and solutions for kinase assay.</b> .....	17
<b>Table 2.1-9. Buffers for HPLC.</b> .....	18
<b>Table 2.1-10. Buffers for chromatography with a Polaris 5 C18 column.</b> .....	18
<b>Table 2.1-11. Buffers for chromatography with a Hypercarb column.</b> .....	18
<b>Table 2.1-12. Media for bacterial culture.</b> .....	19
<b>Table 2.1-13. Media for plant culture.</b> .....	19
<b>Table 2.1-14. <i>Arabidopsis thaliana</i> lines.</b> .....	20
<b>Table 2.1-15. <i>Arabidopsis thaliana</i> crosses.</b> .....	20
<b>Table 2.1-16. <i>Arabidopsis thaliana</i> complementation lines.</b> .....	20
<b>Table 2.1-17. Primers for genotyping.</b> .....	21
<b>Table 2.1-18. Primers for cloning.</b> .....	23
<b>Table 2.1-19. Vectors.</b> .....	24
<b>Table 2.1-20. Constructs.</b> .....	25
<b>Table 2.1-21. Substrate candidates.</b> .....	26
<b>Table 2.2-1. PCR system.</b> .....	31
<b>Table 2.2-2. PCR program.</b> .....	31
<b>Table 2.2-3. Kinase assay system.</b> .....	35
<b>Table 2.2-4. HPLC solvent gradient.</b> .....	35
<b>Table 2.2-5. Coupled enzyme assay system.</b> .....	36
<b>Table 2.2-6. Solvent gradient on the Polaris 5 C18 column for nucleoside analysis.</b> .....	37
<b>Table 2.2-7. Solvent gradient on the Hypercarb column for nucleotide analysis.</b> .....	38
<b>Table 3.2-1. Kinetic constants for AICAr, inosine, and uridine of PINK.</b> .....	51
<b>Table 3.3-1. Kinetic constants for AICAr, guanosine, and inosine of K6-2.</b> .....	69

LIST OF TABLES

---

**Table A-1. Accession numbers used for bioinformatic analysis. .... 102**

# 1 Introduction

## 1.1 Nucleotides

### 1.1.1 Nucleotides are essential for plant development

Nucleotides are indispensable for plants. First, they are the building blocks of RNA and DNA which carry the genetic instructions for development, functioning, growth, and reproduction (Senecoff et al., 1996). Second, some nucleotides act as precursors for several coenzymes, such as flavin adenine dinucleotide (FAD), nicotinamide adenine dinucleotide (NAD), and S-adenosylmethionine (SAM) (Crozier, 2000; Herz et al., 2000; Hanson and Gregory III, 2002). Then, some nucleotides serve as the energy provider in plants for enzymatic reactions that consume energy. In particular, ATP, which is known as a universal energy carrier in cells, can directly participate in reactions requiring energetic coupling *in vivo*. In general, ATP has a strong affinity for metal cations, especially divalent magnesium ions ( $Mg^{2+}$ ), and ATP- $Mg^{2+}$  binding is necessary for most ATP-protein interactions (Storer and Cornish-Bowden, 1976; Garfinkel et al., 1986; Wilson and Chin, 1991). Additionally, nucleotides are pivotal for the biosynthesis of hormones and secondary metabolites (Lim and Bowles, 2004; Zrenner et al., 2006). For example, the cyclic nucleotide cGMP, which is derived from GMP, is involved in plant hormone signaling that leads to the rapid phosphorylation of root proteins (Isner et al., 2012), and xanthosine acts as the precursor to caffeine, an important alkaloid in coffee and tea (Ashihara et al., 2013).

### 1.1.2 Structure

Nucleotides contain a pentose, a nitrogen-containing heterocycle (nucleobase), and up to 3 phosphoryl group(s) (Figure 1 A). Nucleosides are nucleotides without phosphoryl groups. Depending on the number of phosphoryl groups, a nucleotide is either a nucleoside 5'-monophosphate (NMP), -diphosphate (NDP), or -triphosphate (NTP). When an oxygen atom is missing from the 2' carbon position, one speaks of deoxyribonucleotides. The purine nucleobases (adenine, guanine, hypoxanthine, and xanthine) are heterocyclic compounds that contain an imidazole ring combined with a six-membered carbon-nitrogen (pyrimidine) ring, while the pyrimidine nucleobases (uracil, cytosine, and thymine) are only six-membered carbon-nitrogen heterocyclic compounds (Figure 1 B). Adenine, guanine, uracil, and cytosine are constituents of RNA, whereas thymine is present instead of uracil in DNA. In addition,

nucleobases can be modified by adding groups on the side chains. Methylation is the most common form of modification. For example, N<sup>6</sup>-methyladenosine (m<sup>6</sup>A) has been found not only in ribosomal RNA (rRNA) and transfer RNA (tRNA), but also in messenger RNA (mRNA) influencing posttranscriptional regulation (Frye et al., 2018).

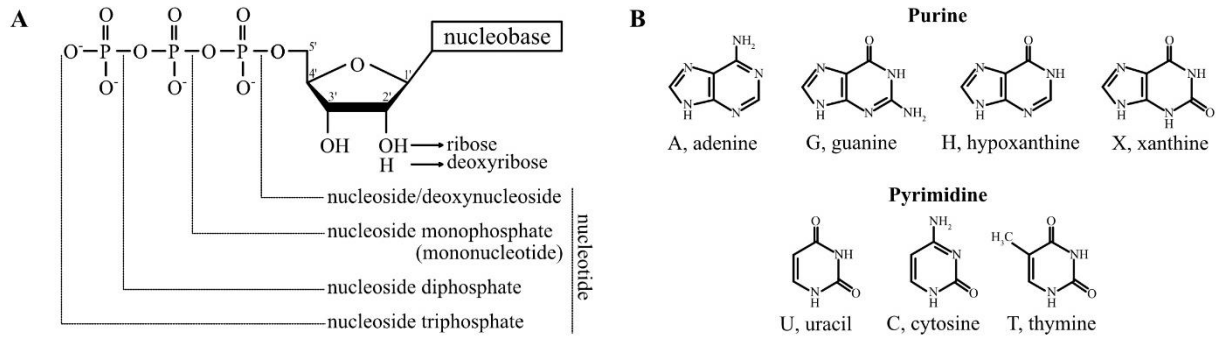


**Figure 1. Structure of nucleosides, nucleotides, and nucleobases.**

(A) Structure of nucleosides and nucleotides. (B) Structure of the nucleobases adenine, guanine, hypoxanthine, xanthine, uracil, cytosine, and thymine.

### 1.1.3 Nucleotide metabolism

Nucleotide metabolism is a complex process. It can be divided into two main categories, purine metabolism and pyrimidine metabolism. Conceptually, each of them can be further divided into the following parts: (i) *de novo* synthesis, which produces nucleotides from molecules of central metabolism through a series of enzymatic reactions, (ii) salvage, which recycles nucleobases and nucleosides to generate nucleoside monophosphates, and (iii) catabolism, which results in the complete degradation of nucleotides that release nutritional resources, such as carbon, nitrogen, and phosphate (Witte and Herde, 2020).

## 1.2 Purine metabolism in plants

### 1.2.1 *De novo* purine biosynthesis

*De novo* purine biosynthesis is essential for plants (Gopaul et al., 1996), and the process uses 5-phosphoribosyl-1-pyrophosphate (PRPP), glutamine, glutamate, glycine, CO<sub>2</sub>, 10-formyl tetrahydrofolate (10-formyl-THF), and aspartate to form IMP, AMP, or GMP. Additionally, several of the reactions involved in this process are energy consuming.

Initially, amidotransferase (ATase), which is also known as 5-phosphoribosylpyrophosphate amidotransferase (PRAT), joins PRPP and glutamine to produce 5-phosphoribosylamine (PRA), which can be further attached to glycine via an amide bond to form ribonucleotide (GAR) by GAR synthase (GARS), and this process consumes ATP. GAR is then transformylated to formylglycinamide ribonucleotide (FGAR) by GAR transformylase (GART). The next step utilizes ATP to convert FGAR to formylglycinamide ribonucleotide (FGAM) with the involvement of FGAM synthase (FGAMS). In addition, 5-aminoimidazole ribonucleotide (AIR) with a closed-loop structure is synthesized by AIR synthase (AIRS), and this step requires ATP. AIR is further converted to 4-carboxy aminoimidazole ribonucleotide (CAIR), which contains carbon and nitrogen structures of the second ring of the purine skeleton. Afterwards, aspartate is added to form N-succinyl-5-aminoimidazole-4-carboxamide ribonucleotide (SAICAR) with the involvement of ATP and SAICAR synthase (SAICARS). Fumarate is then released under the participation of adenylosuccinate lyase (ASL) to build 5-aminoimidazole-4-carboxamide ribonucleotide (AICAR). 5-Aminoimidazole-4-carboxamide ribonucleotide formyltransferase/inosine monophosphate cyclohydrolase (ATIC) catalyzes the last two steps to form inosine monophosphate (IMP) by adding the final carbon from 10-formyl-THF. Subsequently, purine *de novo* synthesis is divided into two branches; one branch is used for AMP synthesis that occurs in the chloroplast, requiring two enzymatic reactions catalyzed by adenylosuccinate synthase (SAMPS) and adenylosuccinate lyase (ASL); and the other branch is used for the GMP synthesis that takes place in the cytosol (two reactions catalyzed by IMP dehydrogenase and GMP synthetase).



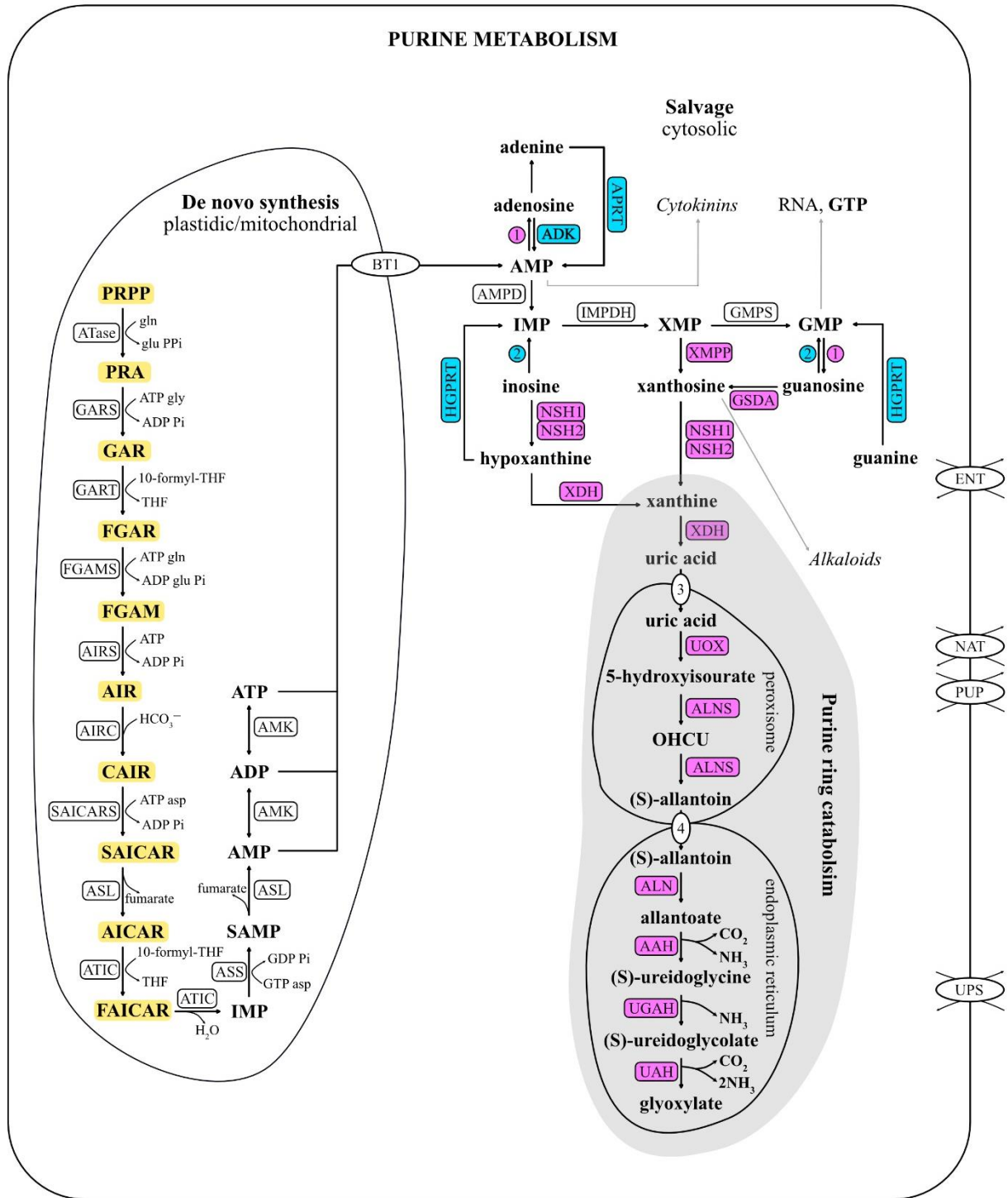


**Figure 2. Scheme of purine metabolism in Arabidopsis.**

The background boxes with yellow shading indicate the precursors and intermediates in the *de novo* purine biosynthesis pathways. The purine ring catabolism pathways are highlighted by light grey shading. The metabolites and enzymes (in boxes with white background) that are involved in purine biosynthesis are glutamine (gln), glutamate (glu), glycine (gly), pyrophosphate (ppi), tetrahydrofolate (THF), 10-formyl-tetrahydrofolate (10-formyl-THF), aspartate (asp), 5-phosphoribosyl-1-pyrophosphate (PRPP), 5-phosphoribosylamine (PRA), glycinamide ribonucleotide (GAR),

## INTRODUCTION

---

formylglycinamide ribonucleotide (FGAR), formylglycinamide ribonucleotide (FGAM), 5-aminoimidazole ribonucleotide (AIR), 4-carboxy aminoimidazole ribonucleotide (CAIR), N-succinyl-5-aminoimidazole-4-carboxamide ribonucleotide (SAICAR), 5-aminoimidazole-4-carboxamide ribonucleotide (AICAR), 5-formaminoimidazole-4-carboxamide ribonucleotide (FAICAR), inosine monophosphate (IMP), adenylosuccinate (SAMP), adenosine monophosphate (AMP), adenosine diphosphate (ADP), adenosine triphosphate (ATP), xanthosine monophosphate (XMP), guanosine monophosphate (GMP), and guanosine triphosphate (GTP). Enzymes: PRPP amidotransferase (ATase), GAR synthase (GARS), GAR transformylase (GART), FGAM synthase (FGAMS), AIR synthase (AIRS), AIR carboxylase (AIRC), SAICAR synthase (SAICARS), adenylosuccinate lyase (ASL), AICAR transformylase/IMP cyclohydrolase (ATIC), adenylosuccinate synthase (ASS), adenylate kinase (AMK), AMP deaminase (AMPD), IMP dehydrogenase (IMPDH), GMP synthetase (GMPS). Enzymes involved in purine catabolism are marked with purple background shading and include: putative nucleotidase(s) (1) guanosine deaminase (GSDA), nucleoside hydrolase 1 (NSH1), nucleoside hydrolase 2 (NSH2), xanthine dehydrogenase (XDH), urate oxidase or uricase (UOX), allantoin synthase (ALNS), allantoin amidohydrolase or allantoinase (ALN), allantoate amidohydrolase (AAH), ureidoglycine aminohydrolase (UGAH), ureidoglycolate amidohydrolase (UAH). Enzymes involved in purine salvage are indicated by blue background shading and are putative inosine/guanosine kinase (2), hypoxanthine guanine phosphoribosyltransferase (HGPRT), adenosine kinase (ADK), and adenine phosphoribosyltransferase (APRT). Transporters are indicated in ellipses with white background and are adenine nucleotide uniporter (Brittle1, BT1), nucleobase transporters (possibly from the nucleobase ascorbate transporter family (NAT) and the purine permease family (PUP) as well as nucleoside transporters (equilibrative nucleoside transporter family, ENT), uric acid transporter (3), and putative allantoin transporter (4). Modified after (Zrenner et al., 2006).

### 1.2.2 Purine salvage

In addition to purine biosynthesis, plants employ another strategy, the salvage pathway, to directly convert nucleobases and nucleosides to nucleotides by recruiting phosphoribosyltransferases and nucleoside kinases. Radioisotope labeling experiments have been used as a primary tool to study the purine salvage pathway by tracking the proportion of isotopically-labeled purine bases or nucleosides in salvage products, such as nucleotides and nucleic acids (Ashihara et al., 2018). However, this method can only be used to study nucleobase and nucleoside salvage since the plant cell does not take up nucleotides (Girke et al., 2014).

Adenine phosphoribosyltransferase (APRT; Figure 2) converts adenine to AMP and has five isoforms in Arabidopsis (Moffatt and Ashihara, 2002; Ashihara et al., 2018). Hypoxanthine and guanine are reutilized by hypoxanthine guanine phosphoribosyltransferase (HGPRT; Figure 2), resulting in the formation of IMP and GMP. In Arabidopsis, the loss-of-function of *HGPRT* results in a significant accumulation of guanine but not hypoxanthine, indicating that HGPRT is mainly necessary for guanine salvage *in vivo* (Schroeder et al., 2018). In contrast to adenine or hypoxanthine, xanthine is not salvaged in Arabidopsis (Yin et al., 2014).

To salvage nucleosides, plants have several nucleoside kinases that form nucleoside monophosphates. There are two cytosolic adenosine kinases (ADK; Figure 2) that phosphorylate adenosine to AMP (Moffatt et al., 2000). ADKs are especially important for adenosine metabolism since adenosine hydrolase or adenosine deaminase have not been found in plants (Witte and Herde, 2020). In Arabidopsis, silencing the adenosine kinase 1 gene (At3g09820) results in the accumulation of adenosine (Lee et al., 2012) and leads to severe growth retardation phenotype (Schoor et al., 2011). Moreover, adenosine kinase is speculated to phosphorylate 5-aminoimidazole-4-carboxamide ribonucleoside (AICAr), producing 5-aminoimidazole-4-carboxamide ribonucleotide (AICAR) which is not only an intermediate of *de novo* purine synthesis but involved in the regulation of the expression of adenine phosphoribosyltransferase (APRT) gene in yeast (Daignan-Fornier and Pinson, 2012; Ceschin et al., 2015). Presumably, plants possess an inosine/guanosine kinase (3; Figure 2), which phosphorylates inosine and guanosine to IMP and GMP; because labeled products were detected when radioactive inosine and guanosine were supplied externally (Ashihara et al., 2018). Remarkably, xanthosine cannot be salvaged to XMP in Arabidopsis (Yin et al., 2014).

The purine salvage pathway is indispensable for plants because some purine bases and nucleosides may be toxic for plant growth (Schroeder et al., 2018; Chen and Witte, 2020). In

addition, the purine salvage pathway consumes less energy and forms nucleotides in a simpler process compared to that of *de novo* synthesis. The compromised adenine and adenosine salvage pathways lead to severe phenotypes. For instance, in Arabidopsis, the *APRT* mutant resulted in male infertility (Gaillard et al., 1998), and the *ADK* mutants manifested growth abnormalities (Moffatt and Ashihara, 2002).

### 1.2.3 Purine catabolism

Contrary to being salvaged, purines can also be completely catabolized in plants. For adenine and adenosine degradation, the compounds must initially be salvaged to AMP, which is subsequently converted to IMP by AMP deaminase (AMPD; Figure 2), as plants lack adenosine deaminase (Dancer et al., 1997). Likewise, guanine must first be salvaged by HGPRT to GMP for degradation (Baccolini and Witte, 2019).

In addition, IMP may be dephosphorylated by the complex of nucleoside hydrolase 1 and nucleoside hydrolase 2 (NSH1 and NSH2; Figure 2) to inosine, which can be further dehydrogenated by xanthine dehydrogenase (XDH; Figure 2) to hypoxanthine, but this route has little contribution for purine catabolism (Baccolini and Witte, 2019). On the contrary, IMP - XMP - GMP - guanosine - xanthosine is the major route of purine catabolism (Dahncke and Witte, 2013; Baccolini and Witte, 2019). Xanthosine is the first common intermediate, mostly from guanosine deamination mediated by guanosine deaminase (GSDA; Figure 2), but also from XMP dephosphorylation catalyzed by XMP phosphatase (XMPP; Figure 2) (Heinemann et al., 2021). Furthermore, xanthosine is hydrolyzed by the NSH1-NSH2 complex, and hypoxanthine is oxidized by xanthine dehydrogenase (XDH; Figure 2), to xanthine. Xanthine is then oxidized by XDH to uric acid, which is transported into the peroxisomes and further oxidized and hydrolyzed to allantoin. The hydrolysis of allantoin in the endoplasmic reticulum (ER) finalizes the complete degradation of the purine ring, leading to the release of ammonia, glyoxylate, and carbon dioxide (Werner and Witte, 2011).

### 1.3 Pyrimidine metabolism in plants

#### 1.3.1 Pyrimidine *de novo* synthesis

The process begins with the condensation of carbamoylphosphate and aspartate catalyzed by aspartate transcarbamoylase (ATCase; Figure 3) which is located in the plastid. Subsequently, carbamoylaspartate is transported to the cytosol and cyclized by dihydroorotase (DHOase; Figure 3) to form dihydro-orotate. The next enzyme, dihydroorotate dehydrogenase (DHODH; Figure 3) is likely located in the intermembrane space of mitochondria, where dihydro-orotate is oxidized to orotate. Orotate is then transported to the cytosol and condensed with PRPP by orotate phosphoribosyltransferase (OPRTase; Figure 3) to orotidine 5'-monophosphate (OMP), which can be further converted to uridine monophosphate (UMP) by UMP synthase (UMPS; Figure 3). In the synthesis of cytidine phosphate (CTP), the phosphorylation of UMP to uridine triphosphate (UTP) must occur, and UTP is aminated to CTP by CTP synthetase (CTPS; Figure 3).

#### 1.3.2 Pyrimidine salvage

Similar to purine salvage, pyrimidine bases and nucleosides can also be salvaged to pyrimidine nucleotides. Uracil can be salvaged by uracil phosphoribosyltransferase (UPRT; Figure 3) in plastids (Mainguet et al., 2009), while the salvage route of cytosine remains unknown. The nucleosides uridine and cytidine are salvaged by uridine-cytidine kinase (UCK; Figure 3) to form UMP and cytidine monophosphate (CMP), which can be further phosphorylated to uridine diphosphate (UDP) and cytidine diphosphate (CDP). UCK plays a crucial role in the pyrimidine salvage pathway. Arabidopsis encodes five UCKs which all contain a uridine kinase (UK) domain and a UPRT domain, but have no UPRT activity (unpublished laboratory data, M. Chen and C-P Witte). UCK1 (At5g40870) and UCK2 (At3g27190) have been reported to be localized in the plastid (Chen and Thelen, 2011). However, Ohler et al. (2019) showed that both UCK1 and UCK2 were cytosolic enzymes which were testified in our laboratory (M. Chen and C-P Witte). In addition, the *UCK1 UCK2* double mutant showed a severe vegetative phenotype (Chen and Thelen, 2011). Unpublished data performed by M. Chen and C-P Witte from our laboratory demonstrated that UCK3 (At1g55810) and UCK4 (At4g26510) are cytosolic bifunctional uridine-cytidine kinases, but the knock-out mutant of *UCK3*, *UCK4*, or the *UCK3 UCK4* double mutant showed no effect on either metabolic profiles or physiological

development. Nevertheless, UCK5 (At3g27440) may not be as critical as others since the expression of the UCK5 gene can only be found in the pollen of dicot plants.

### 1.3.3 Pyrimidine degradation

As central intermediates of pyrimidine metabolism, UMP and CMP are degraded by so far unknown UMP CMP phosphatase(s) (2; Figure 3) to form uridine and cytidine, respectively. Cytidine is deaminated to uridine by cytidine deaminase (CDA; Figure 3); subsequently, uridine is hydrolyzed to uracil by NSH1 in the cytosol (Jung et al., 2009). Cytosolic uracil is further transported into plastids by the plastidic nucleobase transporter (PLUTO; Figure 3). Plastidic uracil is then degraded to dihydrouracil by dihydropyrimidine dehydrogenase (DPYD; Figure 3). The next enzyme, dihydropyrimidine hydrolase (DPYH; Figure 3) is located in the endoplasmic reticulum, where dihydrouracil is hydrolyzed to ureidopropionate. Ureidopropionate is further transported to the cytosol and completely degraded to  $\beta$ -alanine, ammonia, and carbon dioxide by  $\beta$ -ureidopropionase ( $\beta$ -UP; Figure 3). In addition,  $\beta$ -alanine is converted to malonate semialdehyde (malonate-SA; Figure 3).

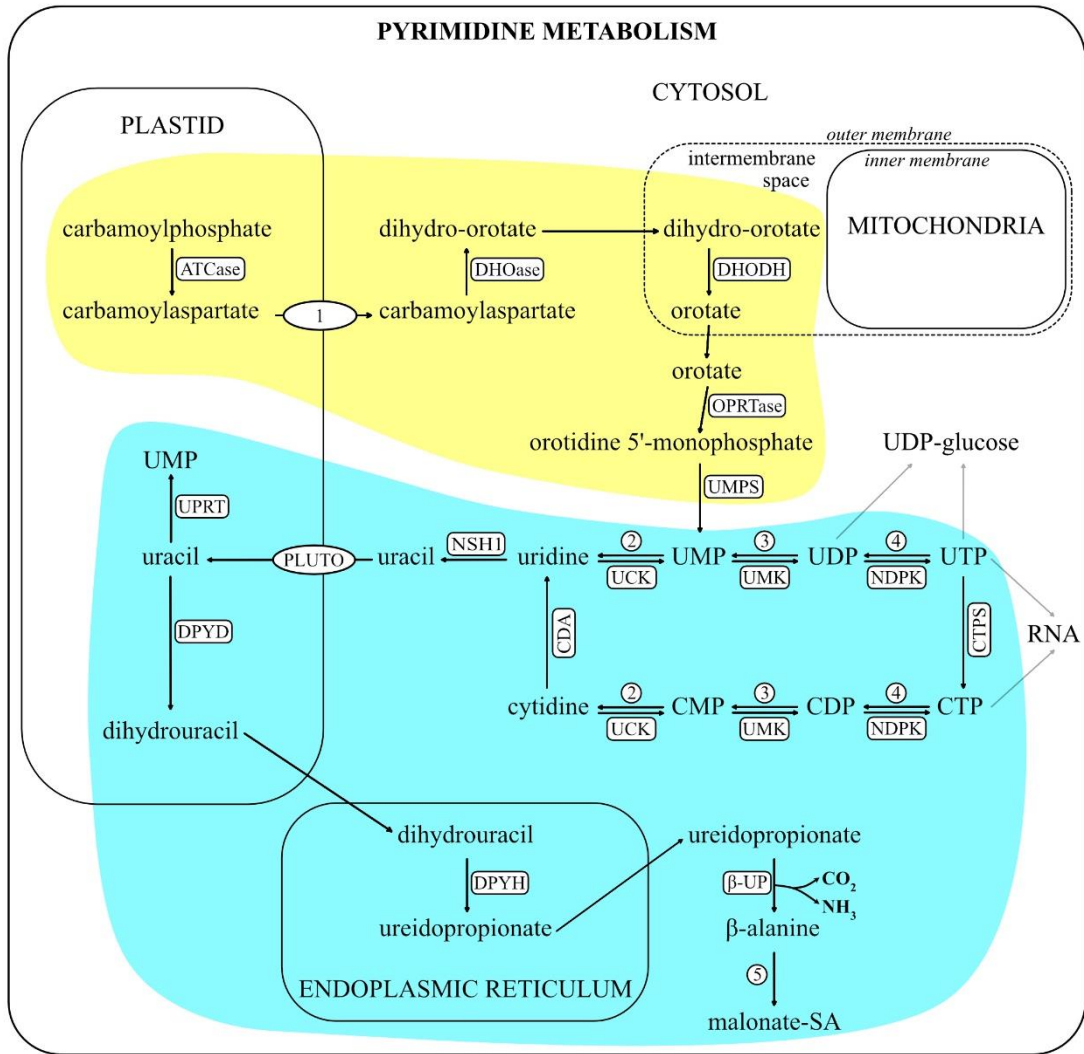


**Figure 3. Scheme of pyrimidine metabolism in Arabidopsis.**

The figure was modified from Zrenner et al. (2006). Pyrimidine *de novo* synthesis is shown in the yellow background, while salvage and degradation are shown in blue. The predicted enzymes are expressed numerically in circles, and the transporters shown in ellipses are putative carbamoyl aspartate transporter (1) and plastidic nucleobase transporter (PLUTO). The enzymes (in boxes with white background) that are involved in pyrimidine metabolism are aspartate transcarbamoylase (ATCase), dihydroorotatase (DHOase), dihydroorotate dehydrogenase (DHODH), orotate phosphoribosyltransferase (OPRTase), UMP synthase (UMPS), UMP kinase (UMK), nucleoside diphosphate kinase (NDPK), CTP synthetase (CTPS), uridine-cytidine kinase (UCK), cytidine deaminase (CDA), putative UMP CMP phosphatase (2), putative UDP CDP phosphatase (3), putative UTP CTP phosphatase (4), nucleoside hydrolase 1 (NSH1), uracil phosphoribosyltransferase (UPRT), dihydropyrimidine dehydrogenase (DPYD), dihydropyrimidine hydrolase (DPYH), β-ureidopropionase (β-UP), and putative β-Ala aminotransferase (5).

## 1.4 PfkB sugar kinases in plants

The phosphofructokinase B-type (PfkB) family is a branch of carbohydrate kinases and is characterized as having an N-terminal glycine rich motif, a C-terminal ATP binding motif (IPR002173), and an NXXE motif (IPR011611) (Guixé and Merino, 2009). A typical PfkB protein has two structural domains, a larger domain composed of a  $\beta$ -sheet between several  $\alpha$ -helices, and a smaller structural domain consisting of another  $\beta$ -sheet which is attached to the large domain by a short loop (Riggs et al., 2017). Through the active site between the two structural domains, PfkB kinases can transfer the phosphate group of ATP from the C-terminal binding domain to the substrate in the closed state of the protein (Riggs et al., 2017). In addition to divalent magnesium, monovalent potassium cations are thought to be cofactors that activate the enzymatic reaction (Andersson and Mowbray, 2002).

In a previous study, a phylogenetic tree (Figure 5) based on the Interpro motif of PfkB sugar kinase (IPR011611) was published (Schroeder et al., 2018). Of all clades in the tree (Figure 5), clade 1 has six subclades (a-f), and some of its subclades (a-d) have fructokinase activity, as described previously by Arsova et al. (2010), while subclades (e, f) have no sugar kinase activity but are involved in chloroplast development (Gilkerson et al., 2012). Enzymes in clade 2 are known as myo-inositol kinases (Kim and Tai, 2011). The Arabidopsis enzyme of clade 3 was characterized and identified as pseudouridine kinase (PUKI), which catalyzes the conversion of pseudouridine to 5'-pseudouridine monophosphate (5'- $\psi$ MP) in the peroxisome (Chen and Witte, 2020). Clade 5 contains ribokinase, mediating the phosphorylation of ribose to ribose-5-phosphate. Ribokinase is involved in ribose recycling from nucleotide catabolism (Riggs et al., 2016; Schroeder et al., 2018). In clade 7, proteins with adenosine kinase activity were identified in Arabidopsis, catalyzing the phosphorylation of adenosine to AMP. ADK1 (At3g09820) and ADK2 (At5g03300) share 89% nucleotide identity (Moffatt et al., 2002). The *ADK1* mutant showed strong development retardation and the *ADK1 ADK2* double mutant is embryo lethal. However, this severe phenotype of *ADK* deficient line may not be directly from the increased adenosine but a result of the impaired synthesis of cytokinin nucleotide, or reduced SAM-dependent methylation led by the adenosine accumulation (Moffatt et al., 2002; Schoor et al., 2011). The protein “necessary for the achievement of RUBISCO accumulation 5” (NARA5) in Arabidopsis in clade 8 was described as important for chloroplast development and the accumulation of chloroplast protein (Ogawa et al., 2009).



Of all 9 clades, the proteins in clades 4, 6, 8, and 9 have unknown functions, while the ADKs in clade 7 may have more functions than those of adenosine kinase. As shown in the right half of Figure 5, the enzymes in clade 3 (PUKI), clade 5 (RBSK), and clade 7 (ADK) are related to nucleotide metabolism. Based on that, we conjectured that some of the proteins of unknown function in the close-by clades may also function in nucleotide metabolism and may have novel nucleoside kinase activities (Figure 4). This idea forms the basis of this study.

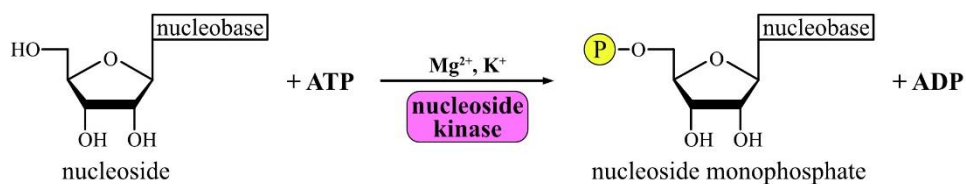


**Figure 4. Scheme of nucleoside kinase activity.**

The letter P in the yellow circle indicates a phosphate group.

The PfkB sugar kinases encoded by At1g06730, At5g43910, At4g28706, At3g09820 (ADK1), At5g03300 (ADK2), At4g27600 (NARA5), and At1g19600 were characterized in this study. In the following, At5g43910 is named kinase 6-1 (K6-1), while At4g28706 is called kinase 6-2 (K6-2), and At1g19600 is referred to as kinase 9 (K9). At1g06730 was identified as plastid inosine kinase (PINK).

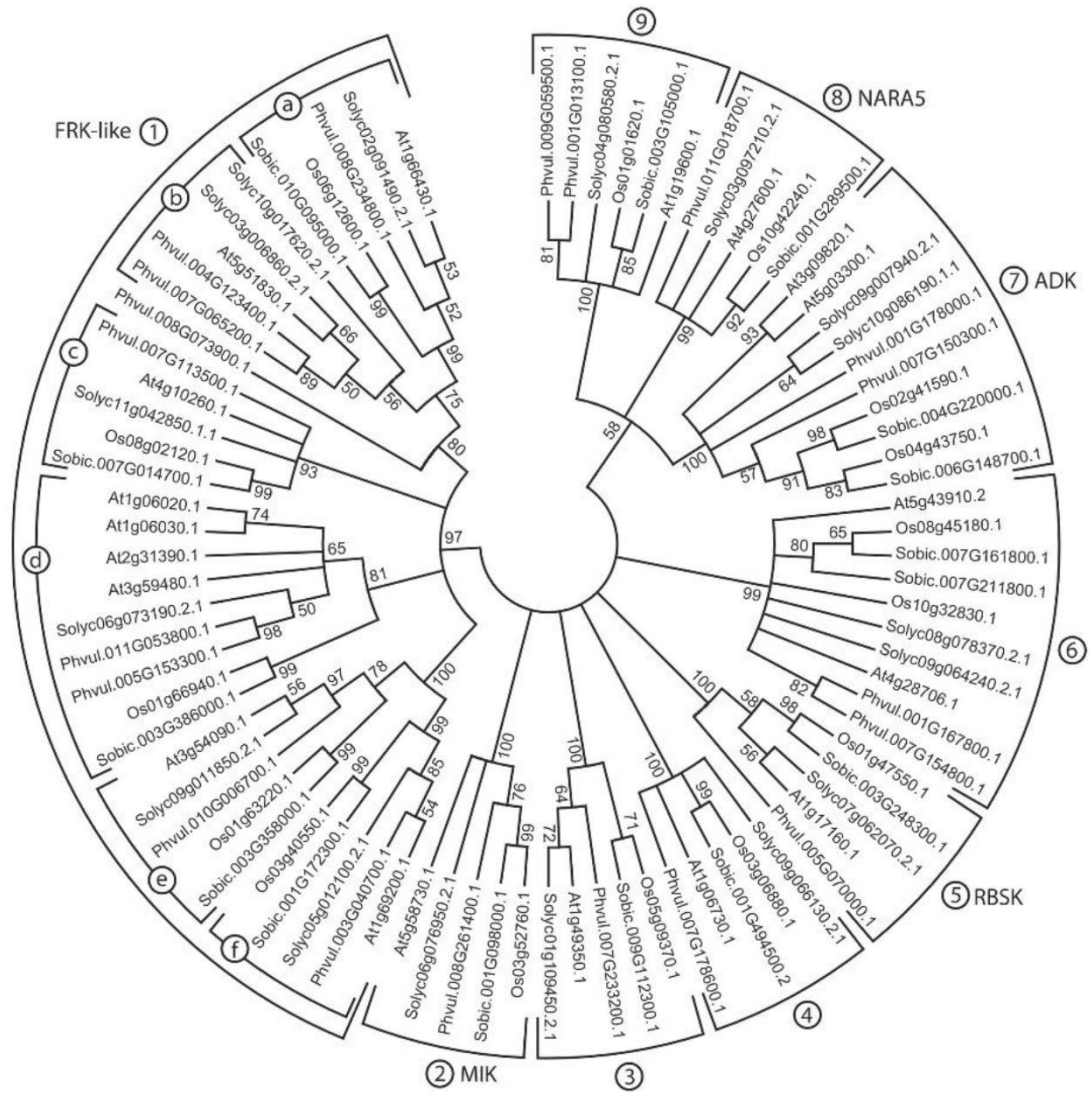


**Figure 5. Phylogenetic analysis of PfkB kinases in plants.**

This tree was reproduced from (Schroeder et al., 2018). To generate the tree, sequences containing the Interpro motif (IPR011611) were aligned from *Arabidopsis thaliana*, *Phaseolus vulgaris*, *Solanum lycopersicum*, *Sorghum bicolor*, and *Oryza sativa*. FRK-like, fructokinase-like; MIK, myo-inositol kinase; RBSK, ribokinase; ADK, adenosine kinase; NARA5, necessary for the achievement of RUBISCO accumulation 5.

### **1.5 Aim of this study**

Although many enzymes involved in nucleotide metabolism of plants have been functionally identified in recent years, for some enzymes, which have been described with their activity, the encoding genes have not yet been found. This study focused on the characterization of phosphofructokinase B-type (PfkB) kinases from *Arabidopsis thaliana*, aiming to identify the biochemically described guanosine and inosine kinase(s) as well as discover novel nucleoside kinases of nucleotide metabolism by using molecular biology, biochemistry, and liquid chromatography coupled with mass spectrometry (LC-MS) technologies.

## 2 Material and Methods

### 2.1 Material

#### 2.1.1 Antibiotics

**Table 2.1-1: Antibiotics.**

Antibiotic	Stock concentration (mg mL <sup>-1</sup> )	Working concentration (µg mL <sup>-1</sup> )
ampicillin (Amp)	100	100
carbenicillin (Carb)	50	50 in liquid, 75 in plates
gentamycin (Gent)	15	15
kanamycin (Kan)	50	50
rifampicin (Rif)	50 <sup>1</sup>	50

<sup>1</sup>Rif was dissolved in dimethyl sulfoxide (DMSO), while the others were dissolved in H<sub>2</sub>O for stock.

#### 2.1.2 Bacterial strains

**Table 2.1-2: Bacterial strains.**

Species	Strain	Resistance
<i>Agrobacterium tumefaciens</i>	C58C1::pCH322 (Voinnet et al., 2003)	Rif <sup>R</sup>
<i>Agrobacterium tumefaciens</i>	GV3101::pMP90RK (Koncz and Schell, 1986)	Rif <sup>R</sup> in the genome, Gent <sup>R</sup> and Kan <sup>R</sup> on the helper plasmid
<i>Escherichia coli</i>	BL21 (DE3) (Novagen)	-
<i>Escherichia coli</i>	K-12 DH10B (Invitrogen)	-

**2.1.3 Buffers and solutions**

**Table 2.1-3. Buffer for *Nicotiana benthamiana* infiltration.**

<b>Buffer</b>	<b>Composition</b>
Infiltration Buffer	10 mM MgCl <sub>2</sub> , 150 μM acetosyringone, 10 mM MES (pH 5.6, adjusted with KOH).

**Table 2.1-4. Buffers for Strep tagged protein extraction and purification.**

<b>Buffer</b>	<b>Composition</b>
Extraction Buffer	100 mM HEPES pH 8, 100 mM NaCl, 5 mM EDTA, 10 mM DTT, 0.005% (w/v) TritonX 100, 100 μg mL <sup>-1</sup> avidin
Washing Buffer	100 mM HEPES pH 8, 100 mM NaCl, 0.5 mM EDTA, 2 mM DTT, 0.005% (w/v) TritonX 100
Elution Buffer	100 mM HEPES pH 8, 100 mM NaCl, 0.5 mM EDTA, 2 mM DTT, 0.005% (w/v) TritonX 100, 10 mM biotin

**Table 2.1-5. Buffers associated with SDS polyacrylamide gel.**

<b>Buffer</b>	<b>Composition</b>
Resolving Gel	10% (w/v) acrylamide: bis-acrylamide (37.5 : 1), 0.1% (w/v) SDS, 375 mM Tris-HCl pH 8.8, 0.075% (w/v) APS, 0.05% (w/v) TEMED
Stacking Gel	4% (w/v) acrylamide: bis-acrylamide (37.5 : 1), 0.1% (w/v) SDS, 125 mM Tris-HCl pH 6.8, 0.1% (w/v) APS, 0.1% (w/v) TEMED
5 × SDS Loading Buffer	10% (w/v) SDS, 500 mM DTT, 300 mM Tris-HCl pH 6.8, 50% (v/v) glycerol, 0.2% bromophenol blue
SDS-PAGE Running Buffer	0.1% (w/v) SDS, 25 mM Tris-HCl, 192 mM glycine

MATERIAL AND METHODS

**Table 2.1-6. Solutions for the colloidal Coomassie stain in SDS-PAGE.**

Buffer	Composition
Fixation Solution	10% (v/v) acetic acid, 40% (v/v) ethanol
Colloidal Coomassie Dye Stock	0.1% (w/v) Coomassie Brilliant Blue G-250, 1% (v/v) phosphoric acid, 10% (w/v) ammonium sulfate
Staining Solution	20% (v/v) methanol, 80% (v/v) Colloidal Coomassie dye stock

**Table 2.1-7. Buffers and solutions for immunoblot.**

Buffer	Composition
Blotting Buffer	48 mM Tris-HCl pH 9.2, 0.5 mM SDS, 20% (v/v) methanol, 40 mM glycine
TBS-T Buffer	20 mM Tris-HCl pH 7.6, 150 mM NaCl, 0.1% (v/v) Tween 20
Blocking Solution	5% (w/v) milk powder in TBS-T buffer
AP Buffer	100 mM Tris-HCl pH 9.5, 5 mM MgCl <sub>2</sub> , 100 mM NaCl
BCIP	50 mg mL <sup>-1</sup> in DMF
NBT	50 mg mL <sup>-1</sup> in 70% (v/v) DMF

**Table 2.1-8. Buffers and solutions for kinase assay.**

Buffer	Composition
5 × Kinase Buffer	200 mM Tris-HCl pH 7.5, 10 mM MgCl <sub>2</sub> , 2.5 mM KCl
Termination Solution	1.2 M HClO <sub>4</sub>
Neutralization Solution	5 M KOH, 2 M K <sub>2</sub> CO <sub>3</sub>

**Table 2.1-9. Buffers for HPLC.**

<b>Buffer</b>	<b>Composition<sup>1</sup></b>
Mobile phase A	10 mM ammonium acetate, 5 mM TBA, pH 6.5 adjusted with ammonium hydroxide
Mobile phase B	5 mM TBA in acetonitrile

<sup>1</sup>All chemicals and reagents were HPLC grade.

**Table 2.1-10. Buffers for chromatography with a Polaris 5 C18 column.**

<b>Buffer</b>	<b>Composition<sup>1</sup></b>
Mobile phase A	10 mM ammonium acetate pH 7.5 adjusted with ammonium hydroxide
Mobile phase B	methanol

<sup>1</sup>All chemicals and reagents are LC-MS grade.

**Table 2.1-11. Buffers for chromatography with a Hypercarb column.**

<b>Buffer</b>	<b>Composition<sup>1</sup></b>
Mobile phase A	5 mM ammonium acetate pH 9.5 adjusted with ammonium hydroxide
Mobile phase B	acetonitrile

<sup>1</sup>All chemicals and reagents are LC-MS grade.

**2.1.4 Media**

**Table 2.1-12. Media for bacterial culture.**

<b>Medium</b>	<b>Composition</b>
LB	0.5% (w/v) yeast extract, 1% (w/v) tryptone, 1% (w/v) NaCl, pH 7.0 <sup>1</sup> ; 1.5% (w/v) agar for solid media
YEB	0.1% (w/v) yeast extract, 0.5% (w/v) meat extract, 2 mM MgSO <sub>4</sub> , 0.5% (w/v) pepetone, 0.5% (w/v) sucrose, pH 7.2 <sup>1</sup> ; 1.5% (w/v) agar for solid media

<sup>1</sup>pH adjusted with NaOH.

**Table 2.1-13. Media for plant culture.**

<b>Medium</b>	<b>Composition</b>
Half-strength MS	0.8% (w/v) phytoagar (Duchefa), 2.45 g L <sup>-1</sup> MS salt (Duchefa), pH 5.7 <sup>1</sup>

<sup>1</sup>pH adjusted with KOH.



2.1.5 Plants

**Table 2.1-14. *Arabidopsis thaliana* lines.**

No. <sup>1</sup>	Name	Locus	Ecotype	Lines	Reference
WT	Col-0	-	Col-0	-	-
KO 29	<i>hgprt</i>	At1g71750	Col-0	GK015E03	(Schroeder et al., 2018)
KO 34	<i>nsh1</i>	At2g36310	Col-0	SALK083120	(Jung et al., 2011)
KO 165	<i>pink</i>	At1g06730	Col-0	SALK_040950	-
KO 220	<i>k6-2</i>	At4g28706	Col-0	SALK_050816	-

<sup>1</sup>Laboratory mutant number.

**Table 2.1-15. *Arabidopsis thaliana* crosses.**

No. <sup>1</sup>	Name	Mother line	Father line
C382	<i>pink hgprt</i>	<i>pink</i>	<i>hgprt</i>
C383	<i>pink nsh1</i>	<i>pink</i>	<i>nsh1</i>

<sup>1</sup>Laboratory cross number.

**Table 2.1-16. *Arabidopsis thaliana* complementation lines.**

No. <sup>1</sup>	Name	Gene	Tag	Resistance in plants
H338	<i>pink::PINK</i>	Col-0	HA-StrepII	BASTA <sup>R</sup>
H338	<i>pink nsh1::C</i>	Col-0	HA-StrepII	BASTA <sup>R</sup>
H338	<i>pink hgprt::C</i>	Col-0	HA-StrepII	BASTA <sup>R</sup>

<sup>1</sup>Laboratory unified clone number.

2.1.6 Primers

Table 2.1-17. Primers for genotyping.

No. <sup>1</sup>	Description	Sequence
448	Left border primer to screen Gabi-Kat lines	ATATTGACCATCATACTCATT GC
1033	Forward primer to amplify <i>actin2</i>	GTGAACGATTCCTGGACCTGC
1034	Reverse primer to amplify <i>actin2</i>	GAGAGGTTACATGTTACCA CAAC
1905	Forward primer to screen <i>nsh1</i> SALK insertion lines	TTCCATGGATTGTGGTATGGA GAATTG
2616	Reverse primer to screen <i>nsh1</i> SALK insertion lines	AAGAGAGACATCTCCTAGTC CG
2023	Forward primer to screen <i>hgp1</i> Gabi-Kat insertion lines	CAATCAGGCAGCTAAGTGTA TTG
2025	Reverse primer to screen <i>hgp1</i> Gabi-Kat insertion lines	GCAATTCCAAATTATTTTGTA CCG
N61	The left border of T-DNA to screen SALK insertion lines	TGGTTCACGTAGTGGGCCATC
P868	Forward primer to screen <i>pink</i> SALK insertion lines	CTGATGAGCGTAGAGCACTT GC
P869	Reverse primer to screen <i>pink</i> SALK insertion lines	CCTTCACACAACACCTCCC
P1807	Forward primer to screen <i>k6-2</i> SALK insertion lines	GTGATCGTGACCTCAGGT
P1808	Reverse primer to screen <i>k6-2</i> SALK insertion lines	GGGTACAAGTCTAGGATCTG
P2849	Forward primer for qRT-PCR of <i>k6-2</i> (At4g28706)	TCATAGGAGCTGTTCTATATG
P2850	Reverse primer for qRT-PCR of <i>k6-2</i> (At4g28706)	CAGAAAGGGTACAAGTCTAG
P2853	Forward primer for genotyping to clone At1g31800	GCTTCGTGATGACTTGATGA

## MATERIAL AND METHODS

---

P2854	Reverse primer for genotyping to clone	TACAAACGAAAACCACAATG
	At1g31800	
P2855	Forward primer for genotyping to clone	CTGAATAGAAGTTGGTAGGA
	At2g31450	
P2856	Reverse primer for genotyping to clone	AATAGCACAAAACCTCACCGT
	At2g31450	
P2857	Forward primer for genotyping to clone	TGATCACGACCGTACAACC
	At3g42057	
P2858	Reverse primer for genotyping to clone	CCGTAGAGGTTGATTCGTGA
	At3g42057	G

---

<sup>1</sup>Laboratory primer number.

**Table 2.1-18. Primers for cloning.**

No. <sup>1</sup>	Description	Sequence
P39	Reverse primer containing XmaI site without stop codon to clone k9 (At1g19600)	TCCCGGGGTTGTGGATGTCAGG AACAG
P708	Forward primer with PstI site to clone k9 (At1g19600)	TCTGCAGAAAATGGTAGCTGAG GCCTTGC
P858	Forward primer with EcoRI site, to clone pink (At1g06730)	TAGAATTCAAAATGTATCACCA CGCTTTTTCCC
P859	Reverse primer containing XmaI site without stop codon to clone pink (At1g06730)	ATCCCGGGAGATGAAGCCTTCA CACAACACC
P1632	Reverse primer containing XmaI site without stop codon to clone k6-1 (At5g43910)	ACCCGGGTGTCCCTAAGAACGT TGCA
P1637	Forward primer with EcoRI site to clone k6-1 (At5g43910)	TGAATTCAAAATGTCATCTTGCT CCGACGAAG
P1633	Reverse primer containing XmaI site without stop codon to clone k6-2 (At4g28706)	ACCCGGGAACCAGAAAGGGTA CAAGTC
P1638	Forward primer with PstI site to clone k6-2 (At4g28706)	TCTGCAGAAAATGCTCTGCTTC ACTCATGTC
P1634	Forward primer with PstI site to clone nara5 (At4g27600)	TCTGCAGAAAATGGCGTTCTCC CTCCTCTCTC
P1635	Reverse primer containing XmaI site without stop codon to nara5 (At4g27600)	ACCCGGGAGACCCAACATCTGT TCGA
P1599	Forward primer with NcoI site to clone adk1 (At3g09820)	TCCATGGCTTCCTCTGATTTCG
P1600	Reverse primer with XmaI site to clone adk1 (At3g09820)	ACCCGGGTAGTTGAAGTCTGG TTTCTCAG
P1639	Forward primer with NcoI site to clone adk2 (At5g03300)	TCCATGGCTTCTTCTTCTAACTA CGATGG
P1606	Reverse primer containing XmaI site without stop codon to clone adk2 (At5g03300)	ACCCGGGTAGTTAAAGTCGGG CT

<sup>1</sup>Laboratory primer number.

2.1.7 Vectors and constructs

Table 2.1-19. Vectors.

Name (No. <sup>1</sup> )	Description	Function
pJET1.2/blunt (-)	AMP <sup>R</sup> , T7 promoter, eco47IR, PlacUV5, Rep (pMB1).	Vector for the cloning and amplification of PCR products.
pET30-CTH (V2)	Kan <sup>R</sup> , T7 promoter, ori f1, ori pBR322, lacI.	Vector containing a His tag for the expression of recombinant proteins in <i>E. coli</i> .
pXCS-YFP (V36)	Amp <sup>R</sup> , BASTA <sup>R</sup> , Carb <sup>R</sup> , p35S, pA35S, ori ColE1, ori RK2, YFP.	Binary vectors for the overexpression of recombinant proteins with C-terminal fused YFP tag in plants.
pXCScpmv-HAStrepII (V69)	Amp <sup>R</sup> , BASTA <sup>R</sup> , Carb <sup>R</sup> , p35S, pA35S, ori ColE1, ori RK2, HA-StrepII, CPMV enhancer.	Binary vectors for the overexpression of recombinant proteins with C-terminal fused HA-StrepII tag in plants.
pXNS2cpmv-StrepII (V90)	Amp <sup>R</sup> , BASTA <sup>R</sup> , Carb <sup>R</sup> , p35S, pA35S, ori ColE1, ori RK2, StrepII, CPMV enhancer.	Binary vectors for the overexpression of recombinant proteins with N-terminal fused StrepII tag in plants.
pXCS-NeonGreen (V165)	Amp <sup>R</sup> , BASTA <sup>R</sup> , Carb <sup>R</sup> , p35S, pA35S, ori ColE1, ori RK2, NeonGreen.	Binary vectors for the overexpression of recombinant proteins with C-terminal fused NeonGreen tag in plants.
pXCScpmv-YFP (V199)	Amp <sup>R</sup> , BASTA <sup>R</sup> , Carb <sup>R</sup> , p35S, pA35S, ori ColE1, ori RK2, YFP, CPMV enhancer.	Binary vectors for the overexpression of recombinant proteins with C-terminal fused YFP tag in plants.

<sup>1</sup>Laboratory vector number.

**Table 2.1-20. Constructs.**

No. <sup>1</sup>	Name (gene)	Vector	Description
H257	Kinase 9 (At1g19600)	V69	Contains the cDNA of kinase 9 and expresses C-terminal HA-StrepII tagged KINASE 9 in plants. Amp <sup>R</sup> in <i>E. coli</i> , Carb <sup>R</sup> in <i>A. tumefaciens</i> , and BASTA <sup>R</sup> in <i>planta</i> .
H338	PINK (At1g06730)	V69	Contains the cDNA of pink and expresses C-terminal HA-StrepII tagged PINK in plants. Amp <sup>R</sup> in <i>E. coli</i> , Carb <sup>R</sup> in <i>A. tumefaciens</i> , and BASTA <sup>R</sup> in <i>planta</i> .
H339	PINK (At1g06730)	V36	Contains the cDNA of pink and expresses C-terminal YFP tagged PINK in plants. Amp <sup>R</sup> in <i>E. coli</i> , Carb <sup>R</sup> in <i>A. tumefaciens</i> , and BASTA <sup>R</sup> in <i>planta</i> .
H723	NARA5 (At4g27600)	V69	Contains the genomic DNA of nara5 and expresses C-terminal HA-StrepII tagged NARA5 in plants. Amp <sup>R</sup> in <i>E. coli</i> , Carb <sup>R</sup> in <i>A. tumefaciens</i> , and BASTA <sup>R</sup> in <i>planta</i> .
H728	Kinase 6-1 (At5g43910)	V69	Contains the cDNA of kinase 6-1 and expresses C-terminal HA-StrepII tagged KINASE 6-1 in plants. Amp <sup>R</sup> in <i>E. coli</i> , Carb <sup>R</sup> in <i>A. tumefaciens</i> , and BASTA <sup>R</sup> in <i>planta</i> .
H731	Kinase 6-2 (At4g28706)	V69	Contains the cDNA of kinase 6-2 and expresses C-terminal HA-StrepII tagged KINASE 6-2 in plants. Amp <sup>R</sup> in <i>E. coli</i> , Carb <sup>R</sup> in <i>A. tumefaciens</i> , and BASTA <sup>R</sup> in <i>planta</i> .
H732	ADK1 (At3g09820)	V90	Contains the cDNA of adk1 and expresses N-terminal StrepII tagged ADK1 in plants. Amp <sup>R</sup> in <i>E. coli</i> , Carb <sup>R</sup> in <i>A. tumefaciens</i> , and BASTA <sup>R</sup> in <i>planta</i> .
H735	ADK2 (At5g03300)	V90	Contains the cDNA of adk2 and expresses N-terminal StrepII tagged ADK2 in plants. Amp <sup>R</sup> in <i>E. coli</i> , Carb <sup>R</sup> in <i>A. tumefaciens</i> , and BASTA <sup>R</sup> in <i>planta</i> .
H835	Kinase 6-2 (At4g28706)	V165	Contains the cDNA of kinase 6-2 and expresses C-terminal NeonGreen tagged KINASE 6-2 in plants. Amp <sup>R</sup> in <i>E. coli</i> , Carb <sup>R</sup> in <i>A. tumefaciens</i> , and BASTA <sup>R</sup> in <i>planta</i> .
H847	PINK (At1g06730)	V2	Contains the cDNA of pink and expresses PINK without a tag. Sequences of His tag were cut out by EcoRI and XhoI. Kan <sup>R</sup> in <i>E. coli</i> .

<sup>1</sup>Laboratory unified clone number.

**2.1.8 Substrate candidates for kinase assay****Table 2.1-21. Substrate candidates.**

No. <sup>1</sup>	Substrate
1	adenosine
2	AICAr
3	guanosine
4	cytidine
5	xanthosine
6	uridine
7	inosine
8	thymidine
9	2'-AMP
10	3'-AMP
11	5'-AMP
12	2'-deoxyxanthosine
13	2'-deoxycytidine
14	2'-deoxyadenosine
15	2'-deoxyguanosine
16	2'-deoxyinosine
17	2'-deoxyuridine
18	N <sup>1</sup> -methyladenosine
19	N <sup>6</sup> -methyladenosine

<sup>1</sup>Substrate screen number.

### 2.1.9 Software and databases

Software and Webtools:

Agilent MassHunter Qualitative Analysis: <https://www.agilent.com/>

Affinity Designer and Affinity Photo: <https://affinity.serif.com/de/>

BLAST: <https://blast.ncbi.nlm.nih.gov/Blast.cgi>

BoxShade: [https://embnet.vital-it.ch/software/BOX\\_form.html](https://embnet.vital-it.ch/software/BOX_form.html)

Endnote: <https://www.endnote.com/>

Genevestigator: <https://genevestigator.com/>

Graphpad: <https://www.graphpad.com/>

ImageJ: <https://imagej.nih.gov/ij/>

InterProScan: <https://www.ebi.ac.uk/interpro/>

Leica LAS X: <https://www.leica-microsystems.com/>

MEGA X: <https://www.megasoftware.net/>

Multiple Primer Analyzer: <https://www.thermofisher.com/de/de/home/brands/thermo-scientific/molecular-biology/molecular-biology-learning-center/molecular-biology-resource-library/thermo-scientific-web-tools/multiple-primer-analyzer.html>

MUSCLE (Multiple Sequence Alignment): <https://www.ebi.ac.uk/Tools/msa/muscle/>

Rstudio: <https://www.rstudio.com/>

Vector NTI: <https://www.thermofisher.com/de/de/home/life-science/cloning/vector-nti-software.html>

Databases:

Arabidopsis eFP browser:

[http://bar.utoronto.ca/efp2/Arabidopsis/Arabidopsis\\_eFPBrowser2.html](http://bar.utoronto.ca/efp2/Arabidopsis/Arabidopsis_eFPBrowser2.html)

Phytozome: <https://phytozome-next.jgi.doe.gov/>

TAIR: <https://www.arabidopsis.org/>

T-DNA Express: [http://signal.salk.edu/cgi-](http://signal.salk.edu/cgi-bin/tdnaexpress?LOCATION=17669013&CHROMOSOME=chr5&INTERVAL=)

[bin/tdnaexpress?LOCATION=17669013&CHROMOSOME=chr5&INTERVAL=](http://signal.salk.edu/cgi-bin/tdnaexpress?LOCATION=17669013&CHROMOSOME=chr5&INTERVAL=)  
[5](http://signal.salk.edu/cgi-bin/tdnaexpress?LOCATION=17669013&CHROMOSOME=chr5&INTERVAL=)



## 2.2 Methods

### 2.2.1 Plants

#### 2.2.1.1 Growth of *Arabidopsis thaliana*

For *Arabidopsis* cultivation, the seeds were sterilized in 70% ethanol for 10 min. After being completely dried on a clean bench, the seeds were sown on soil (Type 0 Nullerde) or half-strength MS plates (Table 2.1-13). After sowing, the seeds were incubated in the dark at 4°C for 48 h to synchronize the germination. Afterwards, the seeds were transferred to the growth chamber set to long-day conditions (16 h light of 85  $\mu\text{mol m}^{-2} \text{s}^{-1}$ , 22°C / 8 h dark, 20°C, 60% relative humidity). Potted plants were fertilized with a solution containing Ferty 3 Mega (0.07%, [w/v]) every 3 days. For the allopurinol application, 500  $\mu\text{L}$  of a 200  $\mu\text{M}$  allopurinol solution was sprayed onto 10-day-old seedlings grown on plates at the onset of light as described by Ma et al. (2016). The dark treatment was performed as described by Schroeder et al. (2018).

#### 2.2.1.2 Growth of *Nicotiana benthamiana*

*N. benthamiana* cultivation was performed as described by Baccolini and Witte (2019). Potted plants were grown under long-day conditions in the chamber. Five-week-old plants were used for the *Agrobacterium tumefaciens* infiltration to express the recombinant proteins.

#### 2.2.1.3 Stable transformation of *Arabidopsis*

The floral dipping method described by Clough and Bent (1998) was used for the stable transformation of *Arabidopsis*. Briefly, an *Agrobacterium* glycerol stock at -80°C was activated on a YEB plate, the bacteria were proliferated in a YEB liquid culture, and re-suspended in a 5% (w/v) sucrose solution to an OD value of 0.5. Six-week-old *Arabidopsis* plants were transformed by dipping the flowers in the resuspension solution of *A. tumefaciens* for 2 min, and two dips were performed in total. Subsequently, the offspring seedlings were selected by glufosinate ammonium (BASTA) application.

### 2.2.2 Microbiology

#### 2.2.2.1 Bacterial cultures

YEB medium (Table 2.1-12) was utilized to cultivate *Agrobacterium tumefaciens* GV3101::pMP90RK. Kanamycin, rifampicin, and gentamicin (Table 2.1-1) were used to screen the GV3101::pMP90RK strain, while carbenicillin (Table 2.1-1) was added to the media to select the strains that had successfully transformed the constructs. Agrobacteria were first grown on a YEP plate (with four antibiotics) for two days and inoculated into liquid YEB cultures (four antibiotics included). Liquid cultures were incubated at 28°C with shaking at 180 rpm for 12 to 16 hours (Witte et al., 2004).

*Escherichia coli* cultures were grown in LB media (Table 2.1-12) with appropriate antibiotics, which were determined by the binary vector (Table 2.1-19). The liquid cultures were incubated overnight at 37°C with shaking at 200 rpm. The LB plates with *E. coli* cultures were incubated upside down at 37°C overnight. Both *A. tumefaciens* and *E. coli* were stored in 25% (v/v) glycerol and frozen at -80°C.

#### 2.2.2.2 Transformation

Chemo-competent cells of *E. coli* strain DH10B (which were homemade) were employed for transformations to amplify plasmids. Fifty nanograms of ice-cold plasmid or ligation product were added to 50 µL DH10B competent cells and placed on ice for 10 min. The mixture was placed in a water bath at 45°C for 45 s and then chilled on ice immediately for 3 min. After adding 500 µL of LB liquid media, the transformed *E. coli* DH10B cells were cultured with shaking for 1 h at 37°C and 200 rpm in an incubator with a rotating platform. Afterwards, 100 µL of *E. coli* cultures were applied to LB solid media in which suitable antibiotics had been incorporated and were incubated upside down overnight in a 37°C incubator.

For the transformation of *A. tumefaciens*, approximately 200 ng of plasmids were added to 50 µL of GV3101::pMP90RK competent cells. The mixture was transferred to an ice-cold electroporation cuvette and electroporated. Agrobacteria cells were added to 500 µL of YEB liquid media and incubated at 28°C with shaking at 180 rpm for 1 h. 10 µL of the cultures were applied to YEB solid media that contained four antibiotics (Kan, Rif, Gent, and Carb) and were incubated upside down for 48 h at 28°C.

### 2.2.3 Molecular biology

#### 2.2.3.1 Nucleic acid extraction and cDNA synthesis

Genomic DNA extraction from *Arabidopsis* was performed as described by Edwards et al. (1991). At room temperature, fresh leaves were collected and ground with 200  $\mu$ L DNA extraction buffer (200 mM Tris-HCl pH 7.5, 200 mM NaCl, 25 mM EDTA) using a Retch Mill. The samples were centrifuged at 13,000g for 3 min after 10  $\mu$ L 10% SDS was added. Afterwards, 75  $\mu$ L of isopropanol was added to 100  $\mu$ L supernatant and incubated for 2 min. The supernatant was discarded after centrifugation for 10 min at 13,000g, and the pellet was washed by centrifugal cleaning with 70% ethanol. DNA was finally dried and re-suspended in 100  $\mu$ L of Milli-Q H<sub>2</sub>O and used directly for PCR.

RNA extraction of *Arabidopsis* was performed with the NucleoSpin<sup>®</sup> RNA Plant (MACHEREY-NAGEL) kit. Briefly, seedlings with a fresh weight of 100 mg were harvested and rapidly frozen in liquid nitrogen. Complete denaturation was performed with the solution containing chaotropic ions. The lysis buffer inactivated RNases directly, and RNA was subsequently bound to the silica membrane. DNA was then fully digested by the following incubation with rDNase solution. After two rounds of washing, salts and metabolites were removed. Pure RNA was eluted with ribonuclease free (RNase-free) H<sub>2</sub>O. Given that RNase, which degrades RNA, is present in almost all biological materials, the relevant reagents and consumables should be RNase-free. All described procedures were performed at 4°C.

For cDNA synthesis, a First Strand cDNA Synthesis Kit (Thermo) was used. 5 mg of purified total RNA were used to synthesize full-length cDNA. Oligo (dT) primer, reaction buffer, dNTP, RNase inhibitor, and transcriptase together with purified total RNA (DNA-free) were mixed to synthesize the cDNA. As with RNA extraction, all reagents and consumables were RNase-free.

#### 2.2.3.2 Gene cloning and manipulation

Genes were cloned with the appropriate restriction recognition sites that were introduced by PCR. For this purpose, Phusion High-Fidelity (HF) DNA polymerase (NEB, 2000 U/mL) was employed. The PCR system was performed as shown in Table 2.2-1, while the PCR program shown in Table 2.2-2 was used. During assembly of the components for PCR, all the chemicals, reagents, and solutions were maintained on ice.

## MATERIAL AND METHODS

**Table 2.2-1. PCR system.**

Component	25 $\mu$ L rxn	50 $\mu$ L rxn	Final conc.
5 $\times$ Phusion buffer	5 $\mu$ L	10 $\mu$ L	1 $\times$
10 mM dNTPs	0.5 $\mu$ L	1 $\mu$ L	200 $\mu$ M
10 $\mu$ M forward primer	1.25 $\mu$ L	2.5 $\mu$ L	0.5 $\mu$ M
10 $\mu$ M reverse primer	1.25 $\mu$ L	2.5 $\mu$ L	0.5 $\mu$ M
Template DNA	variable	variable	approx. 10 ng $\mu$ L <sup>-1</sup>
Phusion DNA polymerase	0.75 $\mu$ L	1.5 $\mu$ L	3% (v/v)
Nuclease-free H <sub>2</sub> O	up to 25 $\mu$ L	up to 50 $\mu$ L	-

**Table 2.2-2. PCR program.**

Step	Temperature	Time
Initial denaturation	98°C	30 s
25-35 Cycles	98°C	10 s
	X <sup>1</sup> °C	30 s
	72°C	30 s
Final extension	72°C	10 min
Hold	4-10°C	-

<sup>1</sup>X (annealing temperature) is determined by the primer melting temperature (T<sub>m</sub>) and was usually set to 5°C below T<sub>m</sub>.

After agarose gel electrophoresis was performed, the PCR products were purified from the gel using NucleoSpin<sup>®</sup> Gel and PCR Clean-up (MACHEREY-NAGEL). To build the constructs for the expression of the genes of interest, NEB restriction enzymes were employed to produce the specific sticky ends, and T4 DNA ligase (NEB) for fragment ligation.

## 2.2.4 Biochemistry

### 2.2.4.1 Antibody preparation

First, the construct H847 (Table 2.1-20) was transformed into BL21 (Table 2.1-2) to express the PINK for rabbit immunization. The production of the protein and the purification of precipitated protein as inclusion body were carried out as previously described by Baccolini and Witte (2019). A single colony of H847-containing *E. coli* was selected on a Kan<sup>R</sup> LB plate and grown in 1.5 L of LB liquid culture to an OD of 0.5. Then, 500  $\mu$ M isopropyl- $\beta$ -Dthiogalactoside (IPTG) was added to the culture to induce protein expression by shaking at 200 rpm at 37°C in an orbital shaker for another 3 hours. *E. coli* cells were pelleted by centrifugation and re-suspended in 80 mL of lysis buffer (0.25% [w/v] sucrose, 1 mM EDTA, 50 mM Tris-HCl pH 8.0). Then, 800 mg of lysozyme were added to the suspension and incubated on ice for 30 min. Ultrasonication was performed on ice to achieve cell disruption in the presence of 200 mL of detergent buffer (1% [w/v] deoxycholic acid, 1% [v/v] nonidet P-40, 200 mM NaCl, 2 mM EDTA, 20 mM Tris-HCl pH 7.5). The pellet was obtained by centrifugation and washed several times using washing buffer (0.5% [v/v] Triton X-100, 1 mM EDTA pH 8.0). The final wash was done with 70% ethanol, and the purified inclusion body was re-suspended in 3 mL of PBS (2.7 mM KCl, 137 mM NaCl, 10 mM Na<sub>2</sub>HPO<sub>4</sub>, 1.8 mM KH<sub>2</sub>PO<sub>4</sub>). Rabbit immunization and antibody purification were performed by immunoGlobe.

### 2.2.4.2 Transient expression in *Nicotiana benthamiana*

Transient protein expression in *N. benthamiana* was performed as described by Werner et al. (2008). Briefly, the Agrobacterium strain C58C1::pCH322 (Table 2.1-2) contains a construct for the expression of the p19 protein of tomato bushy stunt virus, and the Agrobacterium strain GV3101::pMP90RK, that carried the construct of interest, were cultured as described in section 2.2.2.1. The solutions were harvested and re-suspended in infiltration buffer (Table 2.1-3) to an OD of 0.1 and 0.5, respectively. The mixed bacterial solution was infiltrated into six-week-old leaves of *N. benthamiana*. The Agrobacteria-infiltrated leaves of *N. benthamiana* were harvested for protein purification after 3 days of incubation as described previously (section 0). For subcellular localization, the infiltrated *N. benthamiana* plants were incubated for approximately 5 days.

### 2.2.4.3 Protein extraction and purification from planta

Leaves of *N. benthamiana* infiltrated with *A. tumefaciens* were harvested and ground using an ice-cold mortar and pestle in the presence of pre-cooled extraction buffer (Table 2.1-4) (2 mL

per gram of freshly weighed leaf material). The crude extraction was clarified by centrifugation at 20,000g at 4°C for 15 min. The supernatant was transferred to a new 2 mL tube and co-incubated with 40 µL of Streptactin-Macroprep (50% [w/v] slurry, IBA) on a rotating wheel at 4°C for 10 min. After centrifugation at 4°C and 900g for 30 s, the supernatant was discarded, and the pellet was re-suspended in 1 mL of washing buffer (Table 2.1-4). This step was repeated five times to remove unbound compounds. After washing, 75 µL of elution buffer (Table 2.1-4) was added to the pellet, and the mixture was shaken on a thermo shaker at room temperature and 900g for 10 min. The slurry was centrifuged at 900g for 30 s at 4°C, and the supernatant was finally obtained and transferred to a new tube. This step was performed twice to completely elute the Strep-tagged protein. In total, 150 µL of purified protein was obtained and stored at -80°C after being tested for activity.

For protein quantification, Bradford (Serva) was used to quantify the purified protein. BSA solutions of different concentrations served as standards. In general, 10 µL of BSA standards as well as purified protein were loaded into a 384-well plate. 100 µL of Bradford was added to each well that contained BSA standard or extracted protein. After 10 min incubation at room temperature, the calibration curve was obtained by measuring the absorption values of the BSA standards at 595 nm in a plate photometer. The purified protein was quantified using this calibration curve.

#### 2.2.4.4 SDS-PAGE

The purified protein was incubated in SDS solution at 95°C for 10 min before loading. The SDS polyacrylamide (10% resolving gel, 4% stacking gel, Table 2.1-5) was set up in an electrophoresis bath (Rio-Rad). After adding the running buffer (Table 2.1-5), 4 µL of protein ladder and 15 µL of the heat-denatured protein sample were loaded into the slots of the gel. A two-stage electrophoresis procedure was adopted. In the first stage, the apparatus was set to run at 80 volts for 30 minutes, while in the second stage, it was set to run at 120 volts for 1 hour.

#### 2.2.4.5 Colloidal Coomassie stain

After SDS-PAGE, the gel was fixed in fixation solution (Table 2.1-6) by shaking at 25 rpm for 30 min at room temperature, and rinsed two times using Milli-Q H<sub>2</sub>O. Then, 20 mL of staining solution (Table 2.1-6) was added to the gel, and the solutions were incubated from 4 h to overnight with shaking at 25 rpm. Subsequently, the Coomassie-stained gel was washed several times in Milli-Q H<sub>2</sub>O.

### 2.2.4.6 *Immunoblot*

After electrophoresis was performed, the SDS gel was placed on top of a nitrocellulose membrane and this sandwich was placed in the middle of six layers of filter paper soaked in blotting buffer (Table 2.1-7). This assembly was then transferred to a cassette in the Trans-Blot Turbo™ Instrument (Bio-Rad), and the protein was transferred to the nitrocellulose membrane at 25 V for 9 min. Afterwards, the membrane was blocked by incubation with blocking solution (Table 2.1-7) at room temperature for 30 min with shaking at 25 rpm. Two 15 min shaking washes in 25 mL TBS-T (Table 2.1-7) followed, and 2 µL of Anti-Strep-tag 7G8 (Antibody facility iTUBS) together with 10 mL TBS-T was added to the membrane and incubated at room temperature for 1 h with shaking at 25 rpm. After washing twice more in 25 mL of TBS-T, 1 µL of Anti Mouse IgG (whole molecule) conjugated to AP (Sigma) and 10 mL of TBS-T were added to the membrane and incubated for another 1 hour as previously described. The chromogenic reaction was performed after the final washing in TBS-T. 10 mL of AP buffer (Table 2.1-7) containing BCIP and NBT (Table 2.1-7) was added to the membrane and incubated for 10 min at room temperature.

### 2.2.4.7 *Kinase assay and HPLC analysis*

A kinase assay was performed as shown in Table 2.2-3. The reaction was incubated in a 1.5 ml tube at 30°C for 50 minutes. The assay was stopped by adding 25.6 µL of termination solution (Table 2.1-8) followed by a 30 s vortex. A total of 10.4 µL of neutralization solution (Table 2.1-8) was added to neutralize the strong acid, and the solution vortexed for another 30 s. Before loading to the HPLC, high-speed centrifugation at 4°C and 45,000g for 30 min was employed to remove all particles. All chemicals and reagents were HPLC grade.

**Table 2.2-3. Kinase assay system.**

Component	Volume	Final conc.
5 × Kinase Buffer (Table 2.1-8)	10 µL	1 ×
ATP (1 mM)	10 µL	200 µM
Substrate	10 µL	200 µM
Purified protein	10 µL	variable
H <sub>2</sub> O	10 µL	-

HPLC was employed for a qualification analysis of the kinase assay products and the measurements were performed on an Agilent HPLC 1200 system with a Polaris 5 C18 A column (150 × 4.6 mm, Agilent) and detected by a diode array detector (set to 260 nm and 360 nm as detection and reference wavelengths, respectively). 20 µL of sample was injected into the HPLC with a flow rate of 0.65 mL min<sup>-1</sup>. Mobile phase A (Table 2.1-9) was freshly made and filtered by a nylon membrane (47 mm diameter, 0.45 µM pore size). The solvent gradient is shown in Table 2.2-4.

**Table 2.2-4. HPLC solvent gradient.**

Time (min)	Mobile phase A (%)	Mobile phase B (%)	Flow rate	Max. pressure
0.0	95	5	0.65 mL min <sup>-1</sup> <sub>1</sub>	400 bar
2.5	90	10		
4.0	90	10		
6.0	80	20		
12.0	60	40		
15.0	0	100		
20.0	0	100		
20.1	95	5		
25.0	95	5		



2.2.4.8 *Enzyme kinetic constants*

A coupled enzyme assay using pyruvate kinase (PK) and lactate dehydrogenase (LDH) was employed to determine the kinetic constants. ADP and PEP were used by PK to produce ATP and pyruvate, while pyruvate together with NADH was converted to lactate and NAD by LDH. Measurements of the consumption of NADH (detected by its absorbance at 340 nm) indicated the amount of ADP produced in the phosphorylation reaction. It was confirmed that half the amount of the tested enzyme resulted in half the velocity to demonstrate that the assay is not rate-limited by the coupling reaction. The assay was performed as shown in Table 2.2-5. Each reaction in the coupling enzyme assay was placed in a well of a 96-well plate at 22°C and continuously monitored at 340 nm by a photometer.

**Table 2.2-5. Coupled enzyme assay system.**

Component	Stock conc. (mM)	Volume (μL)	Final conc. (mM)
Tris-SO <sub>4</sub> pH 7.5	200	30	40
KCl	1,000	2.5	20
MgCl <sub>2</sub>	200	3	4
PEP	10	30	2
NADH	0.85	30	0.17
Coupled enzyme	Diluted 1:50 in H <sub>2</sub> O	2	3750 times diluted
Tested Enzyme	Variable	15	variable
Substrate	Variable	30	variable
ATP	20	7.5	1

**2.2.5 Metabolite analysis**

Metabolite analysis was accomplished by employing an Agilent HPLC 1200 system (LC) coupled with an Agilent 6460C series triple quadrupole mass spectrometer (MS). For nucleoside measurements, a Polaris 5 C18 column (50 × 4.6 mm, particle size 5 μm, Agilent) was used. The extraction method described by Baccolini and Witte (2019) was used. 50 mg of freshly weighed seedlings, one 7-mm metal bead and five 5-mm metal beads were placed in a 2 mL tube. The sample was rapidly frozen in liquid nitrogen and ground at a frequency of 20

## MATERIAL AND METHODS

Hz for 4 min with an MM400 mill (Retsch). 500  $\mu\text{L}$  of mobile phase A (Table 2.1-10) with internal standards (ISTDs; 0.18  $\text{nmol mL}^{-1}$   $^{13}\text{C5}$ -adenosine, 0.17  $\text{nmol mL}^{-1}$   $^{15}\text{N5}$ -guanosine, 0.73  $\text{nmol mL}^{-1}$   $^{15}\text{N4}$ -inosine, 2  $\text{nmol mL}^{-1}$   $^{15}\text{N2}$ -uridine and 0.65  $\text{nmol mL}^{-1}$   $^{15}\text{N2}$ -xanthine, Cambridge Isotope Laboratories) was added to the tube and incubated for 10 min at 95°C. The sample was chilled on ice and centrifuged at 4°C and 45,000g for 20 min. 20  $\mu\text{L}$  of the supernatant was injected into the LC-MS. The column temperature was set at 25°C, and the solvent gradient was employed as shown in Table 2.2-6. Mobile phase A (Table 2.1-10) was freshly prepared and filtered with a nylon membrane (47 mm diameter, 0.45  $\mu\text{M}$  pore size).

**Table 2.2-6. Solvent gradient on the Polaris 5 C18 column for nucleoside analysis.**

Time (min)	Mobile phase A (%)	Mobile phase B (%)	Flow rate	Max. pressure
0.0	95	5	0.8 $\text{mL min}^{-1}$	400 bar
2.0	95	5		
5.5	85	15		
9.5	15	85		
11.0	15	85		
11.1	95	5		
20.0	95	5		

The nucleotide analysis was performed as described by Straube et al. (2021). Generally, 100 mg of freshly weighed seedlings, one 7-mm bead, and five 5-mm beads were collected in a 2 mL tube. The samples were rapidly frozen in liquid nitrogen and ground at 20 Hz for 4 min with a bead-mill MM400 (Retsch). A 1 mL aliquot of 15% TCA containing ISTDs (1.4  $\text{nmol mL}^{-1}$   $^{15}\text{N5}$ -AMP, 2.7  $\text{nmol mL}^{-1}$   $^{15}\text{N5}$ -GMP, 1.2  $\text{nmol mL}^{-1}$   $^{15}\text{N2}$ -UMP, 4  $\text{nmol mL}^{-1}$   $^{15}\text{N4}$ -IMP, 10  $\text{nmol mL}^{-1}$  ATP and GTP [ribose-3', 4', 5', 5''-D4], 10  $\text{nmol mL}^{-1}$  CTP and UTP [5-D1, ribose-3', 4', 5', 5''-D4], Cambridge Isotope Laboratories) was added to the plant powder and ground again with a mill MM400 at 20 Hz for 2 min. The samples were centrifuged at 30,000g, 4°C for 30 min, and the supernatant (approx. 1 mL) was transferred to 1 mL of DCM/TOA (78/22) solution. The samples were vortexed for 12 s and centrifuged at 5,000g and 4°C for 5 min. The supernatant was mixed with 1 mL  $\text{H}_2\text{O}$  with 0.5% (v/v) acetic acid and passed through a Strata X-AW cartridge that was previously successively equilibrated with 1 mL of methanol, 1 mL of formic acid/methanol/ $\text{H}_2\text{O}$  (2/25/73), and 1 mL of 10 mM ammonium acetate pH 4.5.

After washing with 1 mL of 5 mM ammonium acetate pH 4.5 and 1 mL of methanol, the nucleotides binding to the column were eluted two times with 0.5 mL of ammonia/methanol (20/80). Subsequently, the sample was dried in a vacuum until no liquid was obtained. Before loading, the sample was completely re-suspended in 50  $\mu$ L of 5 mM ammonium acetate pH 9.5/acetonitrile (96/4), and 10  $\mu$ L of the sample was injected into the LC-MS. A Hypercarb column (50  $\times$  4.6 mm, particle size 5  $\mu$ m, Thermo Scientific) was employed for nucleotide separation at 30°C. The solvent gradient was performed as shown in Table 2.2-7. Mobile phase A (Table 2.1-11) was freshly made and filtered with a nylon membrane (47 mm diameter, 0.45  $\mu$ m pore size).

**Table 2.2-7. Solvent gradient on the Hypercarb column for nucleotide analysis.**

Time (min)	Mobile phase A (%)	Mobile phase B (%)	Flow rate	Max. pressure
0.0	96	4	0.60 mL min <sup>-1</sup>	400 bar
10.0	70	30		
10.1	0	100		
11.5	0	100		
11.6	96	4		
20.0	96	4		

### 2.2.6 Bioinformatic analysis

The protein sequences used for bioinformatic analysis were obtained from the Phytozome and NCBI databases. MUSCLE was employed to carry out the Multiple Sequence Alignment. Phylogenetic analysis was performed by Molecular Evolutionary Genetics Analysis X (MEGA X) software using maximum likelihood estimation with 1000 iterations.

### 2.2.7 Statistical analysis

In this work, statistical analyses between two datasets were performed by GraphPad Prism 4 software using unpaired t tests. \*, \*\*, \*\*\*, and \*\*\*\* indicate significant differences at  $P < 0.05$ ,  $P < 0.01$ ,  $P < 0.001$ , and  $P < 0.0001$ , respectively. For multiple datasets, the statistical analyses were carried out as described by Heinemann et al. (2021). R software coupled with RStudio

## MATERIAL AND METHODS

---

and CRAN packages Multcomp and Sandwich were used to perform two-sided Tukey's comparisons. Moreover, the heteroscedasticity of the dataset was considered by the sandwich variance estimator. Different letters represent significant differences at  $P < 0.05$ .

## 3 Results

This chapter comprises three sections. The first section describes the *in vitro* characterization of PfkB kinases, leading to the focus on PINK and K6-2. The second section deals with the identification of PINK, while the third section describes how the function of K6-2 was analyzed.

### 3.1 *In vitro* biochemical analyses of PfkB kinases

The PfkB kinases ADK1 [At3g09820], ADK2 [At5g03300], NARA5 [At4g27600], kinase 6-1 (K6-1) [At5g43910], kinase 6-2 (K6-2) [At4g28706], kinase 9 (K9) [At1g19600], and PINK [At1g06730], (Figure 5) were studied here. Even though ADK1 and ADK2 were characterized as adenosine kinases, they may have other previously undiscovered functions. NARA5 was published as being involved in chloroplast protein accumulation in Arabidopsis, but the biological function is still unknown. Nothing is known about the biochemical and physiological functions of K6-1, K6-2, K9 and PINK. To identify potential substrates, first a biochemical analysis of purified PfkB kinases was conducted.

#### 3.1.1 Cloning, expression, and protein purification of PfkB kinases

To investigate the *in vitro* enzymatic activity, cDNAs of Arabidopsis PfkB kinases were cloned into binary vectors and then transiently expressed in *N. benthamiana* leaves. N-terminally StrepII-tagged ADK1 (construct H732, Table 2.1-20), N-terminally StrepII-tagged ADK2 (construct H735, Table 2.1-20), C-terminally HA-StrepII-tagged NARA5 (construct H723, Table 2.1-20), C-terminally HA-StrepII-tagged K6-1 (construct H728, Table 2.1-20), C-terminally HA-StrepII-tagged K6-2 (construct H731, Table 2.1-20), C-terminally HA-StrepII-tagged K9 (construct H257, Table 2.1-20), and C-terminally HA-StrepII-tagged PINK (construct H338, Table 2.1-20) were purified by Strep affinity chromatography as described in section 2.2.4.3.

After transient expression in *N. benthamiana*, the enzymes were purified, and the purification process was monitored by Coomassie staining and immunoblot after SDS polyacrylamide gel electrophoresis. The following fractions were analyzed: clarified crude extract, extract after incubation with affinity resin, fifth washing solution, elution, and boil off (Figure 6). ADKs (ADK1 and ADK2), K6-1, K6-2, K9 and PINK were successfully obtained with molecular weights in agreement with theoretical ones, 38.0 kDa for ADKs, 40 kDa for K6-1, 43.5 kDa for

## RESULTS

---

K6-2, 37.5 kDa for K9, and 55.4 kDa for PINK. However, NARA5 was barely observed by immunoblot neither in the clarified crude extract nor in the elution fraction, indicating that it was not well expressed, and was also difficult to enrich by purification. Moreover, on immunoblots for ADKs and K6-1, several bands in the higher molecular weight range were observed. When a protein is strongly expressed as in the case of the ADKs, such bands have been observed to be dimers or higher multimers of the protein. Alternatively, such bands could represent high molecular weight interaction partners that were co-purified.

## RESULTS

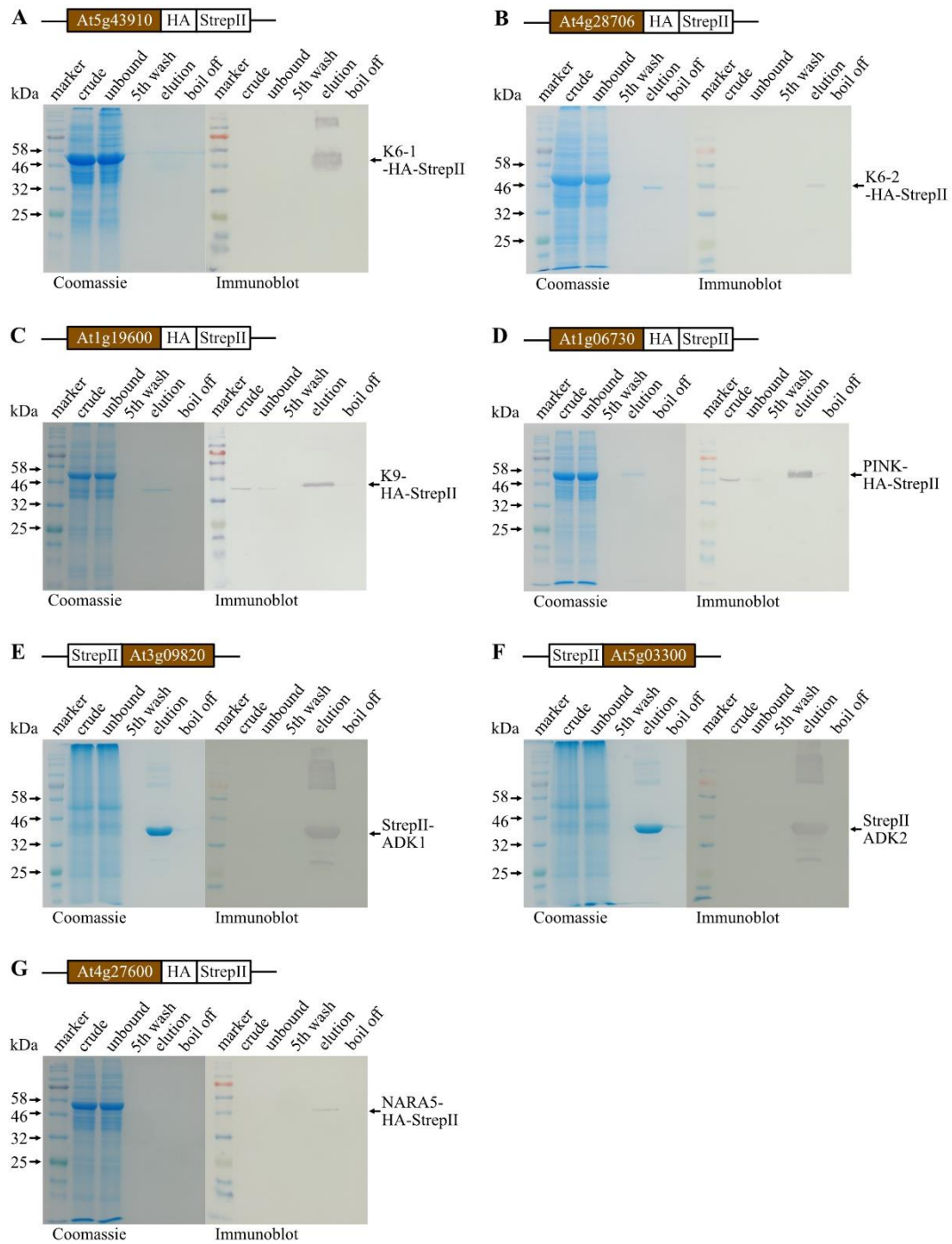


**Figure 6. Affinity purification of Arabidopsis PfkB kinases.**

Coomassie staining and immunoblot of protein fractions from Strep-tactin affinity purification. **(A)** C-terminally HA-StrepII-tagged K6-1. **(B)** C-terminally HA-StrepII-tagged K6-2. **(C)** C-terminally HA-StrepII-tagged K9. **(D)** C-terminally HA-StrepII-tagged PINK. **(E)** N-terminally StrepII-tagged ADK1. **(F)** N-terminally StrepII-tagged ADK2. **(G)** C-terminally HA-StrepII-tagged NARA5. Marker, prestained protein standard; Crude, crude extract of *N. benthamiana* leaves; Unbound, extract after contact with Strep-tactin; 5th wash, fifth washing solution; elution, affinity-eluted protein; boil off, affinity matrix boiled with SDS buffer after elution.

### 3.1.2 Kinase activity screen of PfkB kinases

Putative substrate candidates (Table 2.1-21) were screened in a kinase assay and the reaction was analyzed by reverse phase HPLC with the ion-pairing reagent in the running buffer (section 2.2.4.7). The kinase activity of PfkB kinases from Arabidopsis was determined by the conversion of ATP to ADP, as the two compounds exhibited a stable retention time ( $R_T$ , X-axis) and could be easily separated. The retention time for ADP was approximately 8.3 min compared to 9 min for ATP. The phosphorylation product was another indicator for kinase activity, because this could usually be resolved in the HPLC.

Adenosine kinase 1 (ADK1) and adenosine kinase 2 (ADK2) share the same substrates *in vitro*. In addition to adenosine, they showed kinase activity with AICAr, uridine, inosine, 2'-deoxyadenosine, and N<sup>6</sup>-methyladenosine (Figure 7 and Figure 8). It is not a surprise that they can phosphorylate AICAr because ADKs (ADK1 and ADK2) are proposed to be AICAr kinases in yeast (Daignan-Fornier and Pinson, 2012). In yeast, AICAr was demonstrated to selectively stimulate transcription factor interaction (Rébora et al., 2005; Pinson et al., 2009). However, for plants, such functions have not been shown. In addition, the activities of ADKs, including inosine, uridine, 2'-deoxyadenosine (dA), and N<sup>6</sup>-methyladenosine (m<sup>6</sup>A), suggests that adenosine kinases may be involved in the salvage of these nucleosides.

The kinase K6-2 mediated the phosphorylation of adenosine, AICAr, uridine, inosine, guanosine, and m<sup>6</sup>A to form AMP, AICAR, UMP, IMP, GMP, and m<sup>6</sup>AMP *in vitro* (Figure 9), while another kinase, PINK, was able to phosphorylate AICAr, inosine, and uridine *in vitro* (Figure 10). Unfortunately, of the seven PfkB kinases in Arabidopsis, no activity was found for the substrate candidates of NARA5, K6-1, and K9.



## RESULTS

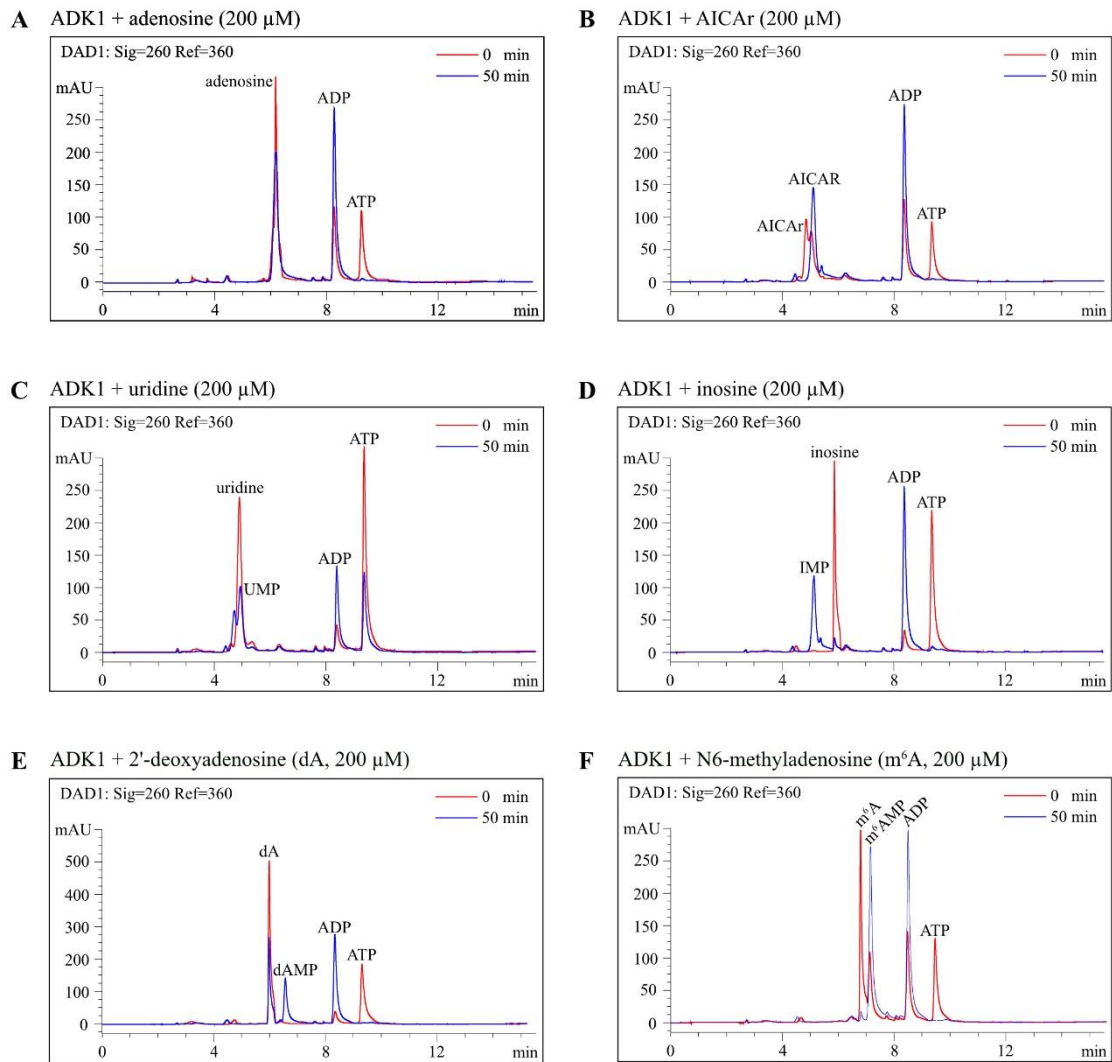


**Figure 7. HPLC analyses of the kinase activity screen for ADK1.**

Kinase assay for ADK1 after 0 min [red curve] and 50 min [blue curve] reaction time, analyzed by HPCL at 260 nm with a 360 nm reference. (A) Absorption of the adenosine-participating kinase assay solutions at 0 min and 50 min. (B) to (F) same as (A) but with different substrates for (B) AICAr, (C) uridine, (D) inosine, (E) 2'-deoxyadenosine, and (F) N<sup>6</sup>-methyladenosine.

## RESULTS

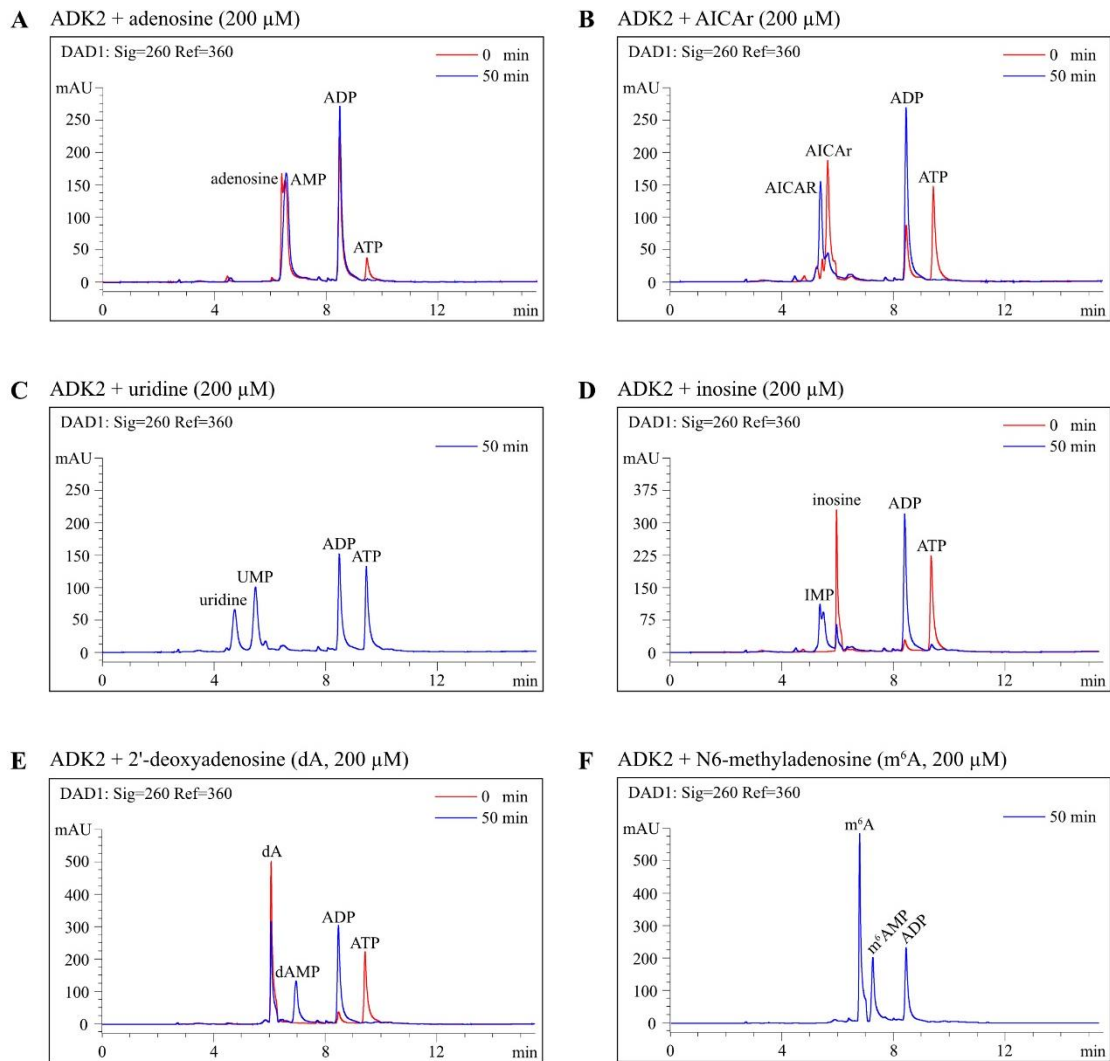


**Figure 8. HPLC analyses of the kinase activity screen for ADK2.**

The ADK2 mediated kinase assay solutions with different reaction times (0 min [red curve], 50 min [blue curve]) were analyzed by HPCL at 260 nm with a 360 nm reference. **(A)** Absorption of the adenosine-participating kinase assay solutions. **(B)** to **(F)** Same as **(A)** but with different substrates for **(B)** AICAr, **(C)** uridine, **(D)** inosine, **(E)** 2'-deoxyadenosine, and **(F)** N<sup>6</sup>-methyladenosine.

## RESULTS

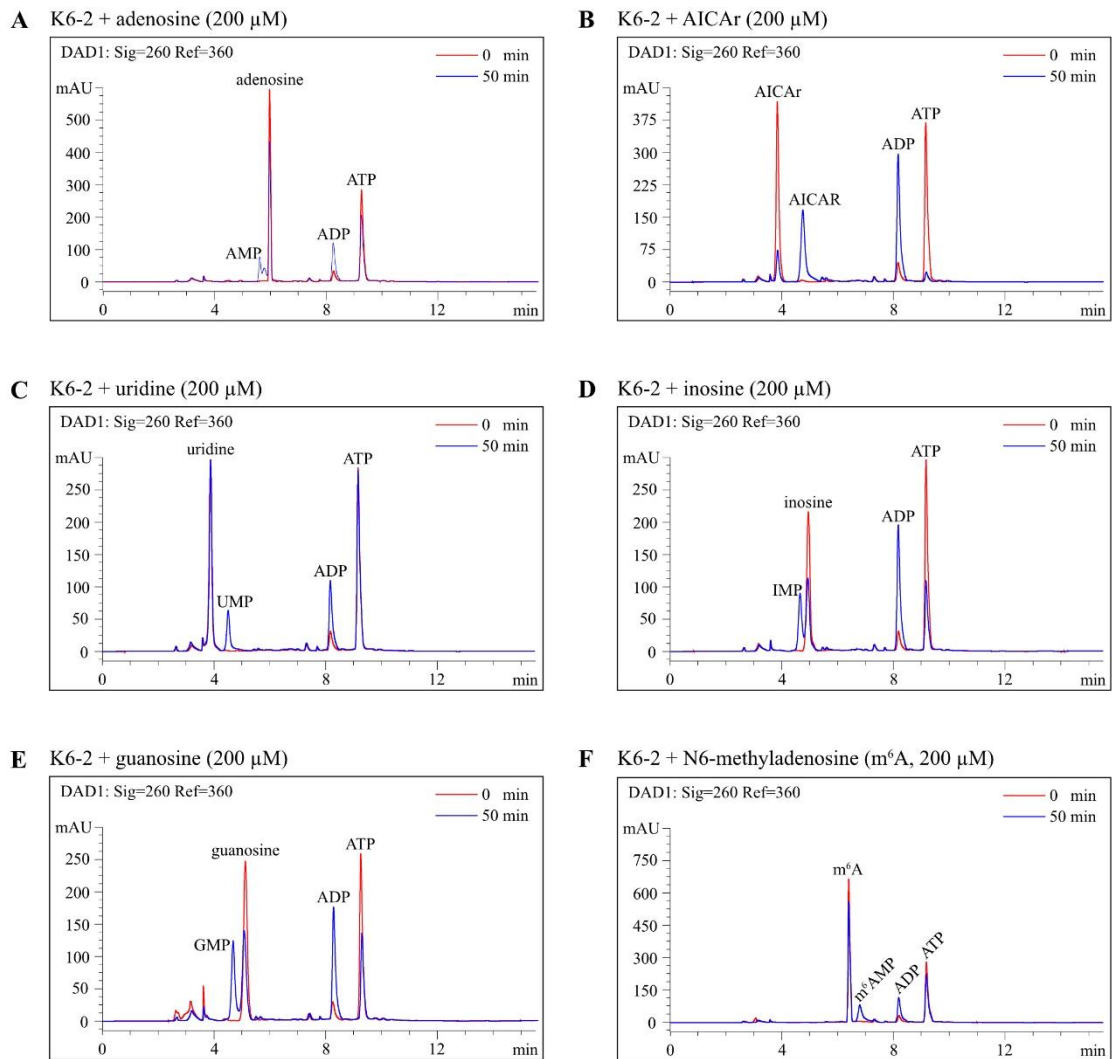


**Figure 9. HPLC analyses of the kinase activity screen for K6-2.**

K6-2 mediated kinase assay solutions of different reaction times (0 min [red curve], 50 min [blue curve]) were analyzed by HPLC at 260 nm with a 360 nm reference. The substrates are (A) adenosine, (B) AICAr, (C) uridine, (D) inosine, (E) guanosine, and (F)  $m^6A$ .

## RESULTS

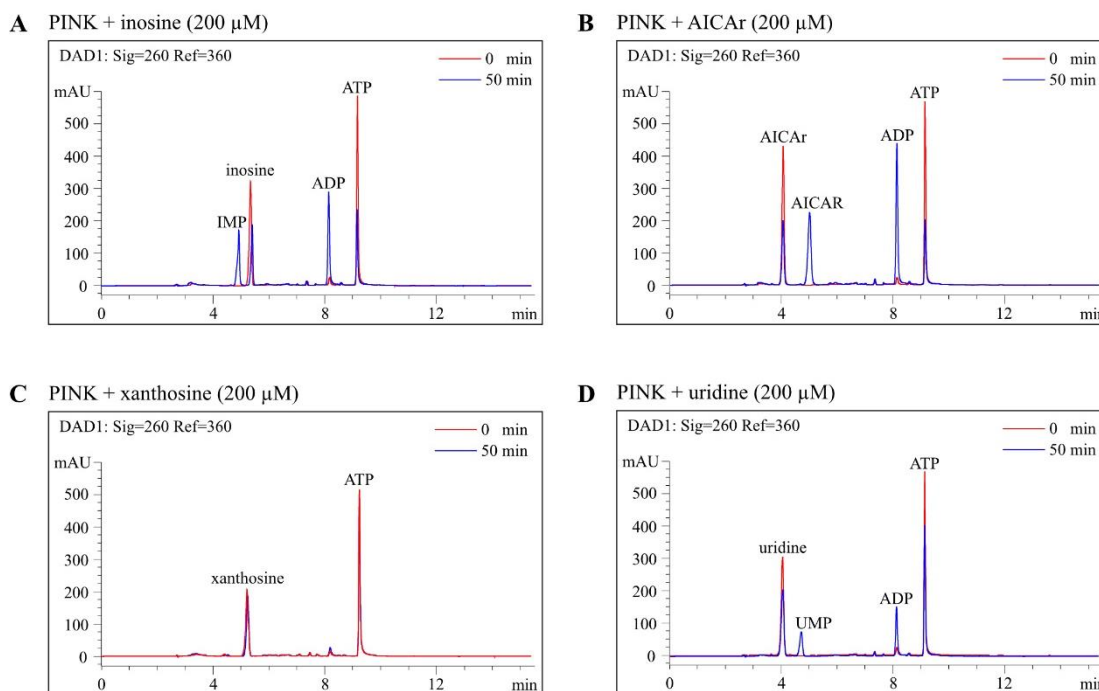


**Figure 10. HPLC analyses of the kinase activity screen for PINK.**

PINK catalyzed kinase assay solutions of different reaction times (0 min [red curves], 50 min [blue curves]) were analysed by HPLC at 260 nm with a 360 nm reference. The substrates shown are (A) inosine, (B) AICAr, (C) guanosine, and (D) uridine.

### 3.1.3 Summary of *in vitro* characterization of PfkB kinases

Of the seven PfkB kinases studied in the substrate screen, kinase activity was observed for adenosine, AICAr, uridine, inosine, 2'-deoxyadenosine, and N<sup>6</sup>-methyladenosine with ADK1 and ADK2 *in vitro*. However, it has already been shown that the ADKs (ADK1 and ADK2) phosphorylate adenosine *in vivo* (Moffatt et al., 2002; Schoor et al., 2011). We decided to focus on the other uncharacterized kinases and therefore not to carry out further research on the ADKs. Additionally, NARA5, K6-1, and K9 were also excluded from further studies, as they had no activity with any of the substrate candidates *in vitro*.

For the uncharacterized kinases PINK and K6-2, nucleoside kinase activity was detected with certain substrates in our screen, which triggered our interest in these kinases. Thus, we focused further analyses on these genes / proteins.

## 3.2 Functional analyses of PINK

Through *in vitro* activity screening, PINK was shown to phosphorylate AICAr, inosine, and uridine (Figure 10). Inosine and uridine are intermediates of purine and pyrimidine metabolism, but it is unknown if AICAr has a function in plants. AIACr is only known as the dephosphorylated version of an intermediate of purine *de novo* biosynthesis. Therefore, it would be interesting to assess if PINK has a biological role as AICAr kinase in Arabidopsis. In addition, investigating whether PINK is an inosine or uridine kinase *in vivo* would be interesting, as this discovery would refine the current model of nucleotide metabolism.

### 3.2.1 Bioinformatic analysis of PINK

PINK was predicted by InterProScan to have a domain of carbohydrate kinase PfkB (IPR011611) (from 122 aa to 404 aa) and be within the ribokinase-like superfamily (IPR029056). To evaluate the conservation of PINK in plants, a phylogenetic tree (Figure 11) based on the protein sequences of certain PfkB kinases from *Arabidopsis thaliana*, *Phaseolus vulgaris*, *Solanum lycopersicum*, *Oryza sativa*, *Sorghum bicolor*, and algae *Chlamydomonas reinhardtii* was constructed (by Claus-Peter Witte) using the MEGA X software. The amino acid sequences were obtained from the Phytozome database and aligned by MUSCLE.

As shown in Figure 11, PINK is present in monocots (*Oryza sativa*, *Sorghum bicolor*), dicots (*Arabidopsis thaliana*, *Phaseolus vulgaris*, and *Solanum lycopersicum*), and the single-cell green algae *Chlamydomonas reinhardtii*, as are the other enzymes of the PfkB kinase family displayed here. PINK sequences of the dicotyledons are more closely related and slightly more distanced from the sequences of the monocyledons, which is not surprisingly also observed in the clade for ADK, PUKI, and RBSK. Overall, the tree shows that PINK is distinct from other PfkB kinases with known nucleoside or ribose substrate, indicating that PINK has a different and conserved function in plants.

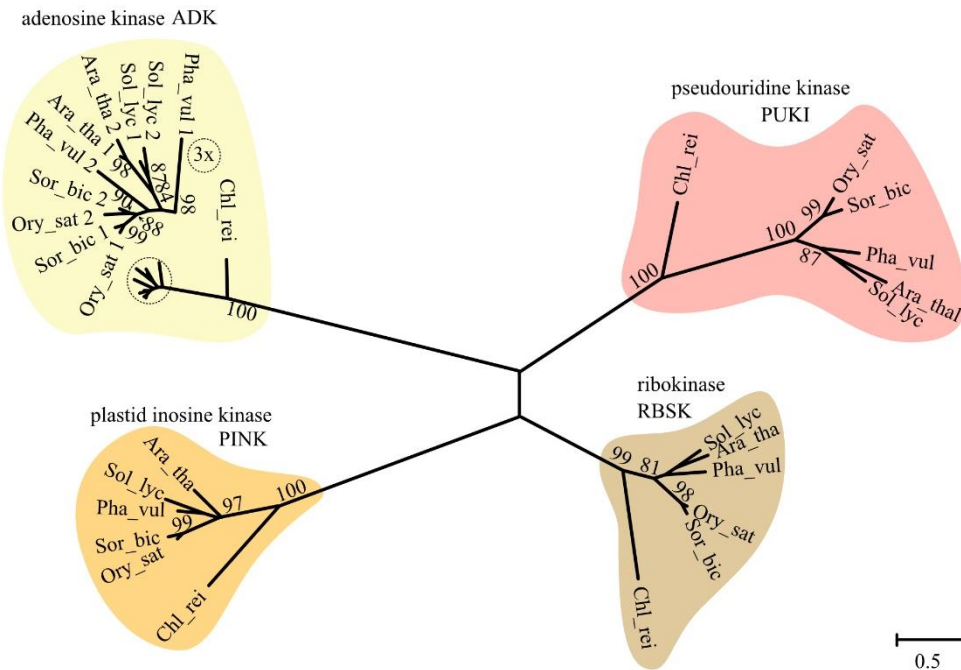


**Figure 11. Phylogenetic analysis of PINK and functionally related PfkB kinases.**

The tree was drawn in MEGA X based on the maximum likelihood method, and the tree with the highest log likelihood (-25233.68) is shown. Only bootstrap values above 80 (1000 iterations) are shown. Ara\_tha, *Arabidopsis thaliana*. Pha\_vul, *Phaseolus vulgaris*. Sol\_lyc, *Solanum lycopersicum*. Ory\_sat, *Oryza sativa*. Sor\_bic, *Sorghum bicolor*. Chl\_rei, *Chlamydomonas reinhardtii*.

### 3.2.2 Subcellular localization of PINK

To investigate the subcellular localization of PINK, a transient expression method in *N. benthamiana* leaves was used (section 2.2.4.2). For this purpose, the cDNA of PINK was cloned into a binary vector (V36; Table 2.1-19), leading to the construct H339 which expresses a C-terminally YFP tagged PINK fusion protein (Table 2.1-20). Three days after infiltration with H339-carrying *Agrobacterium*, the leaves of *N. benthamiana* were collected and analyzed by confocal fluorescence microscopy. Images of three channels (YFP, autofluorescence of chloroplast, and brightfield) were captured (Figure 12).

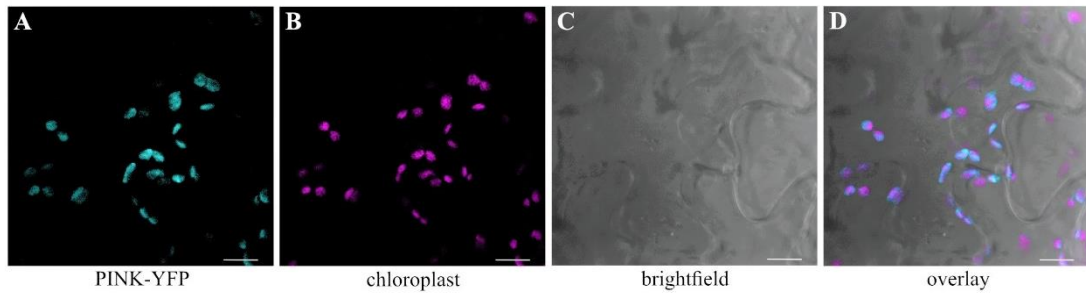


**Figure 12. Subcellular localization of PINK.**

Confocal fluorescence microscopy images of *N. benthamiana* leaves that had transiently expressed PINK-YFP for three days. (A) YFP. (B) Autofluorescence of chloroplasts. (C) Brightfield. (D) Overlay of the three channels. Scale bars = 10 μm.

PINK-YFP (Figure 12 A) and chloroplast autofluorescence (Figure 12 B) were overlapping (Figure 12 D), suggesting that PINK is localized in the chloroplast.

### 3.2.3 Enzyme kinetics of PINK

To further investigate the properties of PINK for the candidate substrates (AICAr, inosine, and uridine), enzyme kinetic analyses (Figure 13) were performed. Initial velocities at various substrate concentrations were determined (as described in section 2.2.4.8) and the data fitted with the Michaelis-Menten equation and a Hanes plot generated.

## RESULTS

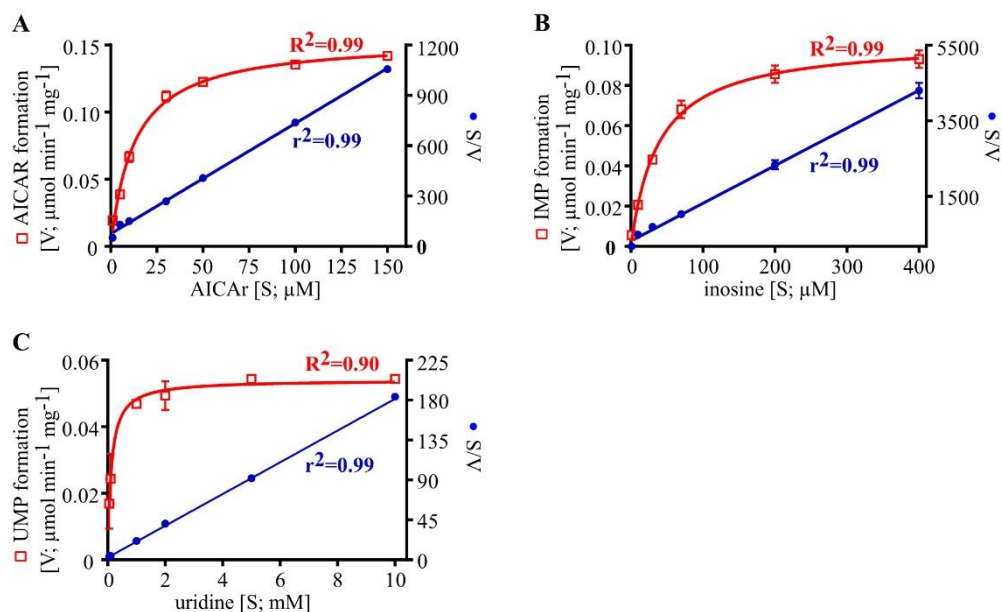


**Figure 13. Kinetic analysis of PINK.**

Determination of the kinetic constants of PINK for (A) AICAr, (B) inosine, and (C) uridine by fitting data with the Michaelis-Menten equation (red curve) and by Hanes plot ( $S/V$ , blue line).  $S$ , substrate concentration;  $V$ , enzymatic velocity. Error bars are SD ( $n = 3$  independent enzymatic reactions).

**Table 3.2-1. Kinetic constants for AICAr, inosine, and uridine of PINK.**

Enzymatic Reaction	$K_m$ ( $\mu\text{M}$ )	$k_{cat}$ ( $\text{s}^{-1}$ )	$k_{cat} / K_m$ ( $\mu\text{M}^{-1} \text{s}^{-1}$ )
PINK, AICAr	$12.83 \pm 0.79$	$0.153 \pm 0.002$	0.0119
PINK, inosine	$38.69 \pm 2.81$	$0.102 \pm 0.002$	0.0026
PINK, uridine	$120.30 \pm 18.53$	$0.054 \pm 0.001$	0.0004

Errors are SD ( $n = 3$  independent enzymatic reactions).

PINK has the lowest  $K_m$  for AICAr, followed by inosine, and the highest for uridine (Table 3.2-1). Moreover, it also shows the highest catalytic efficiency of  $0.0119 \mu\text{M}^{-1} \text{s}^{-1}$  for AICAr, while the next best is  $0.0026 \mu\text{M}^{-1} \text{s}^{-1}$  for inosine and the lowest is  $0.0004 \mu\text{M}^{-1} \text{s}^{-1}$  for uridine (Table 3.2-1), showing that PINK is most active with AICAr, followed by inosine, and is less active with uridine *in vitro*.



### 3.2.4 Characterization of *PINK* variants

To further study the *in vivo* function of PINK, several *Arabidopsis thaliana* lines with varying *PINK* expressions were generated. Homozygotes of the wild type (wt) and *PINK* T-DNA insertion null-mutant (*pink*) were isolated from a segregating mutant population obtained from the Salk T-DNA line collection (Figure 14 B). In addition, knockout mutants of *nsh1* and *hgprt* as described by Baccolini and Witte (2019) were verified, and double mutants of *pink nsh1* and *pink hgprt* were generated by crossing (Figure 14 B). Complementation and overexpression lines were generated in *pink* background (*pink::C*), *pink hgprt* background (*pink hgprt::C*), and *pink nsh1* background (*pink nsh1::C*). A PINK-HA-StrepII expressing transgene as described in section 2.2.1.3 was introduced in these lines, selected by BASTA, and its expression assessed using immunoblot (Figure 14 C).

The PINK gene consists of 2947 base pairs (bps), including a coding region of 1476 base pairs which encode 488 amino acids. In addition, the primer P868 was designed in exon 3, while P869 was designed in exon 5. The T-DNA was inserted in the last exon (E5, Figure 14 A). In addition to PCR, reverse transcription-PCR (RT-PCR) was employed to assess the expression of the intact mRNA of PINK (Figure 14 B).

## RESULTS

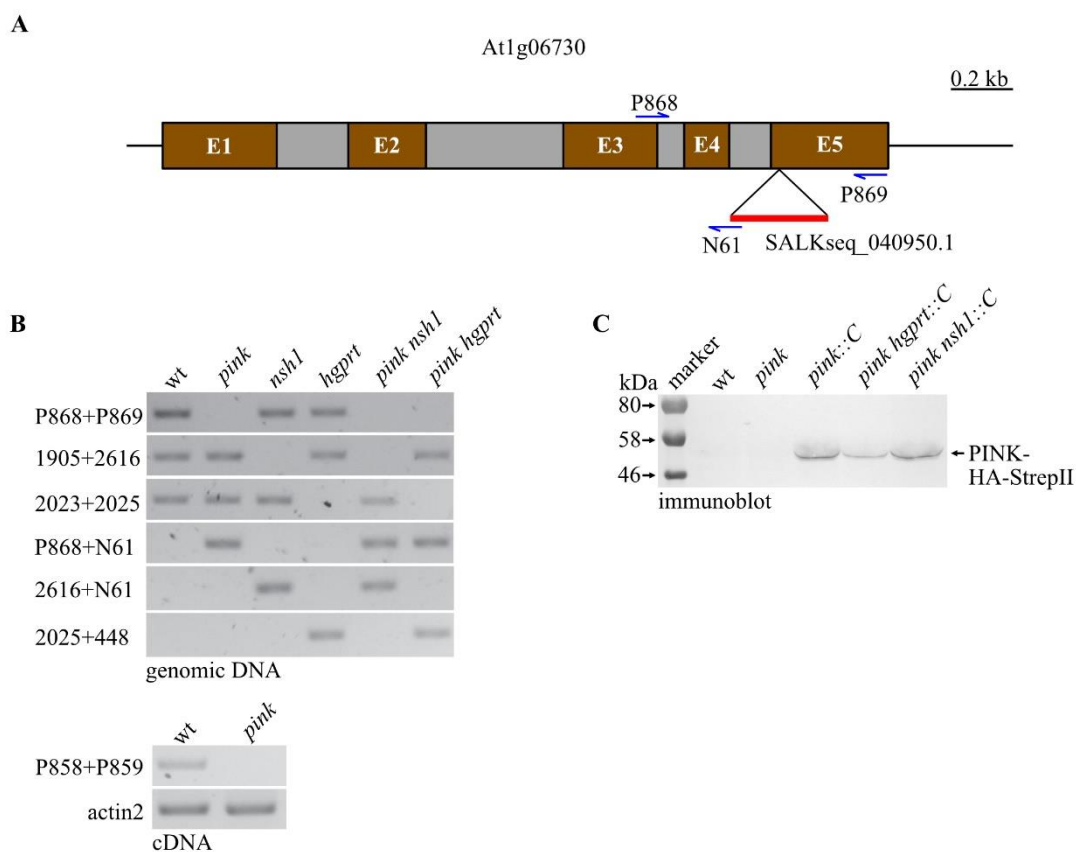


**Figure 14. Characterization of *PINK* variants.**

(A) Scheme of the At1g06730 locus and T-DNA insertion site (triangle) in *pink* (SALKseq\_040950.1). The brown boxes represent the exons, while the grey boxes represent the introns. Note that the E1 shown in this figure begins with the start codon, while the E5 ends with the last stop codon of the coding sequence. The positions of primers P868, P869, and N61 are illustrated. (B) PCR and RT-PCR characterization of segregating homozygous wt, *pink*, *nsh1*, *hgrpt*, *pink nsh1*, and *pink hgrpt*. (C) Immunoblot blot analysis of 10-day-old seedlings of wt, *pink*, *pink::C*, *pink hgrpt::C*, and *pink nsh1::C*. An antibody against the StrepII tag was used for detection.

### 3.2.5 Antibody preparation of PINK

An anti-PINK antibody was generated (immunoGlobe, Germany) to further study PINK in *Arabidopsis thaliana*. For this, inclusion bodies of PINK expressed in *E. coli* were purified (Figure 15 A) and injected into rabbits for antibody production. The resulting polyclonal antibody was able to detect a minimum of 5 ng of affinity purified PINK-HA-StrepII on immunoblots (Figure 15 B). Because PINK has a similar size as ribulose-1,5-bisphosphate carboxylase/oxygenase (RUBISCO), it is problematic to detect PINK in the crude extracts from *Arabidopsis thaliana* since RUBISCO is highly abundant and creates an interfering background

## RESULTS

(Figure 15 B). PINK could not be detected in the wild type but only in the crude extracts of the overexpression line *pink::C* (Figure 15 B).

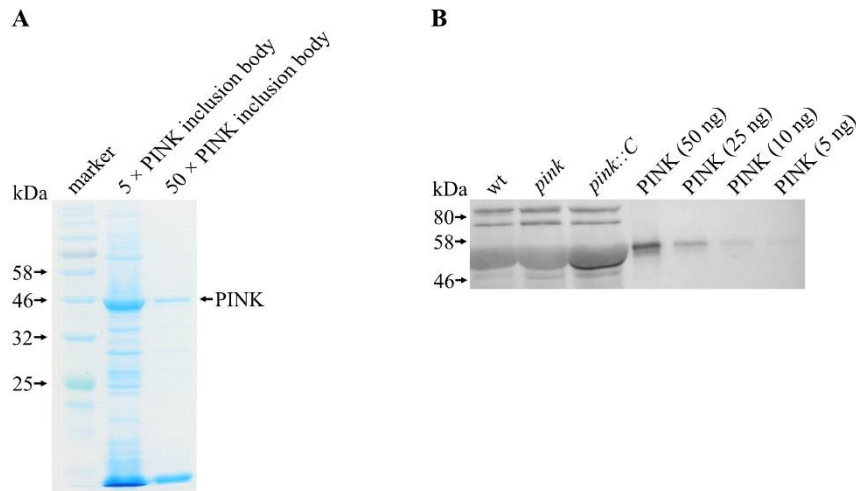


**Figure 15. Inclusion body characterization and detection of PINK with antibodies.**

(A) Coomassie staining after SDS-PAGE of diluted PINK inclusion body. 5, 5-fold diluted preparation; 50, 50-fold diluted preparation. (B) Immunoblot of crude extracts of 10-day seedlings of wild type, *pink*, and *pink::C*. Gradient amounts of PINK-HA-StrepII affinity purified from *N. benthamiana* leaves with 3-day transient expression are shown in the four lanes on the right.

### 3.2.6 Phenotype of the *PINK NSH1* double mutant

The physiological performances of *PINK* mutants were assessed in the context of the *NSH1* mutant. Twenty-one-day-old seedlings of *pink nsh1* showed retarded development compared with that of wild type, *pink*, and *nsh1*, and this phenotype could be compensated in the complementation and overexpression line (*pink nsh1::C*; Figure 16 A). The leaf area was quantified with the ImageJ software. The absence of *PINK* in the *NSH1* background leads to a significantly smaller leaf area and this phenotype is complemented in *pink nsh1::C* (Figure 16 B).

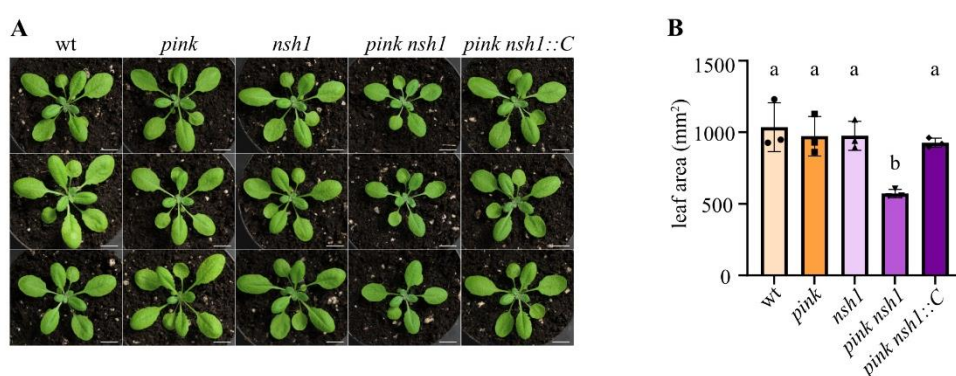


**Figure 16. Phenotype of 21-day-old seedlings of *PINK* variants.**

(A) Images of 21-day-old wild type, *pink*, *nsh1*, *pink nsh1*, and *pink nsh1::C* seedlings. Scale bars = 1 cm. (B) The total leaf area of 21-day-old seedlings of *PINK* variants, which are shown in (A). Error bars are SD (n = 3 biological replicates). Two-sided Tukey's pairwise comparisons were performed for statistical analysis. Different letters indicate significant differences at  $P < 0.05$ .

It is known that the NSH1 and NSH2 complex can hydrolyze inosine and xanthosine, while NSH1 alone degrades uridine. (Baccolini and Witte, 2019). The phenotype observed in 21-day-old seedlings of *pink nsh1* (Figure 16 A) indicates that PINK may share at least one substrate with NSH1 in Arabidopsis. Moreover, no phenotype was observed for the *PINK* single mutant, suggesting that the PINK substrate does not accumulate in *pink* maybe due to the presence of NSH1 and NSH2 complex. To test this hypothesis, to determine potential *in-vivo* substrates, and to investigate the biological function of PINK, metabolite analyses of *PINK* variants were performed.

### 3.2.7 Metabolite analysis of *PINK* variants

#### 3.2.7.1 Metabolite analysis of seedlings varying in *PINK* expression

First, metabolite analysis of 10-day-old wild type and *pink* seedlings was performed under different light conditions to investigate the *in vivo* function of PINK. The reason seedlings were studied under different light conditions was that the analysis of publically available transcriptome data by Genevestigator indicated that purine *de novo* synthesis may be upregulated transcriptionally by light.

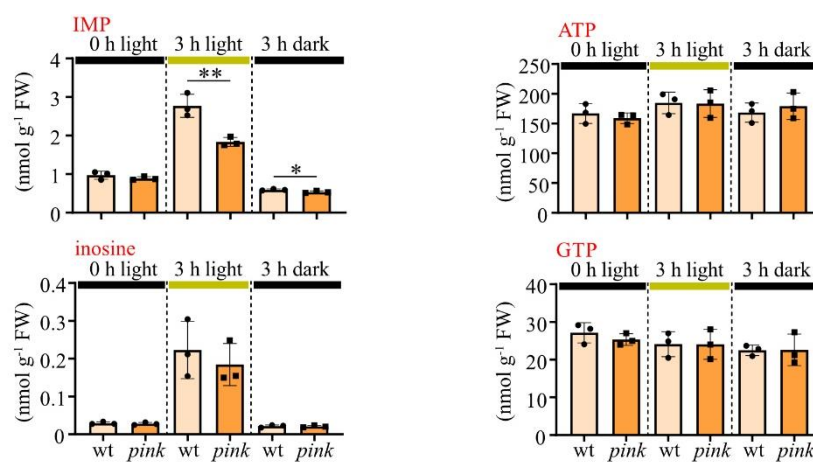


**Figure 17. Metabolite analysis of the *PINK* mutant under different light conditions.**

ATP, GTP, IMP, and inosine contents in 10-day-old wild type and *pink* seedlings grown under long-day conditions (16 h light). Error bars are SD (n = 3 biological replicates, i.e., several seedlings per replicate from different growth plates). An unpaired t test was used for statistical analysis in each treatment group. \* and \*\* indicate significant differences at  $p < 0.05$  and  $p < 0.01$ , respectively. 0 h light, seedlings were harvested at the end of the night, right before the onset of light; 3 h light, seedlings were harvested 3 hours after the end of the night; 3 h dark, seedlings were harvested 3 hours after the end of the normal night, but the night was prolonged. FW, fresh weight.

AICAr, inosine, and uridine are the substrates of PINK *in vitro* (Figure 13), but none of them accumulated in the *PINK* mutant (Figure A-3 C and Figure 17). Interestingly, there was a significant decrease of IMP in *pink* at 3 h of light whereas there was no difference before the onset of light or only a subtle difference at 3 h of prolonged darkness. This results indicate that PINK responds to light and may act as an inosine kinase *in vivo* even though inosine

## RESULTS

accumulation was not observed in *pink*, probably because the accumulation of inosine was prevented by its degradation, catalyzed by the NSH1/NSH2 complex.

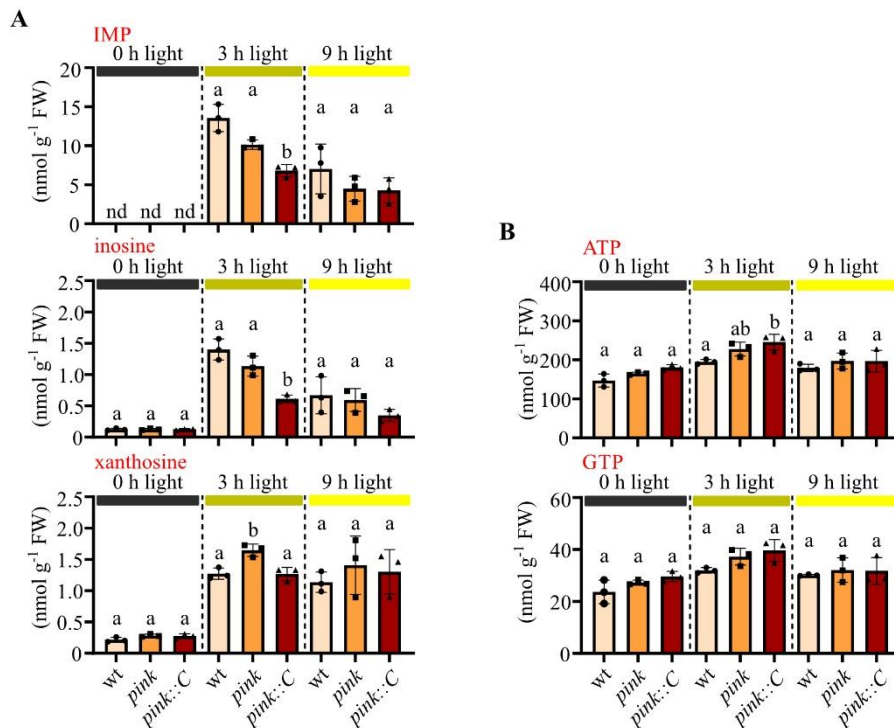


**Figure 18. Metabolite analysis of *PINK* variants with different duration of light.**

(A) IMP, inosine, and xanthosine as well as (B) ATP and GTP contents in 10-day-old seedlings of wild type, *pink*, and *pink::C*. 0 h light, the seedlings were harvested at the end of the night; 3 h light, the seedlings were harvested after 3 hours of light; 9 h light, the seedlings were harvested 9 hours after the end of the night. Error bars are SD (n = 3 biological replicates). The detection limit for IMP in plant matrix was 0.2 nmol g<sup>-1</sup> FW. For statistical analysis, two-sided Tukey's pairwise comparisons were performed separately for each time point. Different letters indicate significant differences at  $p < 0.05$ .

To further investigate how *PINK* responds to light, the metabolite content of seedlings that varied in *PINK* expression was analyzed at different times during the day. The seedlings were harvested immediately before the onset of light (0 h light), at 3 hours after the end of the night (3 h light), and 9 hours after the end of the night (9 h light). There were obvious increases in the content of IMP, inosine, and xanthosine between the end of the night and 3 hours of light (Figure 18 A), indicating that *de novo* purine biosynthesis is stimulated from dark to light as IMP is the product of purine biosynthesis. However, with prolonged light (9 hours), the amounts

## RESULTS

---

of IMP and inosine were decreased compared with that of 3 hours of light (Figure 18 A), suggesting that the purine biosynthesis is stronger induced shortly after the onset of light.

At 3 hours of light, the *PINK* mutant had less IMP in tendency compared to the wild type (Figure 18 A), which is consistent with the data shown in Figure 17, suggesting that PINK may be an inosine kinase *in vivo*. Curiously, instead of being complemented, the amount of IMP became even lower in the complementation and overexpression line (*pink::C*) compared to that of the *PINK* mutant (Figure 18 A), indicating that there are additional ways to regulate the IMP content in plants in addition to the inosine salvage mediated by PINK. Therefore, the hypothesis was born that plastid IMP formation catalyzed by PINK is involved in the feedback inhibition of purine *de novo* biosynthesis in plants, which leads to less total IMP. There is evidence published by Reynolds et al. (1984) demonstrating that IMP directly inhibits the activity of 5-phosphoribosylpyrophosphate amidotransferase (PRAT, also known as ATase; Figure 2) purified from soybean nodules, which is the first enzyme in purine biosynthesis.

The working hypothesis was that inosine is the substrate of PINK *in vivo*. Consistently, at 3 hours of light, a reduction in inosine was observed in *pink::C*, and a decrease in IMP was obtained in *pink* (Figure 18 A), supporting the hypothesis that PINK acts as an inosine kinase *in vivo*.

Surprisingly, at 3 hours of light, the amount of xanthosine was significantly increased in *pink* which was complemented by the transgene in *pink::C* (Figure 18 A). It is interesting because PINK cannot phosphorylate xanthosine (Figure 10 C) which is the first common intermediate in the purine degradation pathway *in vivo*. Thus, the amount of xanthosine might represent the flux through purine catabolism. Additionally, ATP and GTP did not accumulate in the *PINK* mutant, and flux might be increased as a result of stronger *de novo* purine synthesis in *pink* background.

To summarize the above results. After the onset of light, purine biosynthesis is upregulated and PINK becomes activated compared to the end of the dark period (Figure 17 and Figure 18 A). At this time, PINK acts as an inosine kinase *in vivo*, which is supported by the data of IMP decrease in the *PINK* mutant (Figure 17 and Figure 18 A) and inosine decrease in the complementation and overexpression line (*pink::C*) (Figure 18 A). To explain the diminished IMP content in *pink::C*, it was hypothesized that PINK may be involved in the negative feedback inhibition of *de novo* purine biosynthesis by regulating the amount of plastid IMP, which results in less total IMP.

## RESULTS

### 3.2.7.2 Metabolite analysis of seedlings varying in *PINK* expression in the *NSH1* background

To verify the hypothesis proposed in the last section, metabolic analyses of seedlings with different *PINK* expression in the *NSH1* background were performed.

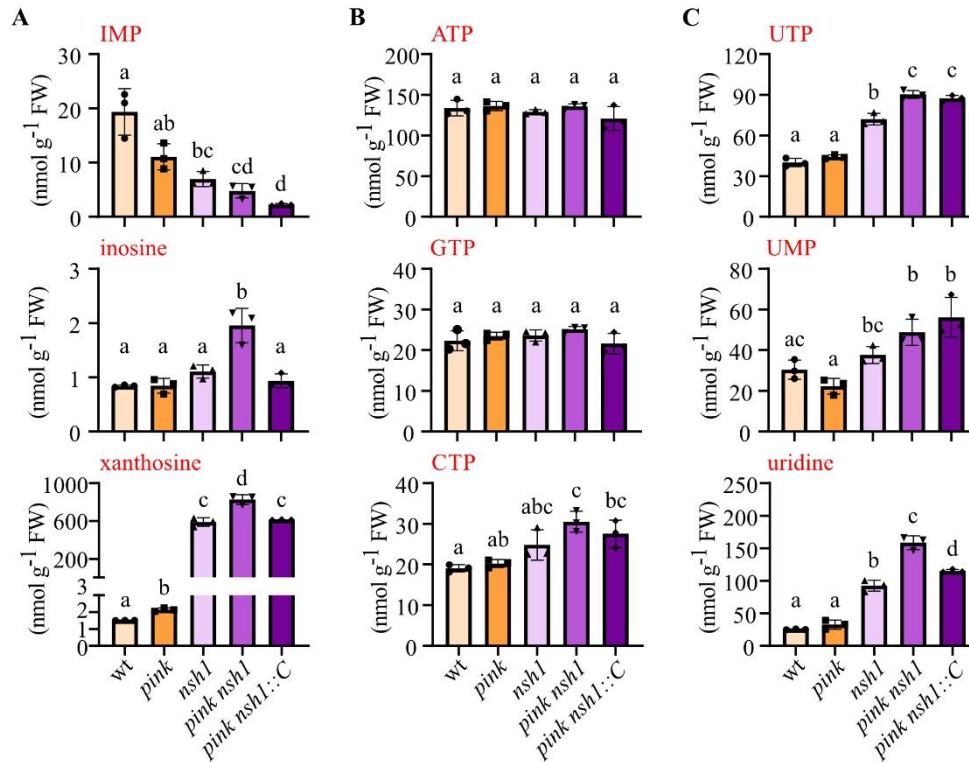


**Figure 19. Metabolite analysis of seedlings varying in *PINK* expression in the *NSH1* background.**

Metabolite analyses in 10-day-old seedlings of wild type, *pink*, *nsh1*, *pink nsh1*, and *pink nsh1::C*. All seedlings were harvested 3 hours after the onset of light. Error bars are SD (n = 3 biological replicates). For statistical analysis, two-sided Tukey's pairwise comparisons were performed. Different letters indicate significant differences at p < 0.05.

The absence of *PINK* in the *NSH1* mutant led to an accumulation of inosine compared with that of *nsh1*, which can be compensated in the complementation and overexpression line (Figure 19 A). This result potentially explains why no inosine accumulation was observed in the *PINK* mutant (Figure 17 and Figure 18 A), as the complex of NSH1 and NSH2 degraded it. More importantly, it demonstrates that *PINK* is catalyzing inosine salvage *in vivo*.

Interestingly, the IMP content decreased in the *NSH1* mutant (Figure 18 A) indicating that there might be additional mechanisms influencing IMP content because in a straightforward model,



## RESULTS

---

the amount of IMP should increase when inosine cannot be degraded in the absence of a functional NSH1-NSH2 complex.

Moreover, xanthosine strongly accumulated in *nsh1*, which was at hundreds of  $\text{nmol g}^{-1} \text{FW}^{-1}$  in contrast to the single digits of  $\text{nmol g}^{-1} \text{FW}^{-1}$  in wild type and *pink* (Figure 19 A). Even so, the absence of *PINK* in the *NSH1* background still led to xanthosine accumulation (Figure 19 A), suggesting the hypothesis that *PINK* should act as a regulator of *de novo* purine biosynthesis because a lack of *PINK* leads to an accumulation of xanthosine, which could reflect the influx from purine synthesis to catabolism. Additionally, compared to *nsh1*, *pink nsh1* and *pink nsh1::C* showed the same tendency of decreased IMP concentrations (Figure 19 A), which were observed previously (Figure 17 and Figure 18 A), indicating that *PINK* is not only involved in the inosine salvage but also should be involved in the feedback regulation of purine synthesis.

In addition to inosine and xanthosine, *pink nsh1* also showed a significant increase in uridine compared to that of *nsh1*, which could be complemented by the *PINK* transgene in *pink nsh1::C* (Figure 19 C). The data suggest that *PINK* salvages uridine in the *NSH1* background. However, there was no difference in uridine or UMP content between *pink* and wild type, leading us to conclude that *PINK* should not be a uridine kinase in the wild type background but can phosphorylate uridine under certain conditions, for example when plants accumulate uridine in the *NSH1* background.

Besides uridine, UTP accumulated in *pink nsh1* compared to *nsh1*, but this effect was not complemented in *pink nsh1::C* (Figure 19 C). For the accumulation in *pink nsh1*, possibility is that the absence of *PINK* might lead to a decrease in chloroplast UMP, resulting in the accumulation of total UTP because the chloroplast UMP acts as a negative regulator of pyrimidine *de novo* synthesis (Bellin et al., 2021). In *pink nsh1::C*, the increases of UMP and UTP could be a result of the enhanced uridine salvage activity.

In this section, evidence is provided that (i) *PINK* is an inosine kinase *in vivo*, and that the presence of the NSH1/NSH2 complex is the reason why no inosine accumulation was observed in *pink*, (ii) *PINK* may be involved in the regulation of purine biosynthesis and influence the size of the purine catabolism pool and (iii) *PINK* may contribute to pyrimidine homeostasis.

## RESULTS

### 3.2.7.3 Metabolite analysis of seedlings varying in *PINK* expression in the *HGPRT* background and upon XDH inhibition via an application of external allopurinol

The idea behind this experiment was to investigate the amount of hypoxanthine in *pink hgpert* seedlings in which XDH was chemically inhibited; and hypoxanthine could neither be salvaged nor degraded. If an accumulation of hypoxanthine was observed in *pink hgpert*, the hypothesis that *PINK* acts as the inosine kinase could be further supported.

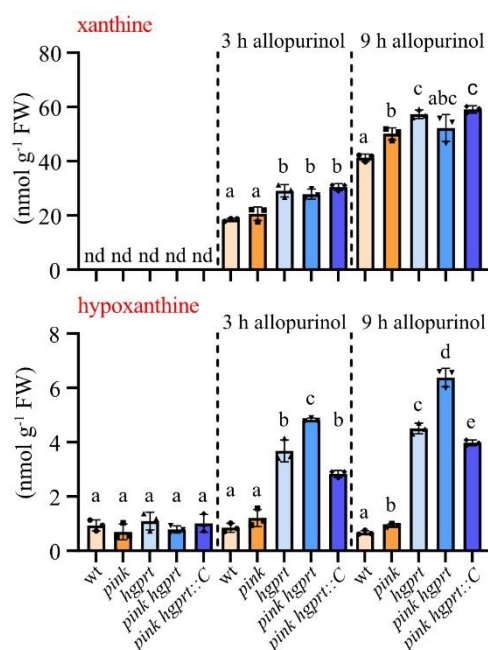


**Figure 20. Metabolite analysis of seedlings varying in *PINK* expression in the *HGPRT* mutant background and upon XDH inhibition during the day.**

Xanthine and hypoxanthine contents in 10-day-old seedlings of wild type, *pink*, *hgpert*, *pink hgpert*, and *pink hgpert::C* before allopurinol treatment, and 3 h and 9 h after allopurinol treatment for XDH inhibition. The seedlings were harvested at the beginning of the day for the samples without allopurinol application, and seedlings treated with allopurinol and sampled 3 h and 9 h later during the day. Error bars are SD (n = 3 biological replicates). The detection limit for xanthine in plant matrix was 1.8 nmol g<sup>-1</sup> FW. For statistical analysis, two-sided Tukey's pairwise comparisons were performed separately for each time point. Different letters indicate significant differences at p < 0.05.

Without the allopurinol treatment, the amount of xanthine and hypoxanthine showed no difference between wild type, *pink*, *hgpert*, *pink hgpert*, and *pink hgpert::C* (Figure 20) due to the activity of xanthine dehydrogenase (XDH; Figure 2), which efficiently oxidizes these compounds. However, after blocking XDH activity with allopurinol, *pink hgpert* showed more

## RESULTS

accumulation of hypoxanthine than *hgp1rt* (Figure 20). This indicates that the extra hypoxanthine is derived from the degradation of inosine that has not been salvaged in the absence of *PINK*, verifying the function of *PINK* as the inosine kinase *in vivo*.

### 3.2.7.4 Metabolite analysis of seedlings with cold treatment of *PINK* variants

Additionally, from the published transcriptome data analyzed by Genevestigator, it was found that purine synthesis genes were induced under cold stress. Thus, to further investigate the physiological role of *PINK*, we performed a metabolic analysis of *PINK* variants under cold stress.

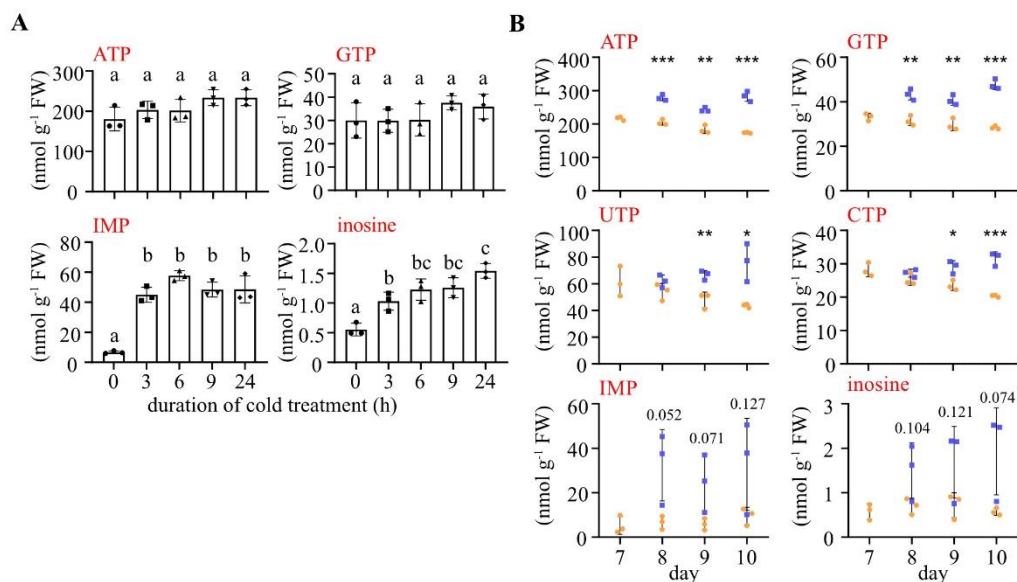


**Figure 21. Metabolite analysis of wild type seedlings with cold treatment.**

(A) ATP, GTP, IMP, and inosine contents of 10-day-old wild type seedlings exposed to 10°C for different times. Two-sided Tukey's pairwise comparisons were performed for the statistical analyses. Different letters represent significant differences at  $P < 0.05$ . (B) Nucleotide and nucleoside contents in wild type seedlings grown under normal long-day conditions up to Day 7 and then either left growing under these conditions for three days (orange data points) or exposed to cold (16 h light period, 10°C throughout; blue data points). For statistical analysis at each time point, an unpaired t test was used. Statistical differences at  $p < 0.05$ ,  $p < 0.01$  and  $p < 0.001$  are indicated by \*, \*\* and \*\*\*, respectively. For IMP and inosine, p values from statistical analyses are indicated in the graph. All plants were harvested 3 hours after daybreak. Error bars are SD ( $n = 3$  biological replicates). FW, fresh weight.

To explore the appropriate timing for the cold treatment, metabolite analysis of wild type seedlings with short and long-term cold treatments (10°C) was performed. After 24 hours of cold treatment, 10-day-old seedlings showed a significant increase in purine nucleotides such as ATP and GTP compared to that of seedlings grown under normal long-day conditions, and

## RESULTS

the difference remained stable at 24 hours, 48 hours and 72 hours (Figure 21 B), suggesting that the cold treatment enhanced purine synthesis and that the enhancement stabilized after 24 hours of cold treatment. Even though the increase in IMP and inosine were not statistically significant, their concentration also increased in tendency and the P values were close to the critical value of significance (0.05) (Figure 21 B). In addition to purines, pyrimidine nucleotides such as UMP, UTP, CMP, and CTP also responded to cold stress and increased after the seedlings were exposed to 10°C for 48 hours (Figure 21 B and Figure A-5 B).

PINK may play a role of purine homeostasis when plants begin sensing cold and are at the stage in which purine content is increasing. Therefore, we quantified the nucleotide content of wild type seedlings during short-term cold treatment to determine the timing of the purine increase. The concentrations of IMP and inosine strongly increased 3 hours after transfer to cold conditions (Figure 21 A), whereas the concentrations of ATP and GTP only increased gradually; in this dataset, ADP and AMP reached statistical significance (Figure A-5 A), while ATP and GTP did not. Then the nucleotide content of wild type, *pink* and *pink::C* was compared without cold stress, with 1 hour of cold stress, and with 3 hours of cold stress – all harvested 3 hours after the end of the night.

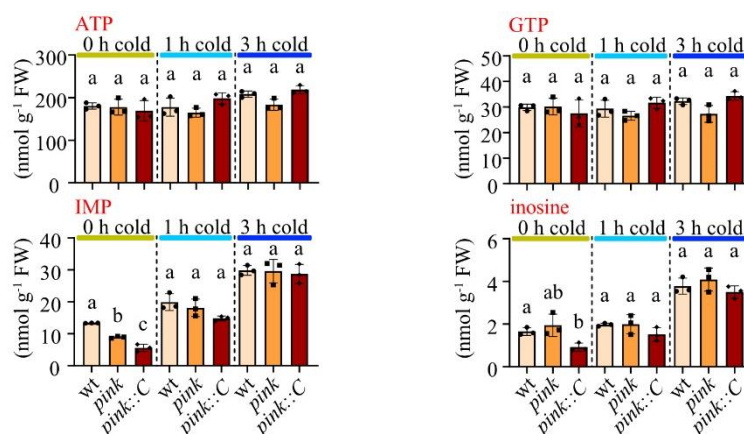


**Figure 22. Metabolite analysis in seedlings of *PINK* variants after short-term cold exposure.**

ATP, GTP, IMP, and inosine contents of 10-day-old seedlings of wild type, *pink*, and *pink::C* without or during 3 hours of cold treatment (10°C). All plants were harvested 3 hours after daybreak. Error bars are SD (n = 3 biological replicates). For statistical analysis at each time point, two-sided Tukey's pairwise comparisons were used. Different letters represent significant differences at  $p < 0.05$ .

As observed before (Figure 17, Figure 18 A, and Figure 19 A), the IMP concentration was lower in *pink* background and was even more reduced in *pink::C* without cold exposure after 3 hours in the light. When seedlings were exposed to cold for 1 hour or 3 hours, the IMP content increased, but the differences between the *PINK* variants vanished. The contents of ATP and GTP were not different between the genotypes under cold stress for different times. The data indicates that the salvage function of *PINK* and its probable contribution to feedback inhibition of purine biosynthesis are of little relevance when the purine biosynthetic pathway is strongly upregulated via cold stress. Other regulatory mechanisms seem to override the feedback inhibition because even in *pink::C*, the IMP concentration matched that of the wild type after 3 hours of cold exposure.

### 3.2.8 Summary of *PINK* functional analyses

In section 3.2 it was shown that (i) AICAr is the best substrate of *PINK* *in vitro*, (ii) *PINK* is localized in the chloroplast, (iii) *PINK* acts as the inosine but not AICAr kinase *in vivo* even though it has better enzymatic efficiency for AICAr *in vitro*, because there was no difference in AICAr content among *PINK* variants, while decreased amounts of IMP in *pink* and inosine in *pink::C* were observed in several independent experiments, (iv) The *in vivo* function of *PINK* as an inosine kinase was further verified via metabolite analysis in the context of *pink nsh1* and *pink hgprt*, (v) *PINK* may be involved in the feedback regulation of *de novo* purine synthesis as the IMP content decreased when *PINK* gene is overexpressed, and the xanthosine content accumulated in the absence of *PINK*, in both wild type and *nsh1* background.

### 3.3 Functional analyses of K6-2

#### 3.3.1 Bioinformatic analysis of K6-2

Phylogenetic analysis based on PfkB kinase 6, adenosine kinase (ADK), ribokinase (RBSK), pseudouridine kinase (PUKI), and plastid inosine kinase (PINK) from *Arabidopsis thaliana*, *Phaseolus vulgaris*, *Solanum lycopersicum*, *Oryza sativa*, *Sorghum bicolor*, and algae *Chlamydomonas reinhardtii* was performed using MEGA X (Figure 23).

The genome of *Arabidopsis* encodes two proteins of the PfkB kinase 6 subunit (K6-1 and K6-2). K6-1 and K6-2 are highly homologous, but K6-2 has a longer N-terminal sequence which potentially is a transit peptide (Figure A-1). Although K6-1 is closely related to K6-2, it did not exhibit any activity to the substrate screen (section 3.1.2).

Similar to PINK, K6-2 is conserved in the plant kingdom and possibly also in algae (Figure 23). In terms of the evolutionary relationship, K6-2 in *Arabidopsis* is the closest to those in *Phaseolus vulgaris*, and *Solanum lycopersicum*, which are also dicotyledons (Figure 23).

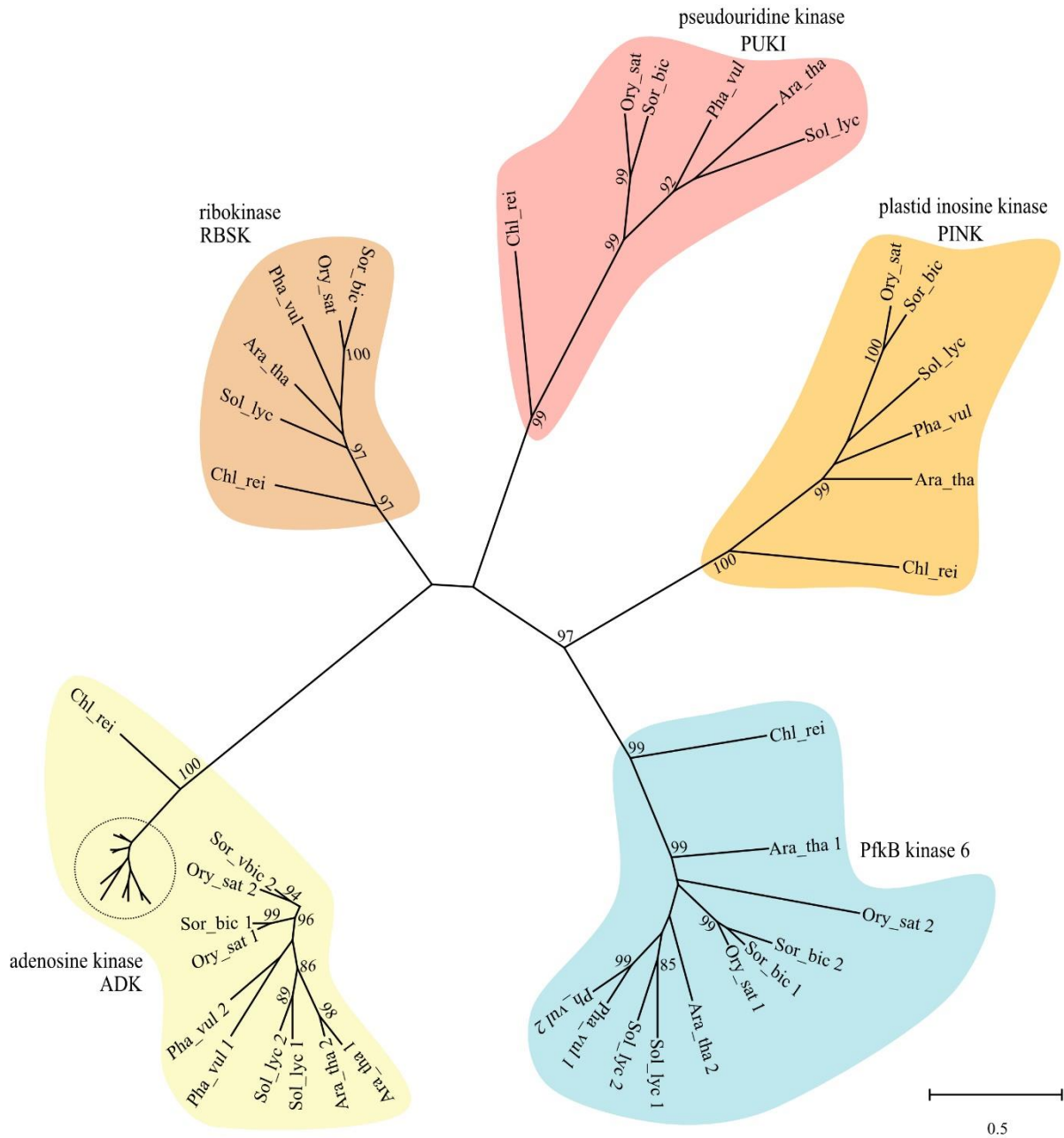


**Figure 23. Phylogenetic analysis of KINASE 6-2 and PfkB nucleoside or ribo-kinases.**

The evolutionary history was inferred by using the maximum likelihood method and JTT matrix-based model. The tree with the highest log likelihood (-25233.68) is shown. Bootstrap values above 80 (1000 iterations) are displayed. *Ara\_tha*, *Arabidopsis thaliana*. *Pha\_vul*, *Phaseolus vulgaris*. *Sol\_lyc*, *Solanum lycopersicum*. *Ory\_sat*, *Oryza sativa*. *Sor\_bic*, *Sorghum bicolor*. *Chl\_rei*, *Chlamydomonas reinhardtii*.

### 3.3.2 Subcellular localization of K6-2

To investigate the subcellular localization of K6-2, the coding sequence of K6-2 was fused to the binary vector V90 (Table 2.1-19) resulting in the construct H835 (Table 2.1-20) which can be used to express a C-terminal NeonGreen tagged K6-2 fusion protein (K6-2-NeonGreen) in *Nicotiana benthamiana* after *Agrobacterium*-mediated transformation.

Similar to PINK, K6-2 is also localized in the chloroplast, as confirmed by confocal fluorescence microscopy (Figure 24). Combined with the result shown in Figure 9, it appears possible that K6-2 is a plastid AICAr, inosine, or guanosine kinase.

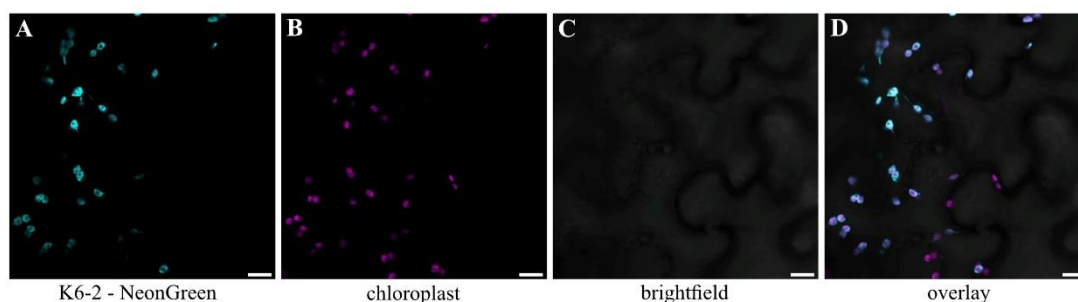


**Figure 24. Subcellular localization of K6-2.**

Confocal fluorescence microscopy images of *N. benthamiana* leaves that transiently expressed C-terminal NeonGreen tagged K6-2. (A) NeonGreen. (B) Autofluorescence of chloroplasts. (C) Brightfield. (D) Overlay of the three channels. Scale bars = 10  $\mu\text{m}$ .

### 3.3.3 Enzyme kinetics of K6-2

To determine the activity of K6-2 for AICAr, inosine, and guanosine, the coupled enzyme assay described in section 2.2.4.8 was performed. Initial velocities were plotted against substrate concentrations and fitted using the Michaelis-Menten equation (red curves) and the data was plotted according to Hanes and fitted by linear regression (blue line, Figure 25).

The Michaelis constants ( $K_m$ ) derived from this analysis of K6-2 for each substrate, the turnover numbers ( $k_{cat}$ ), and the catalytic efficiencies ( $k_{cat}/K_m$ ) are illustrated in Table 3.3-1. Please note that the maximum concentration of guanosine tested was 3 mM and did not reach ten times  $K_m$  due to the solubility limit of guanosine. The kinetic constants of K6-2 for guanosine that are



## RESULTS

shown in Table 3.3-1 were estimated based on the available data and may not be as accurate as those for AICAr and inosine.

In terms of enzyme kinetic constants, K6-2 showed the highest catalytic efficiency for AICAr ( $1.036 \text{ mM}^{-1} \text{ s}^{-1}$ ; Table 3.3-1), followed by guanosine ( $0.296 \text{ mM}^{-1} \text{ s}^{-1}$ ; Table 3.3-1), and the lowest for inosine ( $0.084 \text{ mM}^{-1} \text{ s}^{-1}$ ; Table 3.3-1). In addition, K6-2 has similar  $K_m$  values for AICAr and inosine (Table 3.3-1) that are lower than those for guanosine. Compared to inosine and guanosine, AICAr is the preferred substrate of K6-2 *in vitro*.

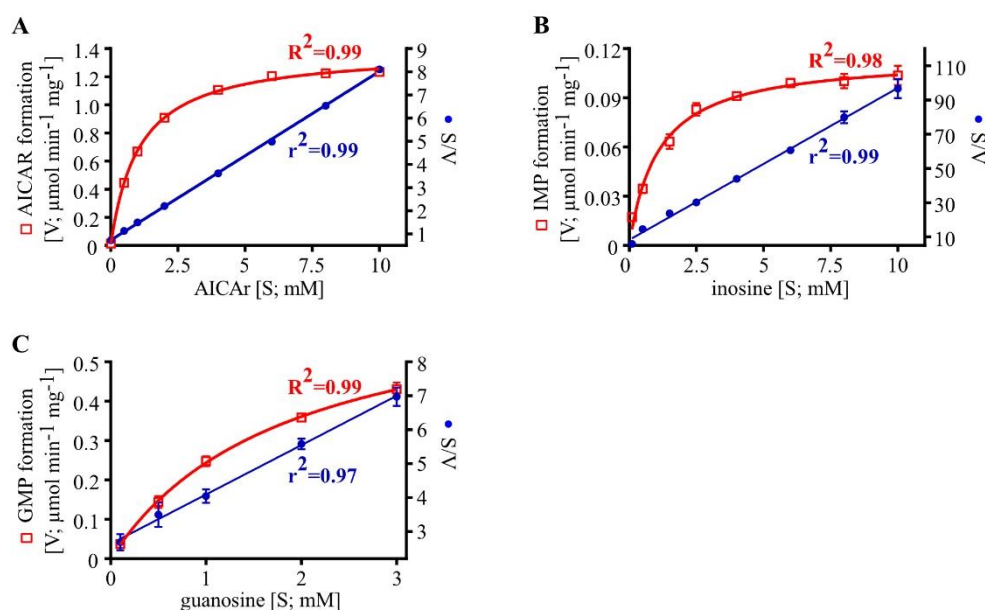


**Figure 25. Kinetic analysis of K6-2.**

Determination of the kinetic constants of K6-2 for (A) AICAr, (B) inosine, and (C) guanosine by fitting data with the Michaelis-Menten equation (red curve) and Hans plot (S/V, blue line). S, substrate concentration; V, enzymatic velocity. Error bars are SD (n = 3 independent enzymatic reactions).

## RESULTS

**Table 3.3-1. Kinetic constants for AICAr, guanosine, and inosine of K6-2.**

Enzymatic Reaction	$K_m$ (mM)	$k_{cat}$ ( $s^{-1}$ )	$k_{cat} / K_m$ ( $mM^{-1} s^{-1}$ )
K6-2, AICAr	$1.058 \pm 0.021$	$1.096 \pm 0.005$	1.036
K6-2, guanosine	$1.855 \pm 0.141$	$0.549 \pm 0.021$	0.296
K6-2, inosine	$1.088 \pm 0.089$	$0.091 \pm 0.002$	0.084

Errors are SD (n = 3 independent enzymatic reactions).

### 3.3.4 Characterization of the K6-2 knock-down mutant

The T-DNA insertion line SALK\_050816 was ordered from the Nottingham Arabidopsis Stock Centre (NASC). Homozygotes of the wild type (wt) and *K6-2* knock-down mutant (*k6-2*) were identified from a segregating mutant population by genomic PCR using primers N61, P1807, and P1808 (Figure 26 B, left). However, intact mRNA of K6-2 was still present in the homozygous mutant line *k6-2* (Figure 26 B, middle). This might be the case because the T-DNA was inserted into an intron (Figure 26 A) and may be spliced out during post-transcriptional processing of the primary transcript of in *k6-2*.

Although the mRNA of K6-2 was still present, its amount was lower than in the wild type (Figure 26 B, middle). To determine the degree of knock down in *k6-2*, real-time quantitative reverse transcription PCR (qRT-PCR) of seedlings of wild type and *k6-2* was performed. The result showed that the SALK\_050816 allele of *K6-2* is a knock-down mutant because it produced significantly less intact mRNA than the wild type (Figure 26 C).

In SALK\_050816, other genes besides At4g28706, including At1g31800, At2g31450, and At3g42057, also were documented to contain a T-DNA insertion ([https://arabidopsis.info/StockInfo?NASC\\_id=550816](https://arabidopsis.info/StockInfo?NASC_id=550816)). To eliminate the potential effects of these genes, plants were selected from the segregating *k6-2* population by genomic PCR that were wild type for the genes in question (Figure 26 B, right).

Furthermore, a K6-2-HA-StrepII complementation and overexpression line of *k6-2* (*k6-2::C*) was generated, selected, and confirmed by immunoblot (Figure 26 D) using anti-Strep antibodies.

## RESULTS

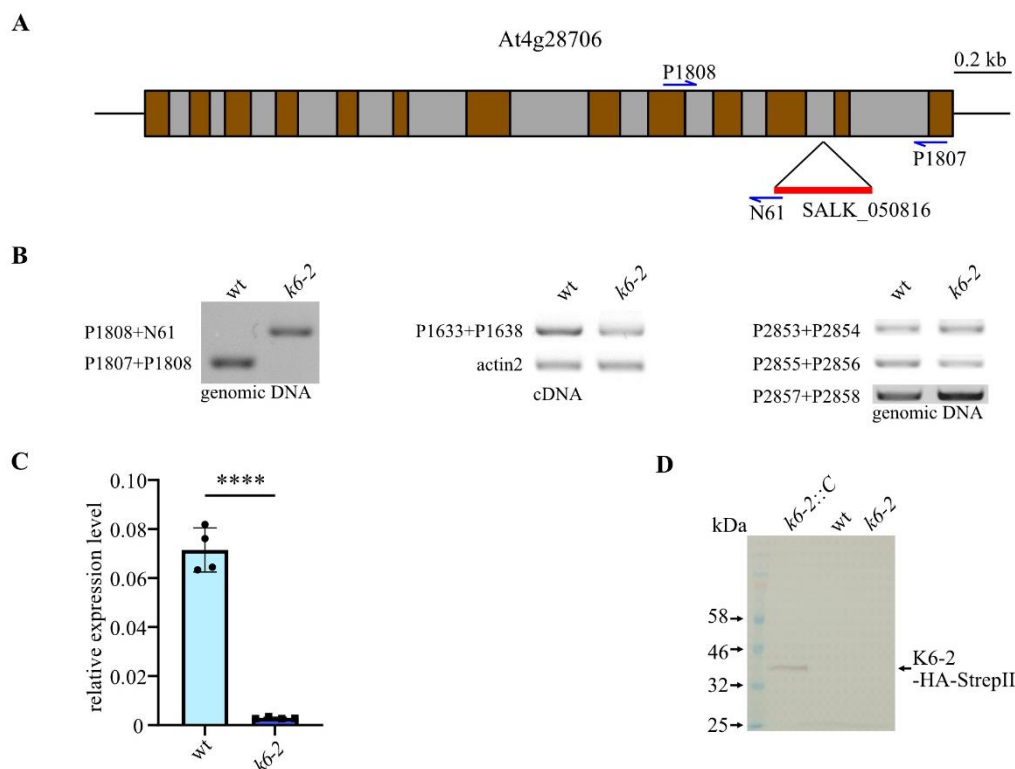


**Figure 26. Characterization of a *K6-2* knock-down mutant.**

(A) Scheme of the At4g28706 locus and T-DNA insertion site (triangle) in *k6-2* (SALK\_050816). The exons are shaded in brown while the introns are shaded in grey. Note that the first exon begins with the start codon, while the last exon ends with the stop codon. The positions of primers P1807, P1808, and N61 are shown. (B) PCR and RT-PCR characterizations of homozygous *k6-2* and wild type lines isolated from a segregating population of *k6-2*. (C) Real-time quantitative reverse transcription PCR (qRT-PCR) of wt and *k6-2*. Error bars are SD (n = 4 biological replicates). An unpaired t test was used for statistical analysis and \*\*\*\* indicates the significant difference at  $P < 0.0001$ . (D) Immunoblot blot analysis of wt, *k6-2*, and *k6-2::C*. An antibody against the Strep-tag was used.

### 3.3.5 Phenotype of the *K6-2* knock-down mutant

To assess the physiological performance, wild type, *k6-2*, and *k6-2::C* were cultured in parallel. Images of 16-day-old *K6-2* variants were taken. Interestingly, seedlings of the knock-down mutant of *K6-2* exhibited yellowing and deformed leaves after the four-leaf stage, and this

## RESULTS

phenotype was complemented in *k6-2::C* (Figure 27 A). Moreover, the leaf area of 16-day-old seedlings of *k6-2* was significantly decreased compared with that of the wild type. This effect was complemented and slightly overcompensated in *k6-2::C* (Figure 27 B).

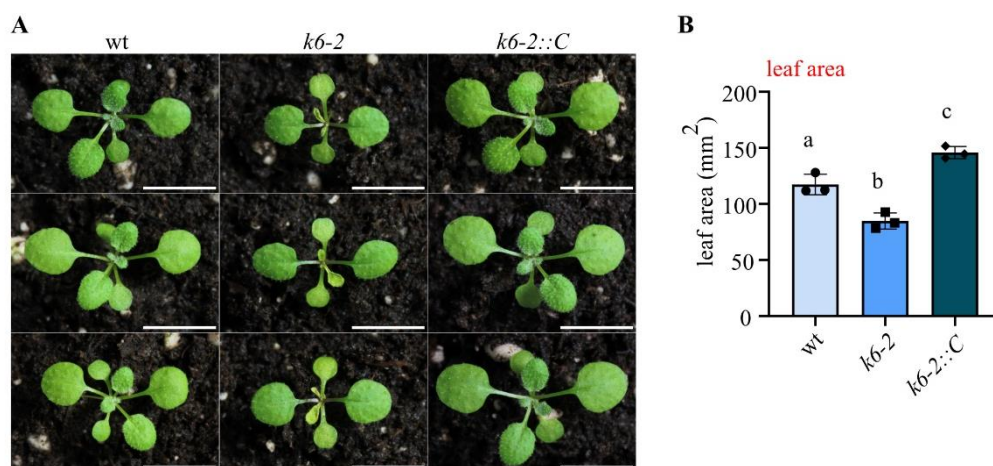


**Figure 27. Phenotype of 16-day-old seedlings with varying *K6-2* expression.**

(A) Images of 16-day-old seedlings with varying *K6-2* expression. Scale bars = 10 mm. (B) Leaf area analysis of wild type, *k6-2*, and *k6-2::C*. Error bars are SD (n = 3 biological replicates). For statistical analysis, two-sided Tukey's pairwise comparisons were performed. Different letters indicate statistical differences at p < 0.05.

### 3.3.6 Metabolite analysis of *K6-2* variants

To investigate the biological function of *K6-2* *in vivo*, metabolite analysis of 10-day-old seedlings that varied in *K6-2* expression was performed. IMP, inosine, and AICAr accumulated in *k6-2* (Figure 28 A) which was complemented by the transgene in *k6-2::C*. It is interesting that all of the accumulated compounds are involved or closely related to *de novo* purine biosynthesis. AICAr, the dephosphorylated form of an intermediate (AICAR) in purine synthesis, is also the best substrate compared to inosine and guanosine *in vitro* (Table 3.3-1). Inosine is also one of the substrates *in vitro*, as shown in Table 3.3-1, and the dephosphorylated form of IMP which is a product of purine biosynthesis. The accumulation of these three compounds (Figure 28 A) indicated that in the knock-down mutant of *K6-2*, purine *de novo* biosynthesis was upregulated, suggesting that *K6-2* is a negative regulator of purine synthesis. Is *K6-2* an AICAr or inosine kinase *in vivo*? The data suggest that *K6-2* is not the inosine kinase *in vivo* because otherwise, a decrease of IMP content in *k6-2* should have been observed,

## RESULTS

whereas the amount of IMP was increased. This indicates that the additional inosine should be derived from an increased amount of IMP rather than a lack of salvage. One of the current working hypothesis is that flux through purine biosynthesis is increased in the absence of K6-2. Consistently, the lower expression of *K6-2* in the knock-down mutants leads to the accumulation of AICAr, which may result in the inhibition of purine *de novo* synthesis.

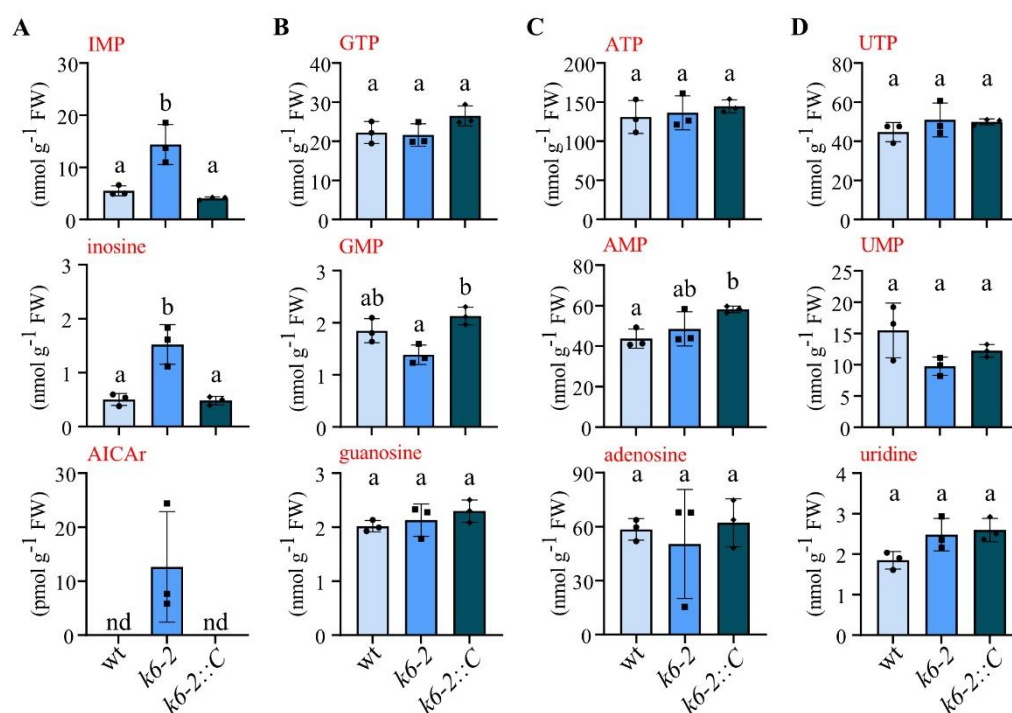


**Figure 28. Metabolite analysis of 10-day-old seedlings varying in *K6-2* expression.**

Metabolite analysis of wild type, *k6-2*, and *k6-2::C*. Error bars are SD ( $n = 3$  biological replicates). The detection limit for AICAr in plant matrix was  $5 \text{ pmol g}^{-1} \text{ FW}$ . For statistical analysis, two-sided Tukey's pairwise comparisons were performed. Different letters indicate statistical differences at  $p < 0.05$ . FW, fresh weight.

Moreover, the GMP content in *k6-2* appeared decreased tendency compared to that in wild type which was complemented in *k6-2::C* (Figure 28 B). Although this data is not yet statistically sound it might be a first hint that K6-2 is involved in the guanosine salvage, but will require further confirmation. The insignificant difference in the amount of GMP between wild type and *k6-2* may be due to the probably small GMP pool in the chloroplast, the organelle where K6-2 is located (Figure 24). Interestingly, GMP is another product of *de novo* purine synthesis and is derived from IMP through catalysis by IMP dehydrogenase and GMP synthase in the cytosol

## RESULTS

---

(Figure 2). If flux through, purine biosynthesis is elevated in *k6-2*, the GMP content should have increased instead of showing a tendency to decrease. Maybe K6-2 has a function in guanosine salvage and its lower expression leads to a decrease in plastid GMP content, which is involved in the feedback regulation of purine biosynthesis, as GMP inhibits the first enzyme of *de novo* purine synthesis (Reynolds et al., 1984). If this model of K6-2 was correct, guanosine accumulation should have been observed, but it was not. This may be explained by the presence of guanosine deaminase (GSDA; Figure 2), which can convert guanosine to xanthosine, preventing the accumulation of guanosine.

In summary, metabolites were analyzed of seedlings that varied in *K6-2* expression and obtained some evidence that (i) *K6-2* should be a negative regulator of purine biosynthesis and that (ii) *K6-2* is probably not an inosine kinase *in vivo* because of the IMP accumulation in *k6-2*. Moreover, two hypotheses of *K6-2* were proposed as follows:

- i. *K6-2* may act as the plastid AICAr kinase *in vivo* as its lower expression led to an accumulation of AICAr resulting in the upregulation of purine *de novo* synthesis.
- ii. *K6-2* may play a role as the plastid guanosine kinase in *Arabidopsis*, downregulating purine synthesis by influencing the plastidic GMP pool.

## 4 Discussion

### 4.1 Characterization of PfkB kinases from Arabidopsis

The PfkB family is known as a branch of carbohydrate kinases including adenosine kinase (ADK), pseudouridine kinase (PUKI), ribokinase (RBSK), necessary for the achievement of RUBISCO accumulation 5 (NARA5), and several others phosphorylating sugars, nucleosides and myoinositol substrates. Some of the PfkB kinases that have been characterized are critical for plant development. The *FLN1* mutant shows an albino phenotype while the *FLN2* mutant results in delayed greening (Gilkerson et al., 2012), the knockout mutant of *NARA5* exhibits severe leaf yellowing (Ogawa et al., 2009), the absence of *PUKI* leads to delayed seed germination (Chen and Witte, 2020), and loss-of-function of *ADKs* results in a severe phenotype of growth retardation (Schoor et al., 2011). Even though the phosphorylation mediated by PfkB kinases requires the participation of ATP, excessive ATP might in some cases result in inhibition due to the binding of ATP to an allosteric site. For example, the state of aggregation of *Escherichia coli* phosphofructokinase 2 (PFK2) and ATP can be shifted from dimer to tetramer, leading to the inhibition of the enzymatic reaction (Baez et al., 2008; Cabrera et al., 2011).

### 4.2 Purine *de novo* purine biosynthesis

Purine *de novo* synthesis results in the formation of IMP, AMP, and GMP and is crucial for plant development. Of the 10 enzymes in this process, 5-phosphoribosylpyrophosphate amidotransferase (PRAT) also known as PRPP amidotransferase (ATase) is the best-studied one. There are three *PRAT* genes in Arabidopsis with different expression patterns. *AtPRAT1* is only expressed in roots and flowers but not leaves, *AtPRAT2* is constitutively expressed and plays a major role in the development of Arabidopsis, and the expression of *AtPRAT3* is very low but is highest in flowers (Bassett et al., 2003; Hung et al., 2004). The T-DNA insertion mutant *AtATase2* (*Atadt2*) showed strong growth retardation and a chloroplast phenotype (van der Graaff et al., 2004), indicating that the purine *de novo* biosynthesis is crucial for Arabidopsis development. Moreover, PRAT can be strongly competitively inhibited by IMP and GMP in soybean (Reynolds et al., 1984) suggesting that plants have a strategy of feedback inhibition to regulate *de novo* purine biosynthesis.

Plants turn on purine biosynthesis in the light, which is not only supported by transcriptional data but also demonstrated in this study as purine contents such as IMP, inosine, and xanthosine are elevated in the early of the day (Figure 18 A). On the contrary, purine synthesis is turned off at night maybe because purine synthesis is energy consuming (Zrenner et al., 2006). During the night, plants consume starch accumulated during the day by photosynthesis to fuel their energetic requirements, and 90% of the starch is depleted by the end of the night (Usadel et al., 2008). When the night is prolonged, as in one of the experiments shown here (Figure 17), the metabolic changes indicating active purine biosynthesis that occur in the light are not observed, showing that it is the light which stimulates purine biosynthesis. Biosynthetic pathways do not only require energy but also carbon and in the case of nucleotide biosynthesis also nitrogen resources. These are more available during the day, which may be an additional reason for the stimulation of purine biosynthesis by light.

In addition, purine biosynthesis can also be upregulated under cold stress. The transcript of the first enzyme (PRAT) of purine synthesis is strongly increased (Klepikova et al., 2019) and the ATP content accumulates in rape and wheat leaves (Sobczyk and Kacperska-Palacz, 1978; Perras and Sarhan, 1984), indicating that the synthesis of purine nucleotides in plants should be enhanced under cold stress. Therefore, we monitored the purine contents of Arabidopsis seedlings at different times during cold treatment (10°C). The data demonstrate that purine synthesis is enhanced at the early stage (within 3 hours) of cold stress (Figure 21) leading later to more ATP and GTP. By contrast, purine catabolism is downregulated in Arabidopsis under cold stress (Figure A-6). Plants may use this strategy to produce more energy substances such as ATP in response to cold stress. Because more energy is required for plants to acclimate to the low temperature, for example, the activity of glucokinase (GlcK) in Arabidopsis is significantly increased under cold stress, requiring more ATP for central carbohydrate interconversions (Nägele et al., 2011).

### **4.3 Functional analysis of PINK**

#### **4.3.1 PINK is an inosine kinase and should be involved in the feedback regulation of purine biosynthesis**

Nucleosides are salvaged to monophosphates by various kinases, such as adenosine kinases (ADKs), pseudouridine kinase (PUKI), and uridine cytidine kinases (UCKs) (Moffatt et al., 2002; Chen and Thelen, 2011; Ohler et al., 2019; Chen and Witte, 2020). In addition, it has



been speculated for a long time that plants may have a guanosine and inosine kinase (IGK) because the externally supplied radioactive guanosine and inosine was found in their salvage products (Ashihara et al., 2018), and an IGK was found in *Escherichia coli*. IGK from *E. coli* has a similar turnover number for guanosine and inosine but of  $K_m$  for guanosine of 6.1  $\mu\text{M}$  and 2100  $\mu\text{M}$  for inosine (Mori et al., 1995; Wang et al., 2020). As the  $K_m$  value for guanosine of *Escherichia coli* IGK is much lower than that for inosine, it acts more likely as a guanosine kinase instead of guanosine/inosine kinase *in vivo*, indicating that in Arabidopsis, there is may be more than one enzyme involved in the salvage of inosine and guanosine.

As the substrate of PINK, inosine is not a major intermediate of purine metabolism in Arabidopsis (Baccolini and Witte, 2019). The source of inosine remains unclear, but may arise from IMP dephosphorylation, transfer RNA turnover, spontaneous deamination of adenosine, and vacuolar RNA degradation. So far, no toxic effects of inosine accumulation in plants have been found. Nevertheless, inosine is involved in the regulation of target of rapamycin (TOR) which is controlling autophagy. The TOR protein complex can negatively control autophagy in Arabidopsis (Liu and Bassham, 2010; Pu et al., 2017) and is regulated by the purine nucleotide level (Kazibwe et al., 2020). Furthermore, external inosine feeding rescues the constitutive autophagic phenotype mediated by TOR in Arabidopsis caused by impaired rRNA turnover (Kazibwe et al., 2020). Thus, PINK may also be involved in the regulation of autophagy by TOR signaling. If external inosine feeding could prevent the autophagic phenotype due to defective rRNA degradation in *pink* background, it would indicate that inosine directly regulates TOR. If not, it would provide evidence that the IMP salvaged by PINK may be one of the upstream signals of TOR.

In this study, some evidence has been shown that PINK might be involved in the feedback regulation of purine *de novo* synthesis by affecting the plastid IMP pool, as the absence of *PINK* leads to xanthosine accumulation while overexpression of *PINK* reduces IMP content in both wild type and *nsh1* background (Figure 18 A, Figure 19 A, and Figure 22). Theoretically, metabolic flux analysis of purine nucleotide biosynthesis could be performed to validate this hypothesis. In particular, labelled  $^{15}\text{N}$  can be used to replace the normal N source followed by quantitative analysis of  $^{15}\text{N}$  labelled purine metabolites. If purine metabolites would be more rapidly labelled in the *PINK* mutant compared to wild type, this would indicate higher flux through the pathway and the hypothesis could be further verified. In addition, metabolite analysis in subcellular fractions could also be done to quantify the plastid and cytosolic IMP pools, respectively. If the plastid IMP pool was larger while cytosolic one was smaller in the

absence of *PINK*, this would provide direct evidence that *PINK* participates in the feedback regulation of *de novo* purine synthesis via moderating the plastid IMP pool. However, neither of these techniques are currently established in our laboratory.

Xanthosine is a central molecule in purine nucleotide catabolism; it can be dephosphorylated from xanthosine monophosphate (XMP) and deaminated from guanosine under the catalysis of XMP phosphatase (XMPP) and guanosine deaminase (GSDA), respectively (Dahncke and Witte, 2013; Heinemann et al., 2021). It is not salvaged to XMP in *Arabidopsis* (Yin et al., 2014) but degraded to xanthine by the complex of NSH1 and NSH2 (Baccolini and Witte, 2019), making it possible for xanthosine to act as a marker of the flux through the purine catabolism in *Arabidopsis*. In this study, one of the pieces of evidence provided for enhanced purine biosynthesis is estimated from the increased xanthosine content, because *Arabidopsis* does not accumulate purine nucleoside triphosphate (Figure 17 B, Figure 18 B, and Figure 19 B) in *pink* or *nsh1* background. Under normal long-day conditions, changes in purine biosynthesis lead to alterations in flux through the catabolic pathway rather than in the content of ATP or GTP. Even though xanthosine accumulated strongly to 390-fold above wild type level in the *NSH1* mutant due to the block of its degradation, 240 nmol g<sup>-1</sup> FW more xanthosine was observed in the *PINK NSH1* double mutant, which even exceeded the combined pool size of ATP and GTP (Figure 19). The result provides strong evidence that the increased flux into the purine degradation pathway led by the absence of *PINK* is most likely a result of upregulated purine *de novo* biosynthesis, since *PINK* shows no activity to xanthosine at all (Figure 10 C). In addition, the growth retardation phenotype observed in the *PINK NSH1* double mutant (Figure 16) may be a result of xanthosine accumulation, as the accumulation of some nucleosides can result in physiological phenotypes, for instance, increased guanosine in the *GSDA* mutant leads to a dark stress phenotype (Schroeder et al., 2018) and the accumulation of pseudouridine in the *PUK1* mutant causes delayed germination (Chen and Witte, 2020).

To facilitate the further study of *PINK*, a polyclonal anti-*PINK* antibody was generated with a good but not very high detection sensitivity (Figure 15 B). However, *PINK* can only be detected in *pink::C* but not in the wild type on immunoblots (Figure 15 B), indicating that *PINK* is rather low abundant in *Arabidopsis*. Additionally, the metabolic phenotype between wild type, *pink*, and *pink::C* can be only observed at the early phase of light (at 3 hours of light) and vanished at the end of the night or the longer light time (9 hours of light) during the normal long-day conditions (Figure 18 A), suggesting the function of *PINK* is only needed by *Arabidopsis* at the early phase of light, a period when purine biosynthesis is higher (Figure 17 and Figure 18).

Moreover, there is no drastic transcriptional changes observed for PINK. Therefore, it can be concluded that PINK is likely encoded by a housekeeping gene dampening the sudden increase of purine metabolic flux due to purine *de novo* biosynthesis at the early stage of light.

#### 4.3.2 PINK under cold stress

Plants have evolved a range of mechanisms to tolerate environmental stresses such as low temperature. The plasma membrane is the primary target of cold stress, resulting in the qualitative and quantitative modifications in its lipid component (Uemura et al., 1995), which can further lead to oxidative damage, cytoskeleton breaking, and disruption of photosynthetic signaling (Sharma et al., 2005). In addition, the data indicates that the purine biosynthesis is also stimulated at low temperature in *Arabidopsis* (Figure 21), and it was thought that the metabolic effect of PINK may be enhanced under this condition.

To further investigate the physiological function of PINK, metabolite quantitative analysis of wild type, *pink*, and *pink::C* is performed under short-term cold stress. However, the metabolic role of PINK seems not important anymore when purine biosynthesis is presumably strongly induced, since the original molecular phenotype, the altered IMP and inosine content in *pink* and *pink::C*, disappears under cold stress (Figure 22). The feedback inhibition of purine synthesis is probably overlaid by some cold-induced mechanisms, and the salvage function of PINK is no longer influencing the purine nucleotide homeostasis under cold stress.

#### 4.3.3 PINK in pyrimidine homeostasis

The absence of *NSH1* leads to uridine accumulation, since *NSH1* is not only crucial for the purine degradation pathway but also involved in pyrimidine catabolism catalyzing uridine to uracil (Jung et al., 2009; Riegler et al., 2011). Interestingly, even more uridine accumulates in the absence of *PINK* in *nsh1* background (Figure 19 C), suggesting that PINK may be involved in uridine salvage *in vivo* as it phosphorylates uridine to UMP *in vitro* (Figure 10 and Figure 13). However, between wild type and *pink*, no effect on uridylates is observed putting into question an *in vivo* function of PINK as uridine kinase (Figure A-3 B and Figure A-4 B). It is possible that PINK does not play a role as a uridine kinase unless the uridine concentration is increased, such as in *nsh1* background, which does not happen in the wild type.

In addition to uridine, UTP also over-accumulated in *pink nsh1* but did not return to the level found in the *NSH1* single mutant when *PINK* was overexpressed in *pink nsh1* (Figure 19 C). However, the increased UTP content observed in *pink nsh1* and *pink nsh1::C* may be from

## DISCUSSION

different pathways. In *pink nsh1*, the accumulation of UTP may be a result of upregulated pyrimidine biosynthesis, because the absence of *PINK* probably leads to a decreased plastid UMP content which has been shown negatively regulates the first two enzymes of pyrimidine *de novo* synthesis (Bellin et al., 2021). Nevertheless, the elevated UTP content in *pink nsh1::C* is likely due to the enhanced uridine salvage.

To further verify whether *PINK* is involved in pyrimidine homeostasis in Arabidopsis, metabolic analysis could be performed in the context of impaired pyrimidine degradation independent of the *NSH1* background, in particular, in the *dihydropyrimidine hydrolase (DPYH)* or  *$\beta$ -ureidopropionase ( $\beta$ -UP)* background. The accumulation of dihydrouracil in the *PINK* *DPYH* double mutant and more ureidopropionate in the *PINK*  *$\beta$ -UP* mutant would be expected if *PINK* was a negative regulator of pyrimidine biosynthesis by controlling the plastid UMP pool.

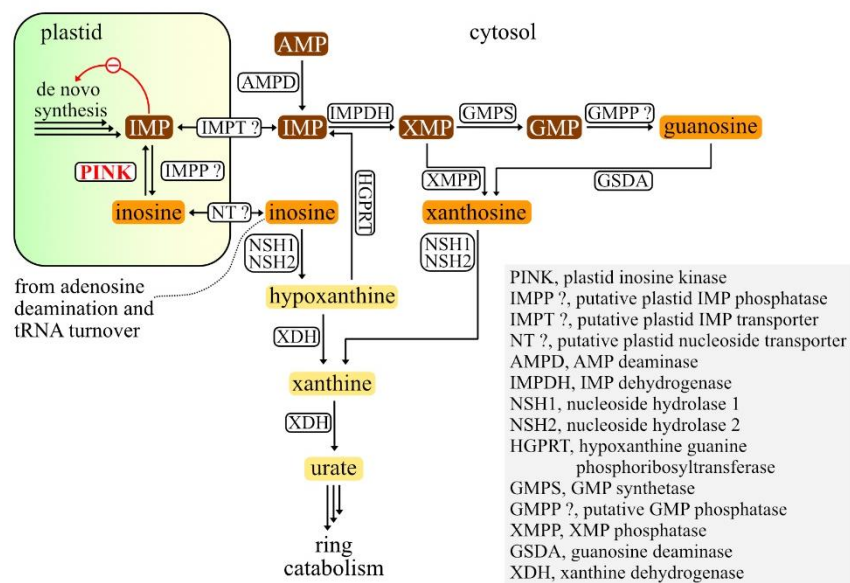


**Figure 29. Model of inosine salvage by PINK in the context of purine metabolism.**

The source of inosine has not been elucidated; it may arise from the turnover of t-RNA, in which inosine occurs or from non-enzymatic adenosine deamination in RNA in general. Moreover, inosine may also be made in plastids from IMP mediated by a putative plastid IMP phosphatase (IMPP ?), which not necessarily is specific for IMP. A putative IMP transporter (IMPT ?) and a putative plastid nucleoside transporter (NT ?) are shown.

## 4.4 Functional analysis of K6-2

### 4.4.1 K6-2 is a negative regulator of purine nucleotide synthesis

K6-2 phosphorylates AICAr, inosine, guanosine, uridine, adenosine, and N<sup>6</sup>-methyladenosine *in vitro* (Figure 9), showing a preference for AICAr, guanosine, and inosine (Figure A-7). The low expression of the enzyme in the *K6-2* mutant leads to the accumulation of IMP, AICAr and inosine (Figure 28). IMP is a product of purine biosynthesis while AICAr is the dephosphorylation form of AICAR which is an intermediate of purine *de novo* synthesis, and inosine could be dephosphorylated from IMP, providing strong evidence that lower expression of K6-2 leads to enhanced purine biosynthesis. To maximize the molecular phenotype, metabolite analysis of the *K6-2* knock-down mutant could be performed in a follow-up study under different light conditions, as the purine biosynthesis is turned on at the early phase of light (Figure 18 A). In particular, the effects of purine contents (AICAr, inosine, and IMP) in *k6-2* would be bigger at 3 h of light than that at the end of the night or 9 h of light if K6-2 negatively regulated purine synthesis. Moreover, metabolic analysis of *K6-2* variants can also be carried out in the context of impaired purine catabolism, for example in the *NSH1* background. It could provide another line of evidence for the suggested negative regulation of purine synthesis by K6-2, if purine compounds over-accumulated in a *K6-2 NSH1* double mutant. Additionally, it is also interesting to perform quantitative metabolite analysis of *K6-2* variants in *pink* background to explore whether their biological functions overlap since both are located in the chloroplast (Figure 12 and Figure 24) and may be involved in the local control of purine *de novo* synthesis. Last but not least, the products of purine nucleotide degradation, such as xanthosine, hypoxanthine and xanthine, could also be quantified in the future work, because upregulated purine synthesis should also result in increased pools of such purine catabolites.

#### 4.4.2 K6-2 may be an AICAr kinase in Arabidopsis

If K6-2 is an AICAr kinase *in vivo*, the upregulated purine synthesis in *k6-2* could be a result of either AICAr accumulation or AICA ribonucleotide (AICAR) decrease. AICAr might serve as a signal stimulating purine biosynthesis, or the potentially reduced level of AICAR in *k6-2* might have a stimulating effect on purine biosynthesis. Investigating these hypotheses is challenging since the elevation of the AICAr concentration in *k6-2* can also originate from stimulated purine *de novo* synthesis and AICAR is not detectable in Arabidopsis with our current LC-MS technique. For further study, the LC-MS technology should be optimized to measure AICAR in plant matrix, for example, by finding the optimal mobile phase gradient or energy source conditions for the detection of this compound.

#### 4.4.3 K6-2 is more likely a guanosine kinase

The tendency of decreased GMP content in *k6-2* and increased amount of GMP and GTP in *k6-2::C* (Figure 28), provides a hint that K6-2 might be a guanosine kinase in Arabidopsis even though there is no guanosine accumulation in *k6-2* (Figure 28). The lack of guanosine accumulation could be explained by active guanosine degradation mediated by guanosine deaminase (GSDA, Figure 29). In addition, the apparently enhanced purine *de novo* synthesis in *k6-2* background might be a result of a decreased plastid GMP pool size, because GMP has been reported to be a feedback inhibitor of PRAT (the first enzyme involved in purine biosynthesis) in different species, such as human (Holmes et al., 1973), *E. coli* (Messenger and Zalkin, 1979), and soybean (Reynolds et al., 1984).

GSDA is responsible for the deamination of guanosine to xanthosine, and the absence of *GSDA* leads to the guanosine accumulation in Arabidopsis (Dahncke and Witte, 2013). Straube et al. (2021) have shown that in addition to guanosine, GMP, GTP, and ATP contents also rise in the *GSDA* mutant as a side effect of the increased guanosine pool. By contrast, the IMP content is significantly reduced in *gsda*, which has been interpreted as a consequence of AMP deaminase (AMPD, Figure 29) inhibition by increased concentrations of GMP. However, the drastic IMP decrease in *gsda* shown by Straube et al. (2021) could also be influenced by the reduced *de novo* purine synthesis, which may be a result of the upregulated plastid GMP pool potentially produced by K6-2.

To assess this model, the *K6-2 GSDA* double mutant should be generated and metabolically analyzed in future work. If there was more guanosine in *k6-2 gsda* than in *gsda*, K6-2 will be identified as a guanosine kinase *in vivo*. Other purine metabolites may also vary in these genetic

backgrounds, for example, there would be more IMP in *k6-2 gsd* than in *gsd*, because the feedback inhibition of purine biosynthesis potentially influenced by K6-2 controlled plastid GMP pool should be downregulated in *k6-2 gsd* if this hypothesis was correct. Metabolite analysis can also be performed in *K6-2* variants with external guanosine feeding. After feeding guanine, fewer products of *de novo* purine synthesis, such as IMP, would be expected if this model was true.

### 4.5 Conclusion

Nucleotide metabolism plays an important role in plants, because next to amino acids, sugars and lipids, nucleotides form the fourth major class of central metabolites. PfkB kinases from *Arabidopsis* with potential nucleoside kinase activity have been characterized in this study, leading to the identification of a plastid inosine kinase (PINK). PINK is validated as involved in inosine salvage through different lines of evidence. Evidence has been provided suggesting that PINK acts as a negative inhibitor of purine *de novo* biosynthesis. In addition, PINK possibly contributes to pyrimidine homeostasis by influencing the plastidic UMP pool.

Another member of the PfkB family, kinase 6-2 (K6-2), has been partially characterized in this work. As PINK, it also may be a negative regulator of purine biosynthesis residing in plastids. However, to fully explore the biological function of K6-2 *in vivo*, further analyses are needed.

## References

- Andersson, C.E., and Mowbray, S.L.** (2002). Activation of ribokinase by monovalent cations. *Journal of Molecular Biology* **315**, 409-419.
- Arsova, B., Hoja, U., Wimmelbacher, M., Greiner, E., Üstün, Ş., Melzer, M., Petersen, K., Lein, W., and Börnke, F.** (2010). Plastidial thioredoxin z interacts with two fructokinase-like proteins in a thiol-dependent manner: evidence for an essential role in chloroplast development in *Arabidopsis* and *Nicotiana benthamiana*. *The Plant Cell* **22**, 1498-1515.
- Ashihara, H., Yokota, T., and Crozier, A.** (2013). Biosynthesis and catabolism of purine alkaloids. In *Advances in Botanical Research* (Elsevier), pp. 111-138.
- Ashihara, H., Stasolla, C., Fujimura, T., and Crozier, A.** (2018). Purine salvage in plants. *Phytochemistry* **147**, 89-124.
- Baccolini, C., and Witte, C.-P.** (2019). AMP and GMP catabolism in *Arabidopsis* converge on xanthosine, which is degraded by a nucleoside hydrolase heterocomplex. *The Plant Cell* **31**, 734-751.
- Baez, M., Merino, F., Astorga, G., and Babul, J.** (2008). Uncoupling the MgATP-induced inhibition and aggregation of *Escherichia coli* phosphofructokinase-2 by C-terminal mutations. *FEBS Letters* **582**, 1907-1912.
- Bassett, E.V., Bouchet, B.Y., Carr, J.M., Williamson, C.L., and Slocum, R.D.** (2003). PALA-mediated pyrimidine starvation increases expression of aspartate transcarbamoylase (pyrB) in *Arabidopsis* seedlings. *Plant Physiology and Biochemistry* **41**, 695-703.
- Bellin, L., Del Caño-Ochoa, F., Velázquez-Campoy, A., Möhlmann, T., and Ramón-Maiques, S.** (2021). Mechanisms of feedback inhibition and sequential firing of active sites in plant aspartate transcarbamoylase. *Nature Communications* **12**, 1-13.
- Cabrera, R., Baez, M., Pereira, H.M., Caniuguir, A., Garratt, R.C., and Babul, J.** (2011). The crystal complex of phosphofructokinase-2 of *Escherichia coli* with fructose-6-phosphate: kinetic and structural analysis of the allosteric ATP inhibition. *Journal of Biological Chemistry* **286**, 5774-5783.
- Ceschin, J., Hürlimann, H.C., Saint-Marc, C., Albrecht, D., Violo, T., Moenner, M., Daignan-Fornier, B., and Pinson, B.** (2015). Disruption of Nucleotide Homeostasis by the Antiproliferative Drug 5-Aminoimidazole-4-carboxamide-1- $\beta$ -D-ribofuranoside Monophosphate (AICAR). *Journal of Biological Chemistry* **290**, 23947-23959.



- Chen, M., and Thelen, J.J.** (2011). Plastid uridine salvage activity is required for photoassimilate allocation and partitioning in Arabidopsis. *The Plant Cell* **23**, 2991-3006.
- Chen, M., and Witte, C.-P.** (2020). A kinase and a glycosylase catabolize pseudouridine in the peroxisome to prevent toxic pseudouridine monophosphate accumulation. *The Plant Cell* **32**, 722-739.
- Clough, S.J., and Bent, A.F.** (1998). Floral dip: a simplified method for Agrobacterium-mediated transformation of Arabidopsis thaliana. *The Plant Journal* **16**, 735-743.
- Crozier, A.** (2000). Biosynthesis of hormones and elicitor molecules. *Biochemistry and Molecular Biology of Plants*.
- Dahncke, K., and Witte, C.-P.** (2013). Plant purine nucleoside catabolism employs a guanosine deaminase required for the generation of xanthosine in Arabidopsis. *The Plant Cell* **25**, 4101-4109.
- Daignan-Fornier, B., and Pinson, B.** (2012). 5-Aminoimidazole-4-carboxamide-1-beta-D-ribofuranosyl 5'-monophosphate (AICAR), a highly conserved purine intermediate with multiple effects. *Metabolites* **2**, 292-302.
- Dancer, J.E., Hughes, R.G., and Lindell, S.D.** (1997). Adenosine-5 [prime]-phosphate deaminase (A novel herbicide target). *Plant Physiology* **114**, 119-129.
- Edwards, K., Johnstone, C., and Thompson, C.** (1991). A simple and rapid method for the preparation of plant genomic DNA for PCR analysis. *Nucleic Acids Research* **19**, 1349.
- Frye, M., Harada, B.T., Behm, M., and He, C.** (2018). RNA modifications modulate gene expression during development. *Science* **361**, 1346-1349.
- Gaillard, C., Moffatt, B., Blacker, M., and Laloue, M.** (1998). Male sterility associated with APRT deficiency in Arabidopsis thaliana results from a mutation in the gene APT1. *Molecular and General Genetics* **257**, 348-353.
- Garfinkel, L., Altschuld, R.A., and Garfinkel, D.** (1986). Magnesium in cardiac energy metabolism. *Journal of Molecular and Cellular Cardiology* **18**, 1003-1013.
- Gilkerson, J., Perez-Ruiz, J.M., Chory, J., and Callis, J.** (2012). The plastid-localized pfkB-type carbohydrate kinases FRUCTOKINASE-LIKE 1 and 2 are essential for growth and development of Arabidopsis thaliana. *BMC Plant Biology* **12**, 1-17.
- Girke, C., Daumann, M., Niopek-Witz, S., and Möhlmann, T.** (2014). Nucleobase and nucleoside transport and integration into plant metabolism. *Frontiers in Plant Science* **5**, 443.

- Gopaul, D.N., Meyer, S.L., Degano, M., Sacchetti, J.C., and Schramm, V.L.** (1996). Inosine-uridine nucleoside hydrolase from crithidia fasciculata. Genetic characterization, crystallization, and identification of histidine 241 as a catalytic site residue. *Biochemistry* **35**, 5963-5970.
- Guixé, V., and Merino, F.** (2009). The ADP-dependent sugar kinase family: Kinetic and evolutionary aspects. *IUBMB Life* **61**, 753-761.
- Hanson, A.D., and Gregory III, J.F.** (2002). Synthesis and turnover of folates in plants. *Current Opinion in Plant Biology* **5**, 244-249.
- Heinemann, K.J., Yang, S.-Y., Straube, H., Medina-Escobar, N., Varbanova-Herde, M., Herde, M., Rhee, S., and Witte, C.-P.** (2021). Initiation of cytosolic plant purine nucleotide catabolism involves a monospecific xanthosine monophosphate phosphatase. *Nature Communications* **12**, 1-9.
- Herz, S., Eberhardt, S., and Bacher, A.** (2000). Biosynthesis of riboflavin in plants. The ribA gene of *Arabidopsis thaliana* specifies a bifunctional GTP cyclohydrolase II/3, 4-dihydroxy-2-butanone 4-phosphate synthase. *Phytochemistry* **53**, 723-731.
- Holmes, E.W., McDonald, J., McCord, J., Wyngaarden, J., and Kelley, W.** (1973). Human glutamine phosphoribosylpyrophosphate amidotransferase. *Journal of Biological Chemistry* **248**, 144-150.
- Hung, W.-F., Chen, L.-J., Boldt, R., Sun, C.-W., and Li, H.-m.** (2004). Characterization of *Arabidopsis* glutamine phosphoribosyl pyrophosphate amidotransferase-deficient mutants. *Plant Physiology* **135**, 1314-1323.
- Isner, J.C., Nühse, T., and Maathuis, F.J.** (2012). The cyclic nucleotide cGMP is involved in plant hormone signalling and alters phosphorylation of *Arabidopsis thaliana* root proteins. *Journal of Experimental Botany* **63**, 3199-3205.
- Jung, B., Hoffmann, C., and Möhlmann, T.** (2011). *Arabidopsis* nucleoside hydrolases involved in intracellular and extracellular degradation of purines. *The Plant Journal* **65**, 703-711.
- Jung, B., Flörchinger, M., Kunz, H.-H., Traub, M., Wartenberg, R., Jeblick, W., Neuhaus, H.E., and Möhlmann, T.** (2009). Uridine-ribohydrolase is a key regulator in the uridine degradation pathway of *Arabidopsis*. *The Plant Cell* **21**, 876-891.
- Kazibwe, Z., Soto-Burgos, J., MacIntosh, G.C., and Bassham, D.C.** (2020). TOR mediates the autophagy response to altered nucleotide homeostasis in an RNase mutant. *Journal of Experimental Botany* **71**, 6907-6920.

- Kim, S.-I., and Tai, T.H.** (2011). Identification of genes necessary for wild-type levels of seed phytic acid in *Arabidopsis thaliana* using a reverse genetics approach. *Molecular Genetics and Genomics* **286**, 119-133.
- Klepikova, A.V., Kulakovskiy, I.V., Kasianov, A.S., Logacheva, M.D., and Penin, A.A.** (2019). An update to database TraVA: organ-specific cold stress response in *Arabidopsis thaliana*. *BMC Plant Biology* **19**, 29-40.
- Koncz, C., and Schell, J.** (1986). The promoter of TL-DNA gene 5 controls the tissue-specific expression of chimaeric genes carried by a novel type of *Agrobacterium* binary vector. *Molecular and General Genetics* **204**, 383-396.
- Lee, S., Doxey, A.C., McConkey, B.J., and Moffatt, B.A.** (2012). Nuclear targeting of methyl-recycling enzymes in *Arabidopsis thaliana* is mediated by specific protein interactions. *Molecular Plant* **5**, 231-248.
- Lim, E.K., and Bowles, D.J.** (2004). A class of plant glycosyltransferases involved in cellular homeostasis. *The EMBO Journal* **23**, 2915-2922.
- Liu, Y., and Bassham, D.C.** (2010). TOR is a negative regulator of autophagy in *Arabidopsis thaliana*. *Plos One* **5**, e11883.
- Ma, X., Wang, W., Bittner, F., Schmidt, N., Berkey, R., Zhang, L., King, H., Zhang, Y., Feng, J., and Wen, Y.** (2016). Dual and opposing roles of xanthine dehydrogenase in defense-associated reactive oxygen species metabolism in *Arabidopsis*. *The Plant Cell* **28**, 1108-1126.
- Manguet, S.E., Gakière, B., Majira, A., Pelletier, S., Bringel, F., Guérard, F., Caboche, M., Berthomé, R., and Renou, J.P.** (2009). Uracil salvage is necessary for early *Arabidopsis* development. *The Plant Journal* **60**, 280-291.
- Messenger, L.J., and Zalkin, H.** (1979). Glutamine phosphoribosylpyrophosphate amidotransferase from *Escherichia coli*. Purification and properties. *Journal of Biological Chemistry* **254**, 3382-3392.
- Moffatt, B.A., and Ashihara, H.** (2002). Purine and pyrimidine nucleotide synthesis and metabolism. *The Arabidopsis Book/American Society of Plant Biologists* **1**.
- Moffatt, B.A., Wang, L., Allen, M.S., Stevens, Y.Y., Qin, W., Snider, J., and von Schwanzenberg, K.** (2000). Adenosine kinase of *Arabidopsis*. Kinetic properties and gene expression. *Plant Physiology* **124**, 1775-1785.
- Moffatt, B.A., Stevens, Y.Y., Allen, M.S., Snider, J.D., Pereira, L.A., Todorova, M.I., Summers, P.S., Weretilnyk, E.A., Martin-McCaffrey, L., and Wagner, C.** (2002).

- Adenosine kinase deficiency is associated with developmental abnormalities and reduced transmethylation. *Plant Physiology* **128**, 812-821.
- Mori, H., Iida, A., Teshiba, S., and Fujio, T.** (1995). Cloning of a guanosine-inosine kinase gene of *Escherichia coli* and characterization of the purified gene product. *Journal of Bacteriology* **177**, 4921-4926.
- Nägele, T., Kandel, B.A., Frana, S., Meißner, M., and Heyer, A.G.** (2011). A systems biology approach for the analysis of carbohydrate dynamics during acclimation to low temperature in *Arabidopsis thaliana*. *The FEBS Journal* **278**, 506-518.
- Ogawa, T., Nishimura, K., Aoki, T., Takase, H., Tomizawa, K.-I., Ashida, H., and Yokota, A.** (2009). A phosphofructokinase B-type carbohydrate kinase family protein, NARA5, for massive expressions of plastid-encoded photosynthetic genes in *Arabidopsis*. *Plant Physiology* **151**, 114-128.
- Ohler, L., Niopek-Witz, S., Mainguet, S.E., and Möhlmann, T.** (2019). Pyrimidine salvage: Physiological functions and interaction with chloroplast biogenesis. *Plant Physiology* **180**, 1816-1828.
- Perras, M., and Sarhan, F.** (1984). Energy state of spring and winter wheat during cold hardening. Soluble sugars and adenine nucleotides. *Physiologia Plantarum* **60**, 129-132.
- Pinson, B., Vaur, S., Sagot, I., Couplier, F., Lemoine, S., and Daignan-Fornier, B.** (2009). Metabolic intermediates selectively stimulate transcription factor interaction and modulate phosphate and purine pathways. *Genes & Development* **23**, 1399-1407.
- Pu, Y., Luo, X., and Bassham, D.C.** (2017). TOR-dependent and-independent pathways regulate autophagy in *Arabidopsis thaliana*. *Frontiers in Plant Science* **8**, 1204.
- Rébora, K., Laloo, B., and Daignan-Fornier, B.** (2005). Revisiting purine-histidine cross-pathway regulation in *Saccharomyces cerevisiae*: a central role for a small molecule. *Genetics* **170**, 61-70.
- Reynolds, P.H., Blevins, D.G., and Randall, D.D.** (1984). 5-Phosphoribosylpyrophosphate amidotransferase from soybean root nodules: kinetic and regulatory properties. *Archives of Biochemistry and Biophysics* **229**, 623-631.
- Riegler, H., Geserick, C., and Zrenner, R.** (2011). *Arabidopsis thaliana* nucleosidase mutants provide new insights into nucleoside degradation. *New Phytologist* **191**, 349-359.
- Riggs, J.W., Rockwell, N.C., Cavales, P.C., and Callis, J.** (2016). Identification of the plant ribokinase and discovery of a role for *Arabidopsis* ribokinase in nucleoside metabolism. *Journal of Biological Chemistry* **291**, 22572-22582.

- Riggs, J.W., Cavales, P.C., Chapiro, S.M., and Callis, J.** (2017). Identification and biochemical characterization of the fructokinase gene family in *Arabidopsis thaliana*. *BMC Plant Biology* **17**, 1-18.
- Schoor, S., Farrow, S., Blaschke, H., Lee, S., Perry, G., von Schwartzberg, K., Emery, N., and Moffatt, B.** (2011). Adenosine kinase contributes to cytokinin interconversion in *Arabidopsis*. *Plant Physiology* **157**, 659-672.
- Schroeder, R.Y., Zhu, A., Eubel, H., Dahncke, K., and Witte, C.P.** (2018). The ribokinases of *Arabidopsis thaliana* and *Saccharomyces cerevisiae* are required for ribose recycling from nucleotide catabolism, which in plants is not essential to survive prolonged dark stress. *New Phytologist* **217**, 233-244.
- Senecoff, J.F., McKinney, E.C., and Meagher, R.B.** (1996). De novo purine synthesis in *Arabidopsis thaliana* (II. the PUR7 gene encoding 5 [prime]-phosphoribosyl-4-(N-succinocarboxamide)-5-aminoimidazole synthetase is expressed in rapidly dividing tissues). *Plant Physiology* **112**, 905-917.
- Sharma, P., Sharma, N., and Deswal, R.** (2005). The molecular biology of the low - temperature response in plants. *Bioessays* **27**, 1048-1059.
- Sobczyk, E.b.A., and Kacperska-Palacz, A.** (1978). Adenine nucleotide changes during cold acclimation of winter rape plants. *Plant Physiology* **62**, 875-878.
- Storer, A.C., and Cornish-Bowden, A.** (1976). Concentration of MgATP<sub>2</sub>-and other ions in solution. Calculation of the true concentrations of species present in mixtures of associating ions. *Biochemical Journal* **159**, 1-5.
- Straube, H., Niehaus, M., Zwittian, S., Witte, C.-P., and Herde, M.** (2021). Enhanced nucleotide analysis enables the quantification of deoxynucleotides in plants and algae revealing connections between nucleoside and deoxynucleoside metabolism. *The Plant Cell* **33**, 270-289.
- Uemura, M., Joseph, R.A., and Steponkus, P.L.** (1995). Cold acclimation of *Arabidopsis thaliana* (effect on plasma membrane lipid composition and freeze-induced lesions). *Plant Physiology* **109**, 15-30.
- Usadel, B., Blasing, O.E., Gibon, Y., Retzlaff, K., Hohne, M., Gunther, M., and Stitt, M.** (2008). Global transcript levels respond to small changes of the carbon status during progressive exhaustion of carbohydrates in *Arabidopsis* rosettes. *Plant Physiology* **146**, 1834-1861.

- van der Graaff, E., Hooykaas, P., Lein, W., Lerchl, J., Kunze, G., Sonnewald, U., and Boldt, R.** (2004). Molecular analysis of “de novo” purine biosynthesis in solanaceous species and in *Arabidopsis thaliana*. *Frontiers in Bioscience* **9**, 1803-1816.
- Voinnet, O., Rivas, S., Mestre, P., and Baulcombe, D.** (2003). Retracted: An enhanced transient expression system in plants based on suppression of gene silencing by the p19 protein of tomato bushy stunt virus. *The Plant Journal* **33**, 949-956.
- Wang, B., Grant, R.A., and Laub, M.T.** (2020). ppGpp coordinates nucleotide and amino-acid synthesis in *E. coli* during starvation. *Molecular Cell* **80**, 29-42. e10.
- Werner, A.K., and Witte, C.-P.** (2011). The biochemistry of nitrogen mobilization: purine ring catabolism. *Trends in Plant Science* **16**, 381-387.
- Werner, A.K., Sparkes, I.A., Romeis, T., and Witte, C.-P.** (2008). Identification, biochemical characterization, and subcellular localization of allantoate amidohydrolases from *Arabidopsis* and soybean. *Plant Physiology* **146**, 418-430.
- Wilson, J.E., and Chin, A.** (1991). Chelation of divalent cations by ATP, studied by titration calorimetry. *Analytical Biochemistry* **193**, 16-19.
- Witte, C.-P., and Herde, M.** (2020). Nucleotide metabolism in plants. *Plant Physiology*.
- Witte, C.-P., Noël, L., Gielbert, J., Parker, J., and Romeis, T.** (2004). Rapid one-step protein purification from plant material using the eight-amino acid StrepII epitope. *Plant Molecular Biology* **55**, 135-147.
- Yin, Y., Katahira, R., and Ashihara, H.** (2014). Metabolism of purine nucleosides and bases in suspension-cultured *Arabidopsis thaliana* cells. *European Chemical Bulletin* **3**, 925-934.
- Zrenner, R., Stitt, M., Sonnewald, U., and Boldt, R.** (2006). Pyrimidine and purine biosynthesis and degradation in plants. *Annu. Rev. Plant Biology*. **57**, 805-836

## **Acknowledgement**

First of all, I would like to thank my supervisor Prof. Dr. Claus-Peter Witte, who is moral, wise and venerable. I am grateful to him for the opportunity to start my PhD career at our institute. I have learned a lot from him, not only about the capability to solve scientific problems, but also about his attitude towards life. The experience I obtained from the institute of plant nutrition will be a precious gift in my future life.

I want to give my thanks to Assoc. Prof. Dr. Mingjia Chen for introducing me to Prof. Witte and the helpful suggestions for practical issues. Many thanks to Dr. Marco Herde and Dr. Marina Varbanova-Herde for the critical discussion of my PhD project. Thanks to Dr. Nieves Medina Escobar, a kind and optimistic colleague and lab manager, who keeps our laboratory well organized. Special thanks to Dr. Markus Niehaus for the valuable advice on plant culture.

I appreciate Pro. Dr. Hans-Peter Braun for acceptance of being my co-referee of my dissertation and Prof. Dr. Thomas Pfannschmidt for being the chair of my PhD defense committee.

I extend my thanks to our former and current members in our group, Dr. Chiara Baccolini, Dr. Rebekka Schröder, Dr. Linda Ewert, Dr. Katharina Johanna Heinemann, Dr. Nabila Firdoos, Mr. Henryk Straube, Mr. Jannis Rinne, Miss. Luisa Voß for their company and the unforgettable moment we shared at our institute. Special thanks to André Specht, Hildegard Thölke and Iris Wienkemeier for their technical and paperwork support.

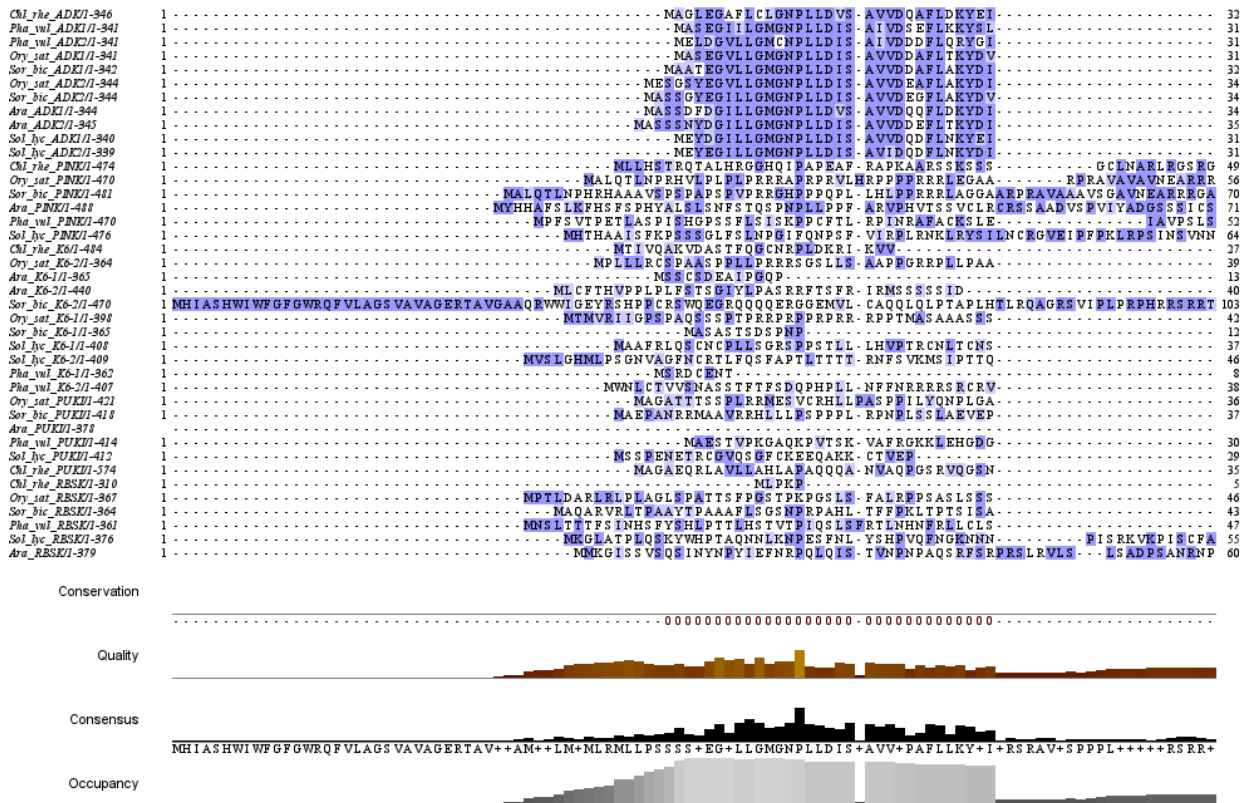
Moreover, I thank the China Scholarship Council (CSC) for the fellowship supporting my stay in Germany. Thanks to the Chinese Embassy in Germany, and the Chinese General Consulate in Hamburg for the help with my life in Germany.

Last but not least, I would like to give my special thanks to my family. Without their love and support, I would never have been able to complete my PhD study in Germany.

# Appendix of Figures

**Figure A-1. Multiple protein sequence alignment of PfkB kinases.**

Protein sequences for ADKs, PUKI, RBSK, PINK, and KINASE 6 from *Arabidopsis thaliana*, *Phaseolus vulgaris*, *Solanum lycopersicum*, *Oryza sativa*, *Sorghum bicolor*, and the algae *Chlamydomonas reinhardtii* were obtained from the Phytozome database. Subsequently, the alignment was obtained using the online tool Muscle (EBI) and the light (dark) blue indicates the similar (identical) amino acid. The conservation, quality, consensus, and occupancy can be found beneath the aligned sequences. The names of the protein being analysed are listed on the left and the Arabic numerals represent the sequential position of the amino acids.





APPENDIX

Table with multiple columns listing protein sequences from various species including Chl\_yke\_ADKI-346, Pha\_wtl\_ADKI-341, Ory\_sat\_ADKI-341, Sor\_btc\_ADKI-342, Ory\_sat\_ADKI-344, Sor\_btc\_ADKI-344, Ara\_ADKI-344, Sol\_hyc\_ADKI-340, Sol\_hyc\_ADKI-339, Chl\_yke\_PNKI-474, Ory\_sat\_PNKI-470, Sor\_btc\_PNKI-470, Ara\_PNKI-470, Pha\_wtl\_PNKI-474, Sol\_hyc\_PNKI-476, Chl\_yke\_K6-404, Ory\_sat\_K6-211-364, Ara\_K6-211-363, Ara\_K6-211-440, Sor\_btc\_K6-211-470, Ory\_sat\_K6-211-398, Sol\_hyc\_K6-211-365, Sol\_hyc\_K6-11-408, Chl\_yke\_K6-211-409, Pha\_wtl\_K6-211-362, Pha\_wtl\_K6-211-407, Ory\_sat\_PUKI-421, Sor\_btc\_PUKI-418, Ara\_PUKI-378, Pha\_wtl\_PUKI-414, Sol\_hyc\_PUKI-412, Chl\_yke\_PUKI-574, Chl\_yke\_RBSKI-310, Ory\_sat\_RBSKI-367, Sor\_btc\_RBSKI-364, Pha\_wtl\_RBSKI-361, Sol\_hyc\_RBSKI-376, Ara\_RBSKI-379.

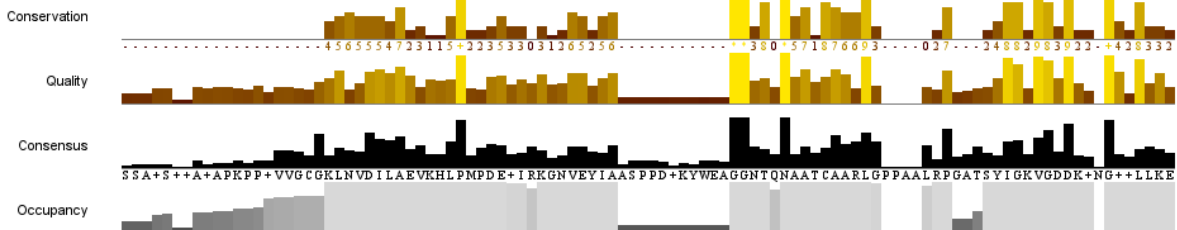
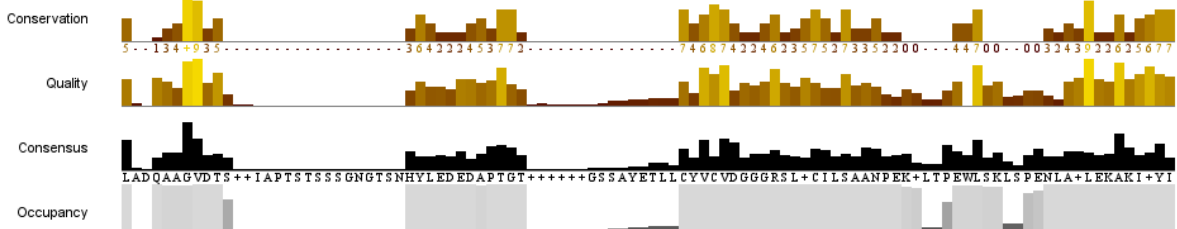
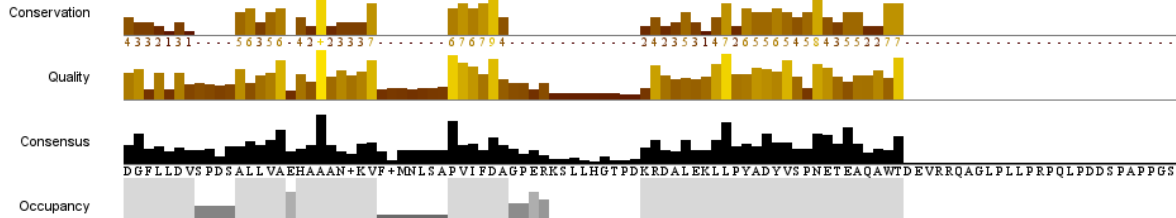


Table with multiple columns showing protein sequence alignments for species like Chl\_yke\_ADKI-346, Pha\_wtl\_ADKI-341, Ory\_sat\_ADKI-341, Sor\_btc\_ADKI-342, Ory\_sat\_ADKI-344, Ara\_ADKI-344, Sol\_hyc\_ADKI-340, Sol\_hyc\_ADKI-339, Chl\_yke\_PNKI-474, Ory\_sat\_PNKI-470, Sor\_btc\_PNKI-470, Ara\_PNKI-470, Pha\_wtl\_PNKI-474, Sol\_hyc\_PNKI-476, Chl\_yke\_K6-404, Ory\_sat\_K6-211-364, Ara\_K6-211-363, Ara\_K6-211-440, Sor\_btc\_K6-211-470, Ory\_sat\_K6-211-398, Sol\_hyc\_K6-211-365, Sol\_hyc\_K6-11-408, Chl\_yke\_K6-211-409, Pha\_wtl\_K6-211-362, Pha\_wtl\_K6-211-407, Ory\_sat\_PUKI-421, Sor\_btc\_PUKI-418, Ara\_PUKI-378, Pha\_wtl\_PUKI-414, Sol\_hyc\_PUKI-412, Chl\_yke\_PUKI-574, Chl\_yke\_RBSKI-310, Ory\_sat\_RBSKI-367, Sor\_btc\_RBSKI-364, Pha\_wtl\_RBSKI-361, Sol\_hyc\_RBSKI-376, Ara\_RBSKI-379.

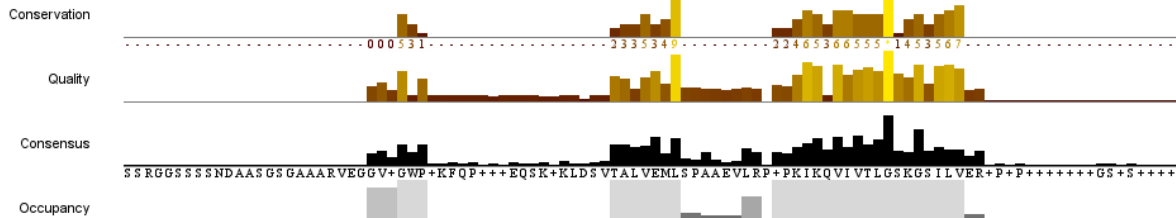


# APPENDIX

<p><i>Chl_yhe_ADEK1-346</i>  <i>Pha_wtl_ADK11-341</i>  <i>Pha_wtl_ADK11-341</i>  <i>Ory_sat_ADK11-341</i>  <i>Sor_bic_ADK11-342</i>  <i>Ory_sat_ADK11-344</i>  <i>Sol_lyc_ADK11-344</i>  <i>Chl_yhe_ADK11-339</i>  <i>Chl_yhe_PNNK1-474</i>  <i>Ory_sat_PNNK1-470</i>  <i>Sor_bic_PNNK1-481</i>  <i>Ara_PNNK1-488</i>  <i>Pha_wtl_PNNK1-470</i>  <i>Sol_lyc_PNNK1-476</i>  <i>Chl_yhe_K61-404</i>  <i>Ory_sat_K6-211-364</i>  <i>Ara_K6-211-365</i>  <i>Ara_K6-211-440</i>  <i>Sor_bic_K6-211-470</i>  <i>Ory_sat_K6-111-398</i>  <i>Sor_bic_K6-111-365</i>  <i>Sol_lyc_K6-111-408</i>  <i>Sol_lyc_K6-211-409</i>  <i>Pha_wtl_K6-111-362</i>  <i>Pha_wtl_K6-211-407</i>  <i>178 DANLS PD</i>  <i>Sor_bic_PUKU1-418</i>  <i>Ara_PUKU1-371</i>  <i>Pha_wtl_PUKU1-412</i>  <i>Sor_bic_PUKU1-412</i>  <i>Chl_yhe_PUKU1-574</i>  <i>Chl_yhe_RBSK1-310</i>  <i>Ory_sat_RBSK1-367</i>  <i>Sor_bic_RBSK1-364</i>  <i>Pha_wtl_RBSK1-361</i>  <i>Sol_lyc_RBSK1-376</i>  <i>Ara_RBSK1-379</i></p>	<pre> 165 TGFFITVSPASIEHVAKHCAENDKIYANGLSAPFIVQVPP.....FKKVLMDSPYIDFLFGNEIEAALAA.....330 164 AGFFITVSPDSIQLVAEHAANKLFSMNLSPAFICEF.....FRBLERALPYDVFVFGNETEARTFS.....327 164 AGFFITVSPDSIQLVAEHAANKLFSMNLSPAFICEF.....FKALVFLPYDVFVFGNETEARTFS.....327 164 AGFFITVSPDSIQLVAEHAANKLFSMNLSPAFICEF.....FRDAQEKVLPYDVFVFGNETEARTIFA.....327 165 AGFFITVSPDSIQLVAEHAANKLFSMNLSPAFICEF.....FRDAQEKVLPYADYVFGNETEARTIFA.....328 167 AGFFITVSPDSIQLVAEHAANKLFSMNLSPAFICEF.....FRDAQEKALPYADYVFGNETEARTIFA.....330 167 AGFFITVSPDSIQLVAEHAANKLFSMNLSPAFICEV.....FRDAQEKALPYDVFVFGNETEARTFA.....330 167 AGFFITVSPDSIQLVREHAANNKVFVFMNLSPAFICEF.....FKDVOEKCLPYDVFVFGNETEARTFS.....330 168 AGFFITVSPDSIQLVSEHAANNKVFVFMNLSPAFICEF.....FKDVOEKFLPYDVFVFGNETEARTFS.....331 164 AGFFITVSPDSIQLVAEHAANNKIFSMNLSPAFICEF.....FRDPQEKALPYDVFVFGNETEARTFS.....327 163 AGFFITVSPDSIQLVAEHAANNKVFVFMNLSPAFICEF.....FKDQOEVKLPYDVFVFGNETEARTFS.....326 243 NGFIIDDELQVQAVCVLDAISQGA.....AIFDPPGRRCQTMIEGP.....RRAALDLLDLSDCVMLMTEEAHVVT.....310 227 NGYAFDELFPDVISSAIDCAIDAGT.....AVFFDPPGRGKSLHGLTLDORALEHSLRLSDVLLTSDAESLT.....296 239 NGYAFDELFPDVIASSIDCAIDSGT.....AVFFDPPGRGKSLHGLTLDORALEHSLRFSDVLLTSDAESLT.....308 242 NGYDFDDFSPFIMSTIDYAAKVG.....AIFDPPGRGKSLKGTDPERRALAHFLRMSDVLLTSDAEVALT.....311 228 NGYDFDELSPGAILSEMEYAVEVGT.....SIFDPPGRGKSLTSGSPDEQRALNQLRMSDVLLTSDAESLA.....297 234 NGYDFDELSPALLESALCAVESGT.....SIFDPPGRGKSLIAGRREBQIIGLITMSVLLTSDAEASLT.....303 161 DERTFEA.....ALLVA-REARRGIT.....PVVVEA-ER.....LRPGQLLEADFFVTSAAHPDQWT.....314 185 DGYSD EM.....ALAVA-KOADMCKI.....PILVDAEER.....TRELGLLGLSLASVIVCNGKFPPEKW.....240 151 NGRSREA.....ELLVA-QKAHSKNI.....PILINA-EK.....KRTGLDELIDLADYAICTSNFPQEW.....204 187 DVRLHET.....ALLVA-KEASRKKI.....PILVDT-EK.....KRDGLDDELFPADYVVCENFPQWT.....240 255 DVRLHET.....ALLVA-EASQRKI.....PILIDA-ER.....KREGLDELNFASVYVVCYAKFPQWT.....308 183 DVRLHET.....ALLVA-EASQRKI.....PILIDA-ER.....KRDGLDELNFASVYVVCYAKFPQWT.....236 150 DVRLHET.....ALLVA-EASRRKI.....PILIDA-EK.....KREGLDELNFATVYVVCYAKFPQWT.....203 178 DEVEQTEELVAEVA-REARRGIT.....PILVDA-ES.....KREVDDELNFATVYVVCYAKFPQWT.....335 193 DGRLEHT.....AAVVA-EAARRGI.....PILIDA-ER.....KREGLDELNFASVYVVCYAKFPQWT.....246 146 DGRLEHT.....ALVVA-HEAVKKNI.....PILMDA-ER.....LREGLDDELNFATVYVVCYAKFPQWT.....199 185 DGRLEPDT.....ALVVA-QEAVKKNI.....PILIDA-ER.....PREGLDDELNFATVYVVCYAKFPQWT.....234 178 DANLS PD.....SLEAAKIAHESGV.....PVVVEPVSVA.....KGSRIAPIAKYVITVTSVNEIELVAMA.....238 174 DANLPEP.....SLEAAKIAHESGV.....PVVVEPVSVA.....KSRRIAPVAEYITVTSVNEIELVAMA.....230 135 DANLSSIL.....ALEASCKIAEESV.....PVVVEPVSVA.....KSRRIASIAKYVITVTSVNEIELVAMA.....191 167 DANMHP.....SLEAAKMAIDMEG.....PVVVEPVSVA.....KSRRIASIAKYVITVTSVNEIELVAMA.....233 178 DANLSSIL.....SLEAAKIAHESGV.....PVVVEPVSVA.....KSRRIASIAKYVITVTSVNEIELVAMA.....235 185 EANLS EG.....ALEYVCRTAARV.....PVVVEPVSVA.....KAARLRLPYATVTSVNEIELVAMA.....208 139 QREIPEP.....VNVVAKLAAAGV.....PVVVEPVSVA.....EGPIDPTLPLCALLSPNETELARLT.....194 194 QREIPDW.....VNAQAAKAGV.....PVVVEPVSVA.....DAPVPEGLLSVDFVSPNETELARLT.....249 191 QREIPDW.....VNAQAAKAGV.....PVVVEPVSVA.....DAPVPEGLLSVDFVSPNETELARLT.....246 191 QREIPDY.....VNAQAAKAGV.....PVVVEPVSVA.....DGPVPEGLLSVDFVSPNETELARLT.....246 206 QREIPDF.....VNIQVAKAARV.....PVVVEPVSVA.....DSPPELLELRCVEVSPNETELARLT.....261 208 QREIPDS.....INIQVAKAARV.....PVVVEPVSVA.....DTPINELLSVDFVSPNETELARLT.....263 </pre>
--	---

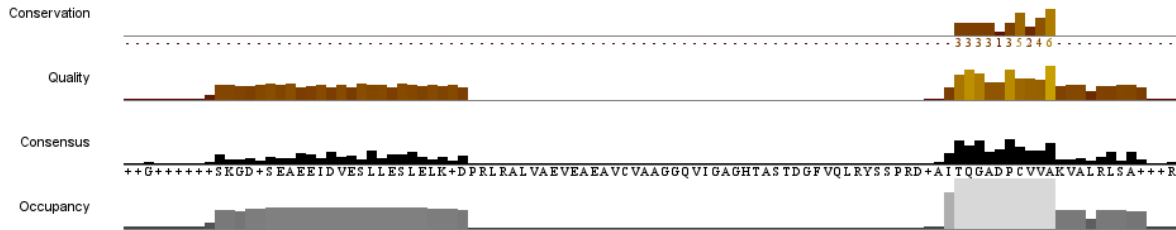


<p><i>Chl_yhe_ADEK1-346</i>  <i>Pha_wtl_ADK11-341</i>  <i>Pha_wtl_ADK11-341</i>  <i>Ory_sat_ADK11-341</i>  <i>Sor_bic_ADK11-342</i>  <i>Ory_sat_ADK11-344</i>  <i>Sor_bic_ADK11-344</i>  <i>Ara_ADK11-344</i>  <i>Ara_ADK11-345</i>  <i>Sol_lyc_ADK11-340</i>  <i>Sol_lyc_ADK11-339</i>  <i>Chl_yhe_PNNK1-474</i>  <i>Ory_sat_PNNK1-470</i>  <i>Sor_bic_PNNK1-481</i>  <i>Ara_PNNK1-488</i>  <i>Pha_wtl_PNNK1-470</i>  <i>Sol_lyc_PNNK1-476</i>  <i>Chl_yhe_K61-404</i>  <i>Ory_sat_K6-211-364</i>  <i>Ara_K6-211-365</i>  <i>Ara_K6-211-440</i>  <i>Sor_bic_K6-211-470</i>  <i>Ory_sat_K6-111-398</i>  <i>Sor_bic_K6-111-365</i>  <i>Sol_lyc_K6-111-408</i>  <i>Sol_lyc_K6-211-409</i>  <i>Pha_wtl_K6-111-362</i>  <i>Pha_wtl_K6-211-407</i>  <i>Ory_sat_PUKU1-418</i>  <i>Ara_PUKU1-371</i>  <i>Pha_wtl_PUKU1-412</i>  <i>Sor_bic_PUKU1-412</i>  <i>Chl_yhe_PUKU1-574</i>  <i>Chl_yhe_RBSK1-310</i>  <i>Ory_sat_RBSK1-367</i>  <i>Sor_bic_RBSK1-364</i>  <i>Pha_wtl_RBSK1-361</i>  <i>Sol_lyc_RBSK1-376</i>  <i>Ara_RBSK1-379</i></p>	<pre> 231 .....ASRGWE.....GLSLEEV.....AKKMSRMPKANGCRP RVVV.....363 231 .....KVGWGE.....GIVEVEE.....AKKMSRMPKANGCRP RVVV.....359 232 .....KVGWGE.....DDNVEEI.....ALKISQPLKASGTHKRITV.....259 232 .....KVRGWE.....TENVEEI.....ALKISQPLKASGTHKRITV.....259 231 .....KVRGWE.....TENIEEI.....ALKISQPLKASGTHKRITV.....260 239 .....KVRGWE.....TENVEEI.....ALKISQPLKASGTHKRITV.....262 231 .....KVRGWE.....TENVEEI.....AWKISQPLKASGTHKRITV.....262 231 .....KVRGWE.....DDVEEI.....AKKMSQPLKASGTHKRITV.....262 233 .....KVRGWE.....TENVEEI.....ALKISQPLKASGTHKRITV.....331 232 .....KVRGWE.....DDNVEEI.....ALKISQPLKASGTHKRITV.....259 237 .....RVHGWE.....DDNVEEI.....ALKISQPLKASGTHKRITV.....258 311 .....GLQDAE.....EAAKRWL.....ARFNARAQVVVVKMGANGAVLCTE.....347 297 .....NIRNPI.....QAGQELL.....KR-GIRTKVWVVKMGSKGSIMV.....340 309 .....TIRNPI.....QAGQELL.....KR-GVRTKQVVVKMGSKGSIMV.....342 310 .....GIRNPI.....RAGQELLRN.....GKGTWVVKMGSKGSIMV.....345 298 .....GIEDPI.....LAGQEFF.....KR-GIRTKVWVVKMGSKGSIMV.....331 304 .....GIEDPI.....LAGQELLN.....GKGTWVVKMGSKGSIMV.....337 215 .....GEAVLA.....DALATA.....HR-LPSARWVITLGRGVSLLFRPPPPAGTGGGSGSGNGS.....269 241 .....SVPSP.....SALLEIE.....LQ-YPRACFAVVTLGGNGMMLER.....276 241 .....GAPSSP.....SALLSML.....LR-LPKLKFVIMTLGEGCVMMLER.....240 241 .....EVSSTP.....GALVSM.....LR-LPKLKFVITVSGEGCLMMLER.....274 309 .....GASSIP.....AALVSM.....SR-LPNIKFVITVLEKGLMLER.....344 237 .....GASSIP.....VALVSM.....LR-LPNIKFVITVLEKGLMLER.....273 206 .....GASSIP.....VALVSM.....LR-LPNIKFVITVLEKGLMLER.....239 247 .....EASIP.....AALVSM.....LR-LPNIKFVITVLEKGLMLER.....271 247 .....EASIP.....TALVSM.....LR-LPKVVFVITVLEKGLMLER.....282 200 .....EASTVP.....KALVSM.....LR-LPNIKFVITVLEKGLMLER.....235 235 .....EASTVP.....QALVSM.....LM-LPNIKFVITVLEKGLMLER.....274 231 .....NSLSPPEKYTVKMEQSKNKAKAVEYLFEMLSPAMFFLL.....EKGIKLLITVLSGNGVVIC.....292 231 .....NSLSPVKNYVHKIEQPKESDAVEYLFEMLSPAMFFLL.....EKGIKLLITVLSGNGVVIC.....288 192 .....NALCARNLPHFRSDEN.....KL-SIEDMFAKPAIIVLL-KNGVWVVKMGSKGSIMV.....246 224 .....NALSGSDEFPQLKESQKRNISWVLEPQLKPAIIVLL.....EKGVVWVVKMGSKGSIMV.....279 221 .....NAVSGHDIQPIRRDDSTL.....SKESFPQTKPAIIVLL-DKGVVWVVKMGSKGSIMV.....277 269 <b>SSRGSSSSSNDAAASGSAAARVEGGGVS</b>GGNGGAGAGDP<b>VAELLR</b>OLTAFAEVVLL<b>LOGTLG</b>VVVLGSLGAAIITL<b>GPAP</b>EDAAAAAGSSSSS.....371 195 .....GLP.....DTEAQVQAAAEQLM-SAGVKSVLVKGADGSLLL.....231 250 .....GMP.....TETFEQISRAAGACH-KMGVKEVLVKGSGSALF.....286 247 .....GMP.....TETFEQISRAAGACH-KMGVKEVLVKGSGSALF.....283 247 .....GMP.....TOSFEQIAAALKCH-ELGVKQILVKGSGSALF.....283 262 .....KMP.....TGNFEQISNAVEQCY-DMGVNQVLVKGSGSALF.....308 264 .....GMP.....TETFEQISQVAKCH-KLGVKQILVKGSGSALF.....308 </pre>
---	--



# APPENDIX

<i>Chi_yhc_ADEK1-346</i>	263	.....FTGGCDFTIVA.....	273
<i>Pha_ywl_ADEK1-341</i>	260	.....ITQGADPVCVA.....	270
<i>Pha_ywl_ADEK1-341</i>	260	.....ITQGADPVCVA.....	270
<i>Ory_sai_ADEK1-341</i>	260	.....ITQGADPVCVA.....	270
<i>Sor_bic_ADEK1-342</i>	261	.....ITQGADPVCVA.....	271
<i>Ory_sai_ADEK1-344</i>	263	.....ITQGCDPVCVA.....	273
<i>Sor_bic_ADEK1-344</i>	263	.....ITQGCDPVCVA.....	273
<i>Ara_ADEK1-344</i>	263	.....ITQGADPVCVA.....	273
<i>Ara_ADEK1-345</i>	264	.....ITQGADPVCVA.....	274
<i>Sor_bic_ADEK1-340</i>	260	.....ITQGADPVCVA.....	269
<i>Sol_bic_ADEK1-339</i>	259	.....ITQGADPVCVA.....	269
<i>Chi_yhc_PUNK1-474</i>	348	.....GDAESHGSGAA.....	358
<i>Ory_sai_PUNK1-470</i>	331	.....TKSAVSSAPAS.....	340
<i>Sor_bic_PUNK1-481</i>	343	.....TKSTVSCAPAA.....	352
<i>Ara_PUNK1-488</i>	346	.....TKSSVSVAPAA.....	355
<i>Pha_ywl_PUNK1-470</i>	332	.....TASNIAICAPG.....	341
<i>Sol_bic_PUNK1-476</i>	338	.....TKSSITCAPAA.....	347
<i>Chi_yhc_K6-1-404</i>	270	<b>GNGSGNGSGSGGGVAVVAPGVRALHDVLELELPRRLRALVAEVEAEAVCVAAAGGQVIGAGHTAS TDGFPVQLRYSS PRDRA</b> .....QEAATAAAVAARERAAALNADSGR.....	373
<i>Ory_sai_K6-2/1-364</i>	277	.....GKDGGENYETEDVDIENVAESILRLKVD.....	321
<i>Ara_K6-2/1-365</i>	241	.....CSSEVSGSEEBETDIDELHESLKOSID.....	283
<i>Ara_K6-2/1-440</i>	277	.....ASKAEVFESEQETDIESLLETLEKHKVD.....	321
<i>Sor_bic_K6-2/1-470</i>	345	.....STTDASEAGEIDAALFESLEKHKVD.....	389
<i>Ory_sai_K6-1/1-398</i>	273	.....STTDASEAEIDVESLLESLEKKEV.....	317
<i>Sor_bic_K6-1/1-365</i>	240	.....STIDASEADKIDIEALLESLEKKEV.....	284
<i>Sol_bic_K6-1/1-408</i>	272	.....AEADLQSEEDVDLEFKKMGQSLD.....	315
<i>Sol_bic_K6-2/1-409</i>	283	.....TEMQVLLPEEMDVEVLFKKNLEED.....	336
<i>Pha_ywl_K6-1/1-362</i>	236	.....FNFGPSTEEQVQDLESLEKKN.....	279
<i>Pha_ywl_K6-2/1-407</i>	275	.....RV.DGQSTEEVNVDSLLESLEKKN.....	317
<i>Ory_sai_PUKK1-421</i>	293	.....CKESTSLMDQRKSEMMSTP.....	333
<i>Sor_bic_PUKK1-418</i>	289	.....CKEHTNFMKDQRKCKQTRFSKQ.....	330
<i>Ara_PUKK1-371</i>	247	.....SKGNPKKALNIDRRFLRSGEVFKK.....	281
<i>Pha_ywl_PUKK1-414</i>	280	.....NKGQPRHFENPPEKTRSGFGGQLY.....	317
<i>Sol_bic_PUKK1-412</i>	278	.....SKAEFNLQRLAFKNGMSPT.....	317
<i>Chi_yhc_PUKK1-574</i>	372	<b>STGLEPVDACSSCSSCGMSGSGSSYDAVAR</b> .....	428
<i>Chi_yhc_RBSK1-310</i>	232	.....PPGPOPLRQA.....	242
<i>Ory_sai_RBSK1-367</i>	287	.....IEGGEPIRQP.....	296
<i>Sor_bic_RBSK1-364</i>	284	.....VEGEEPIRQP.....	293
<i>Pha_ywl_RBSK1-361</i>	284	.....VEGEEKIQP.....	293
<i>Sol_bic_RBSK1-376</i>	299	.....TKGEEPIRQP.....	308
<i>Ara_RBSK1-379</i>	301	.....IQGEEKIQS.....	310



<i>Chi_yhc_ADEK1-346</i>	274	.....VGF.....	325
<i>Pha_ywl_ADEK1-341</i>	271	.....EDG.....	322
<i>Pha_ywl_ADEK1-341</i>	271	.....EDG.....	322
<i>Ory_sai_ADEK1-341</i>	271	.....EDG.....	322
<i>Sor_bic_ADEK1-342</i>	272	.....EDG.....	323
<i>Ory_sai_ADEK1-344</i>	274	.....DDG.....	325
<i>Sor_bic_ADEK1-344</i>	274	.....DDG.....	325
<i>Ara_ADEK1-344</i>	274	.....EDG.....	325
<i>Ara_ADEK1-345</i>	275	.....EDG.....	326
<i>Sol_bic_ADEK1-340</i>	270	.....EDG.....	326
<i>Sol_bic_ADEK1-339</i>	270	.....EDG.....	326
<i>Chi_yhc_PUNK1-474</i>	359	.....RVTLASIAALPKAEAVDITGAGDSFIESLYGVGTGMSLPGEMRLGAVV.....	452
<i>Ory_sai_PUNK1-470</i>	341	.....-APTTIYMGAVKVDVVDITVGCSDSFAAIIVMGFINGWAPDVTLGLANAV.....	406
<i>Sor_bic_PUNK1-481</i>	353	.....FKIDVVDITVGCSDSFTAIIAFGFLHNLPAVSTLTLANAV.....	379
<i>Ara_PUNK1-488</i>	356	.....FKINVVDITVGCSDSFTAIIAFGFLHLDPAVNTLTLANAV.....	391
<i>Pha_ywl_PUNK1-470</i>	342	.....PKVEVVDITVGCSDSFVAIIALGYIRNMDLVNLTIANAV.....	394
<i>Sol_bic_PUNK1-476</i>	348	.....PKVNVVDITVGCSDSFVAIIAYGIRHMLVNTLAIANAV.....	380
<i>Chi_yhc_K6-1-404</i>	274	<b>GAAYAGSGTSAAGAGGGGGGAAGS</b> SGLVA.....	374
<i>Ory_sai_K6-2/1-364</i>	322	.....BSGNIFA.....	360
<i>Ara_K6-2/1-365</i>	284	.....GNVTE.....	337
<i>Ara_K6-2/1-440</i>	322	.....GVGTMTE.....	377
<i>Sor_bic_K6-2/1-470</i>	390	.....GVGSISE.....	445
<i>Ory_sai_K6-1/1-398</i>	318	.....GIGSISE.....	373
<i>Sor_bic_K6-1/1-365</i>	285	.....GIGSING.....	340
<i>Sol_bic_K6-1/1-408</i>	316	.....GIGVVSSE.....	371
<i>Sol_bic_K6-2/1-409</i>	327	.....GIGTITE.....	382
<i>Pha_ywl_K6-1/1-362</i>	280	.....GIGTVFE.....	335
<i>Pha_ywl_K6-2/1-407</i>	318	.....GIGTVSE.....	373
<i>Ory_sai_PUKK1-421</i>	334	.....RTCVHFPAVS-ASVVSITGAGDCLVGGVLSALCGFDIISVAIGVAI.....	384
<i>Sor_bic_PUKK1-418</i>	331	.....RTCVHFPAIS-ASVISITGAGDCLVGGVLSALCGFDIISVAIGVAI.....	381
<i>Ara_PUKK1-371</i>	282	.....SIFANHPPTIE-ARKVKLITGAGDCLVGGTVASISDLDLISLAVGLAS.....	337
<i>Pha_ywl_PUKK1-414</i>	318	.....HIFAVHFPPLA-ASVVRILTGAGDCLVGGTFLSICAGLDIMQSIVAGV.....	374
<i>Sol_bic_PUKK1-412</i>	319	.....NIFAVHFPALB-ASVVRILTGAGDCLVGGTFLSICAGLDIMQSIVAGV.....	373
<i>Chi_yhc_PUKK1-574</i>	428	<b>YCRCRIRGANISHVHPGPPPSFLNRS</b> LTSAAVAGAGPAAAAATAS PPPPAARAPYRLD VVHLRALD.....	531
<i>Chi_yhc_RBSK1-310</i>	243	.....AIRAEQVVDITGAGDCTATYAVAVLQKAPARALRFASAA.....	283
<i>Ory_sai_RBSK1-367</i>	297	.....IIPATEVVDITGAGDTFTSAFAVALVEGPKKEECMRFAAAA.....	337
<i>Sor_bic_RBSK1-364</i>	294	.....IIPATEVIDITGAGDTFTSAFAVALVEGPKKEECMRFAAAA.....	334
<i>Pha_ywl_RBSK1-361</i>	294	.....IIPAKTVVDITGAGDTFTAAFAVALVEGSKKEECLRFAAAA.....	334
<i>Sol_bic_RBSK1-376</i>	309	.....IIPAAKVVDITGAGDTFTAAFAVALVEGSKKEECLRFAAAA.....	349
<i>Ara_RBSK1-379</i>	311	.....IIPAAQVVDITGAGDTFTAAFAVANVEGSKHEECLRFAAAA.....	351



APPENDIX

<i>Chi_yhe_ADKI1-346</i>	336	ANVIQRSGCTF	FAKPTFTWN	346
<i>Pha_ywl_ADKI1-341</i>	333	ANVIQRSGCTY	PEKPDFH	341
<i>Pha_ywl_ADKI1-341</i>	333	ANVIQRPGCTY	PEKPDFH	341
<i>Ory_sat_ADKI1-341</i>	333	ANVIQRSGCTY	PEKPDFN	341
<i>Sor_bic_ADKI1-342</i>	334	ANVIQRPGCTY	PEKPDFN	342
<i>Ory_sat_ADKI1-344</i>	336	ANVIQRSGCTY	PEKPDFN	344
<i>Sor_bic_ADKI1-344</i>	336	ANVIQRSGCTY	PEKPDFN	344
<i>Ara_ADKI1-344</i>	336	SNVVIQRSGCTY	PEKPDFN	344
<i>Ara_ADKI1-345</i>	337	SNVVIQRSGCTY	PEKPDFH	345
<i>Sol_hyc_ADKI1-340</i>	332	SNVIQRSGCTY	PEKPDFA	340
<i>Sol_hyc_ADKI1-339</i>	332	SNVIQRPGCTY	PEKPDF	339
<i>Chi_yhe_PNKI1-474</i>	407	GGATATGRGAGRNV	VARPETVLRLLGEGAAGGVNAEQRAAFQAKGLLQOLAKAQRGLAQGLSAAA	474
<i>Ory_sat_PNKI1-470</i>	380	GAATATGCGAGRNV	AHLDKVLQLLRESNINEDDTPWSELI EASFCEVSVLSK-TAVNSFSDR-LVHVPTCNVVSNLLS MLEAVSERSTVQA	470
<i>Sor_bic_PNKI1-481</i>	392	GAATATGCGAGRNV	ARLDKVLQLLKEADLNEEDT-WTELI EAGNSLCIEVSIMS G-MARNGFGGER-LVHVPTKVVSDILPMFEAVSERSAVQA	481
<i>Ara_PNKI1-488</i>	395	GAATANGCGAGRNV	AKRHQVVDLMKASKLNDEKFFEQLLAEENSESRINLLSKGMIKDGRSNKQIETISMEKVVSELLELLELGRCCVKAAS	488
<i>Pha_ywl_PNKI1-470</i>	381	GAATANGCGAGRNV	ARLEKVVIELRSSNLS EDDDFWFDILEKNVVSQEIITVLSN-VMNGNRNH-LNLVSEFDNVAS ELLPRLERLPESTVGNVST	470
<i>Sol_hyc_PNKI1-476</i>	387	GAATATGCGAGRNV	ASLGKVVQLKERNLNEDK EKWDEVLNDNVNSRDTLLSK-VMVNGNSQ-VHRVSLQKVSV EVELKLEFPKMTGSPK	476
<i>Chi_yhe_K6-1-484</i>	453	AAAKCNRIGARGL	ETRCSSLRDLLHEEGR	484
<i>Ory_sat_K6-2/1-364</i>	361	-----RHQM	-----	364
<i>Ara_K6-1/1-365</i>	338	AACCCRGLGARTSL	PYRTDPNLATFLGT	365
<i>Ara_K6-2/1-440</i>	378	AGCS CRALGARTSL	PHRTDPRLVPFLSSASWRKLRNFEFVNGSSVIGGIS CVSIHNRANRE	440
<i>Sor_bic_K6-2/1-470</i>	446	AGCGCRGLGARS SL	PHVTD PRLAGY	470
<i>Ory_sat_K6-1/1-398</i>	374	AACGCRGLGARTAL	PHRTDPRLVAY	398
<i>Sor_bic_K6-1/1-365</i>	341	AGCGCRGLGARS SL	PHRTD QRLVGY	365
<i>Sol_hyc_K6-1/1-408</i>	372	AGTGCRALGARAGL	PGLTDPRLKPFELVNDQNVAATLL	408
<i>Sol_hyc_K6-2/1-409</i>	383	AAIKCRALGARAGL	PRSTDHRLSPFLV	409
<i>Pha_ywl_K6-2/1-362</i>	336	AASKCRAIGARTGL	PYHTD PCLAFNG	362
<i>Pha_ywl_K6-2/1-407</i>	374	AGAKCRDLGARSGL	PYRADPRLSFILEKLGSSS	407
<i>Ory_sat_PUKI1-421</i>	385	AKSSVES EANI PDKFSA	ATIADDAERTLLS AKMNVCK	421
<i>Sor_bic_PUKI1-418</i>	382	AKASVES EANI PDDISA	AS IADDAQCVLHSAKVVVWCK	418
<i>Ara_PUKI1-371</i>	338	AKAAVES DDNV PPEFKL	DLISGD AELVYNGAKMLMVHQSME	378
<i>Pha_ywl_PUKI1-414</i>	375	AKAAVEA EANV PNTFML	SAIADDAKSYSNKLVLFHQSME	414
<i>Sol_hyc_PUKI1-412</i>	373	AKVVVEVES NVDP EYCL	ARLADDAERS VYSSATMNLIGQSKL	412
<i>Chi_yhe_PUKI1-574</i>	532	AKRAVQSVSNVPELCAADWAPNEADAEAVAATARRYSFPAAVS	-----	574
<i>Chi_yhe_RBSK1-310</i>	284	ASICVQRGAMPSSL	PARAEVDTLLAKQ	310
<i>Ory_sat_RBSK1-367</i>	338	ASLCVQVKGAIPSM	PD RKSVMDDLLESVQVE	367
<i>Sor_bic_RBSK1-364</i>	335	ASLCVVRVKGAIPSM	PD RKSVMKLLDSAKVE	364
<i>Pha_ywl_RBSK1-361</i>	335	ASLCVQVKGASPSM	PD RKS VLDILINRQ	361
<i>Sol_hyc_RBSK1-376</i>	350	ASLCVQVKGAIPSM	PEKRAVFNLLQSA	376
<i>Ara_RBSK1-379</i>	352	ASLCVQVKGAIPSM	PD RKSVMKLLKQSI	379

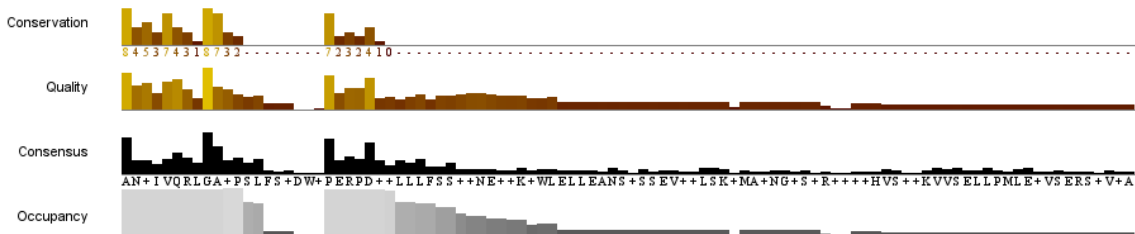


**Figure A-2. Expression overviews of *pink* and *k6-2* in Arabidopsis.**

Expression overviews of (A) *pink* and (B) *k6-2* were obtained from Arabidopsis eFP Browser 2.0. From yellow to red, sequentially representing higher gene expression (indicated).

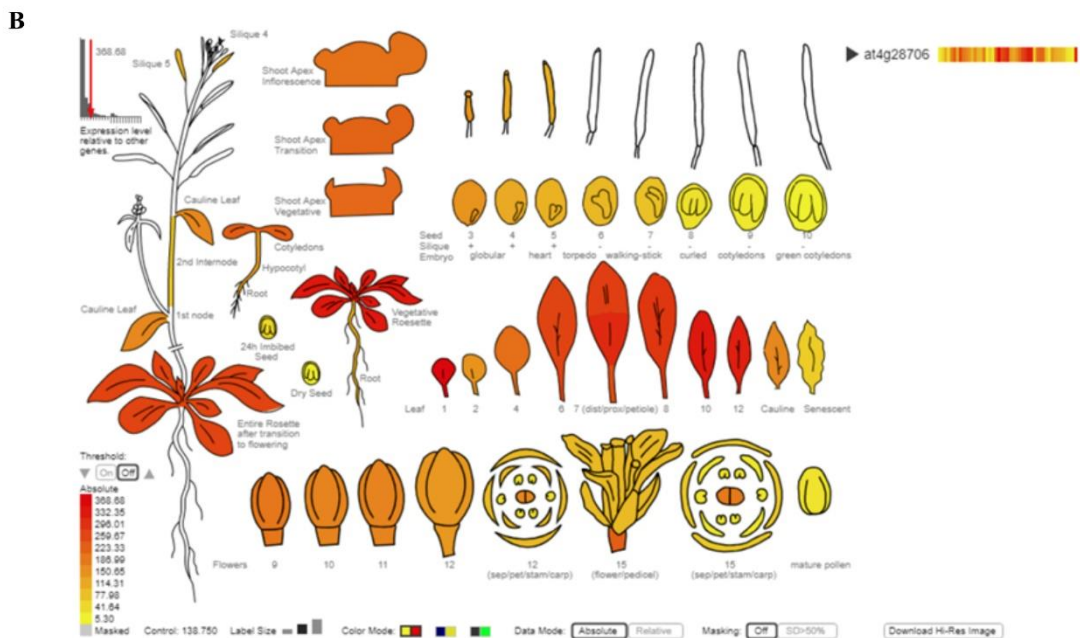
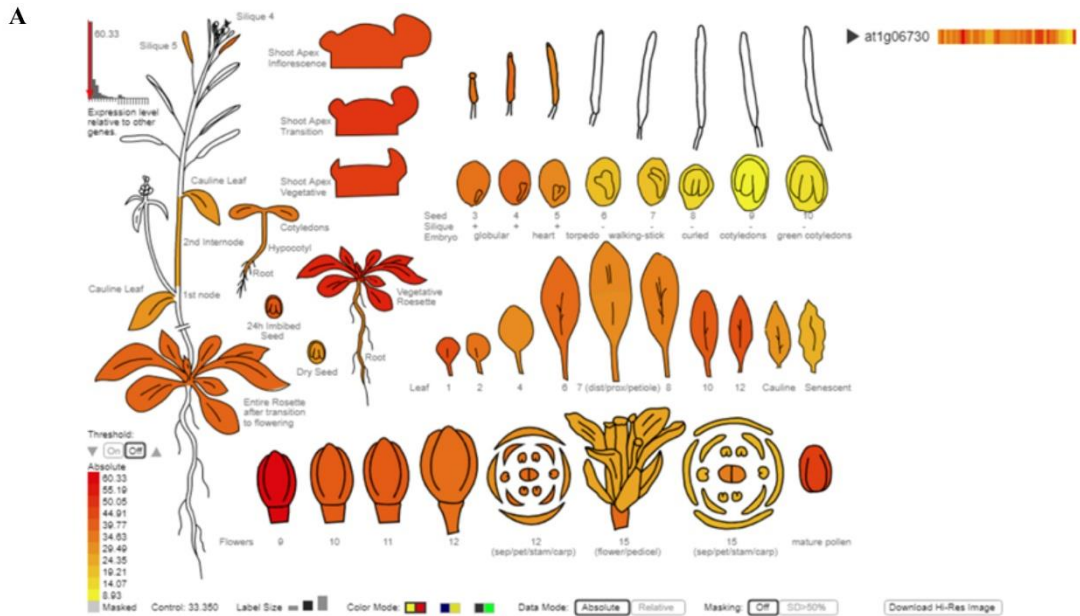


### Figure A-3. Metabolite analysis in seedlings of the *PINK* mutant under different light conditions.

(A) Purine, (B) pyrimidine, and (C) AICAr contents in 10-day-old seedlings of wild type and *pink*. Error bars are SD (n = 3 biological replicates). An unpaired t test was used for statistical analysis in each treatment group. 0 h light, the seedlings were harvested at the end of the night; 3 h light, the seedlings were harvested 3 h after the end of the night; 3 h dark, the seedlings were harvested 3 h after the end of the normal night, but the night was prolonged and these seedlings were not exposed to light. FW, fresh weight.

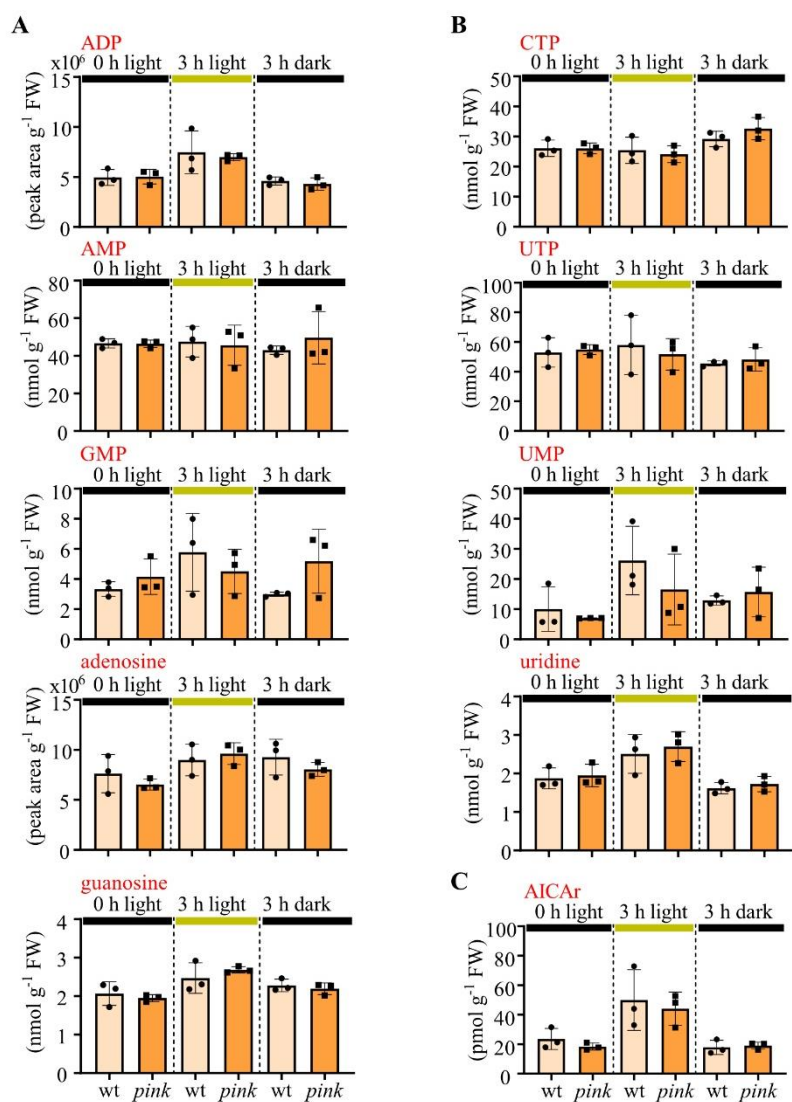


**Figure A-4. Metabolite analysis in seedlings of *PINK* variants with different durations of light.**

(A) Purine, (B) pyrimidine, and (C) hypoxanthine contents in 10-day-old seedlings of wild type, *pink*, and *pink::C*. 0 h light, the seedlings were harvested at the end of the night, right before the onset of light; 3 h light, the seedlings were harvested 3 h after the end of the night; 9 h light, the seedlings were harvested 9 h after the end of the night. Error bars are SD (n = 3 biological replicates). The detection limit for hypoxanthine in plant matrix was 0.1 nmol g<sup>-1</sup> FW. Two-sided Tukey's pairwise comparisons were performed separately for each time point for statistical analyses. Different letters indicate significant differences at p < 0.05.

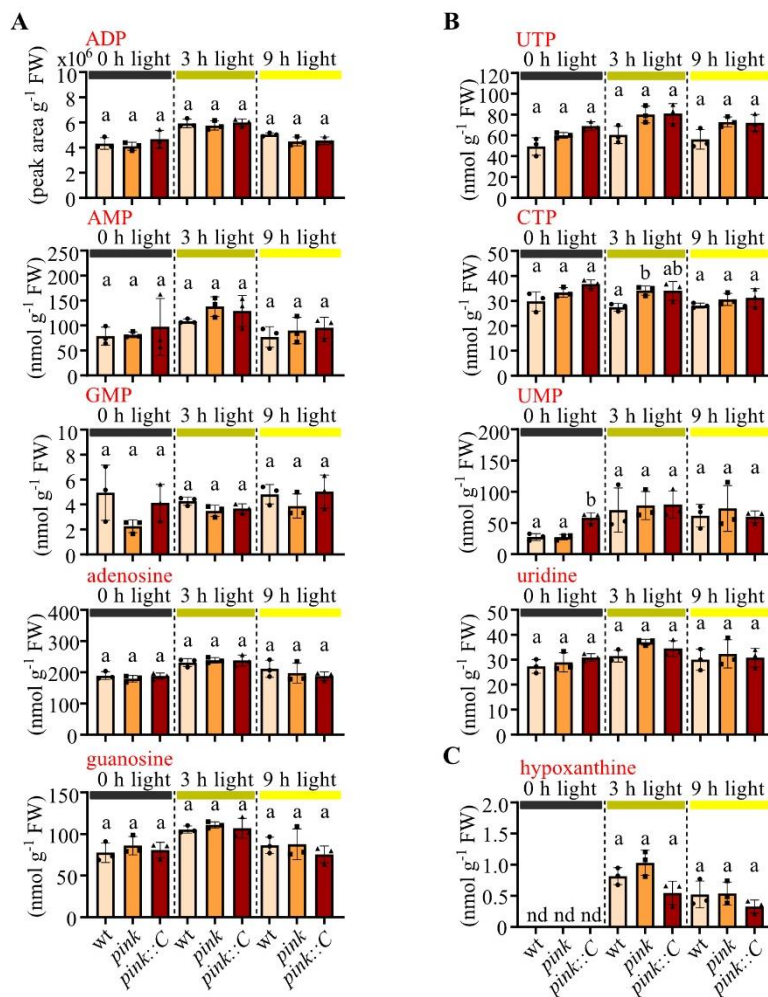


**Figure A-5. Metabolite analysis of Arabidopsis wild type seedlings with cold treatment.**

(A) Metabolic contents of 10-day-old wild type seedlings exposed to 10°C for different times. Two-sided Tukey's pairwise comparisons were performed for the statistical analyses. Different letters represent the significant differences at  $P < 0.05$ . (B) Nucleotide and nucleoside content in wild type seedlings grown at normal long-day condition up to day 7 and then either left growing under these conditions for three days (orange data points) or exposed to cold (16 h light period, 10°C throughout; blue data points). For statistical analysis at each time point, an unpaired t test was used. Statistical differences at  $p < 0.05$ ,  $p < 0.01$  and  $p < 0.001$  are indicated by \*, \*\* and \*\*\*, respectively.

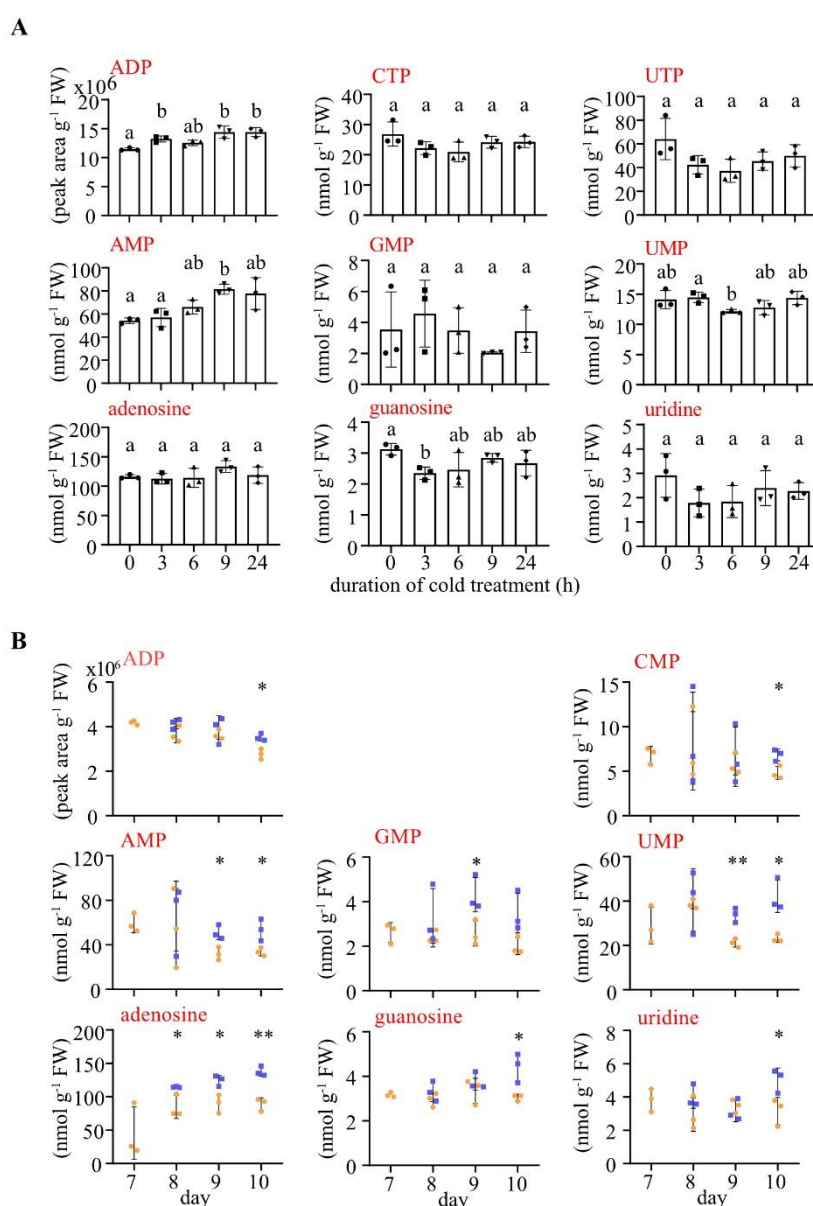


**Figure A-6. Metabolite analysis in seedlings of *PINK* variants with short-term cold exposure.**



APPENDIX

Metabolic contents of 10-day-old seedlings of wild type, *pink*, and *pink::C* without or during 3 hours of cold treatment(10°C). All plants were harvested 3 hours after the onset of light. Error bars are SD (n = 3 biological replicates). For statistical analysis at each time point, two-sided Tukey's pairwise comparisons were used. Different letters represent statistical differences at  $p < 0.05$ .

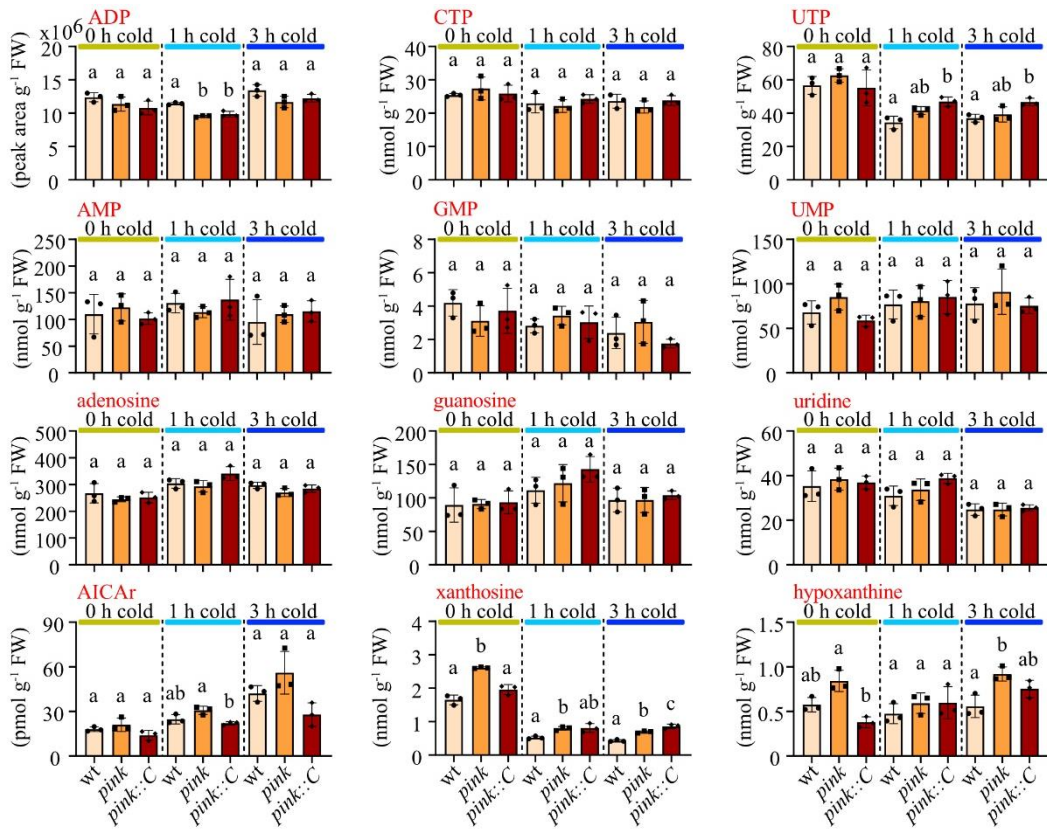
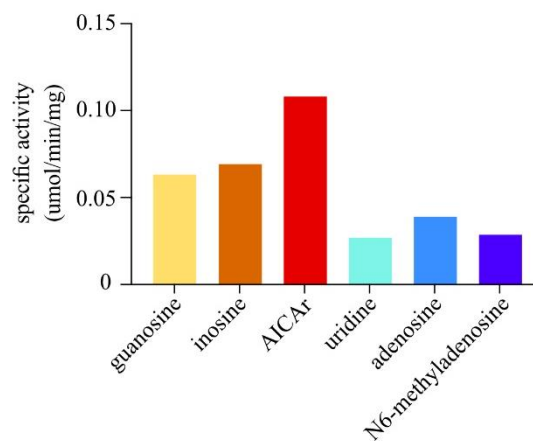


**Figure A-7. Specific activity of K6-2.**

Specific activity of K6-2 for guanosine, inosine, AICAr, uridine, adenosine, and N<sup>6</sup>-methyladenosine. The results are derived from the HPLC analysis (Figure 9) and calculated by ADP formation after 50 min reaction (velocity rates maybe not linear).



## Appendix of Tables

**Table A-1. Accession numbers used for bioinformatic analysis.**

Species	Protein	Accession number
<i>Arabidopsis thaliana</i>	ADK1	At3g09820.1
	ADK2	At5g03300.1
	PUKI	At1g49350.1
	RBSK	At1g17160.1
	PINK	At1g06730.1
	Kinase 6-1	AT5G43910.2
	Kinase 6-2	At4g28706.1
<i>Phaseolus vulgaris</i>	ADK1	Phvul.001G178000.1
	ADK2	Phvul.007G150300.1
	PUKI	Phvul.007G233200.1
	RBSK	Phvul.005G070000.1
	PINK	Phvul.007G178600.1
	Kinase 6-1	Phvul.001G167800.1
	Kinase 6-2	Phvul.007G154800.1
<i>Solanum lycopersicum</i>	ADK1	Solyc09g007940.2.1
	ADK2	Solyc10g086190.1.1
	PUKI	Solyc01g109450.2.1
	RBSK	Solyc07g062070.2.1
	PINK	Solyc09g066130.2.1
	Kinase 6-1	Solyc08g078370.2.1
	Kinase 6-2	Solyc09g064240.2.1
<i>Oryza sativa</i>	ADK1	LOC_Os02g41590.1
	ADK2	LOC_Os04g43750.1
	PUKI	LOC_Os05g09370.1
	RBSK	LOC_Os01g47550.1
	PINK	LOC_Os05g09370.1
	Kinase 6-1	LOC_Os08g45180.1
	Kinase 6-2	LOC_Os10g32830.1
<i>Sorghum bicolor</i>	ADK1	Sobic.004G220000.1
	ADK2	Sobic.006G148700.1
	PUKI	Sobic.009G112300.1

APPENDIX

---

	RBSK	Sobic.003g248300.1
	PINK	Sobic.001G494500.2
	Kinase 6-1	Sobic.007g161800.1
	Kinase 6-2	Sobic.007g211800.1
<i>Chlamydomonas reinhardtii</i>	ADK	Cre03.g204601.t1.1
	PUKI	Cre17.g701100.t1.2
	RBSK	Cre10.g424500.t1.2
	PINK	Cre09.g387050.t1.2
	Kinase 6	Cre01.g045640.t1.2

---

## Curriculum Vitae

### Personal Data

---

Name: Xiaoguang Chen  
Gender: Male  
Nationality: P.R. China  
Date of Birth: March 6<sup>th</sup>, 1991  
Place of Birth: Shangqiu, Henan, P.R. China

---

### Education

---

11.2018 - present      Ph.D. candidate  
Department of Molecular Nutrition and Biochemistry of Plants  
Gottfried Wilhelm Leibniz Universität Hannover  
Supervisor: Prof. Dr. Claus-Peter Witte

10.2017 - 10-2018      Ph.D. candidate  
Institute of Immunology  
Universität Duisburg-Essen  
Supervisor: Prof. Dr. Karl Sebastian Lang

09.2014 - 07.2017      Master student. Institution of Plant Protection  
Chinese Academy of Agricultural Sciences  
Supervisor: Prof. Dr. Lihua Guo

09.2010 - 07.2014      Bachelor student. Plant quarantine  
Henan Agricultural University

---

## Publications

Zhu, C., Liu, X., Wang, W., Chen, X., Gao, S., Qian, M., Yang, N., Xu, Y., and Chen, M. (2021). Plant Sample Preparation for Nucleoside/Nucleotide Content Measurement with An HPLC-MS/MS. *Journal of Visualized Experiments: Jove*.

Zhang, L<sup>+</sup>., Chen, X<sup>+</sup>., Bhattacharjee, P., Shi, Y., Guo, L., and Wang, S. (2020). Molecular characterization of a novel strain of *Fusarium graminearum* Virus 1 infecting *Fusarium graminearum*. *Viruses* 12, 357.

Chen, X., He, H., Yang, X., Zeng, H., Qiu, D., and Guo, L. (2016). The complete genome sequence of a novel *Fusarium graminearum* RNA virus in a new proposed family within the order *Tymovirales*. *Archives of Virology* 161, 2899-2903.